AD NUMBER

AD818913

NEW LIMITATION CHANGE

TO

Approved for public release, distribution unlimited

FROM

Distribution authorized to U.S. Gov't. agencies and their contractors; Critical Technology; JUN 1967. Other requests shall be referred to U.S. Army Engineer Waterways Experiment Station, Vicksburg, MS.

AUTHORITY

USAEWES ltr dtd 24 Jan 1972

Technical Report No. RA076R1000

Contract Report No. 3-166

Final Report

RESEARCH STUDY FOR THE DESIGN OF A PORTABLE VTOL BLAST CONTROLLING PLATFORM

June 1967 - FHR 3462

By

W.M. Dervin, R.S. Moss, and
F.H. Ringler

Sponsored by

U.S. Army Materiel Command

Conducted for

U.S. Army Engineer Waterways Experiment Station
CORPS OF ENGINEERS
Vicksburg, Mississippi

Under

Contract No. DACA 39-67-C-0003

By

FAIRCHILD HILLER
Republic Aviation Division
Farmingdale, Long Island, New York 11735

Technical Report No. RA076R1000

Contract Report No. 3-166

Final Report

RESEARCH STUDY FOR THE DESIGN OF A PORTABLE VTOL BLAST CONTROLLING PLATFORM

June 1967 - FHR 3462

By

W.M. Dervin, R.S. Moss, and
F.H. Ringler

Sponsored by

U.S. Army Materiel Command

Conducted for

U.S. Army Engineer Waterways Experiment Station
CORPS OF ENGINEERS
Vicksburg, Mississippi

Under

Contract No. DACA 39-67-C-0003

By

FAIRCHILD HILLER
Republic Aviation Division
Farmingdale, Long Island, New York 11735

FOREWORD

This report covers work conducted from 16 January 1967 through 30 June 1967 by Fairchild Hiller, Republic Aviation Division under Contract No. DACA39-67-C-0003, "Research Study for the Design of a VTOL Blast Controlling Platform." The contract was negotiated under 10 U.S.C. 2304(a)(11) and sponsored by U.S. Army Materiel Command. Payment is to be made by Special Disbursing Agent, U.S. Army Engineer Waterways Experiment Station, Corps of Engineers, P.O. Box 631, Vicksburg, Mississippi. Supplies and services obtained are authorized by and chargeable to Military Allotment 21X2040 708-3508 P5910 (5022-66) S22-079.

Mr. John J. Brown was the Fairchild Hiller Program Manager. Mr. Michael Picchiello and Mr. Frank Ringler were in charge of development of the design concept. Mr. Daniel Dayboch and Mr. Warren Dervin conducted the thermodynamic study under the direction of Mr. Carl Roberts. Mr. Aaron Merkin and Mr. Robert Moss were responsible for the structural analysis which was supervised by Mr. William Harris. Design requirements were formulated by Mr. Richard Oliveto and Mr. Frank Dellosso. The material survey was conducted by Mr. Julius Stock under the direction of Mr. Henry Kleindienst.

ABSTRACT

The feasibility of the concept for a portable blast-diverting platform for vertical takeoff and landing (VTOL) aircraft was previously demonstrated by scale model tests. The platform would be assembled in the field from modules. Each module consists of a structural base containing air-deflector vanes and a load-bearing, gridded top. The platform would direct aircraft exhaust blast away from the aircraft and into the air to prevent terrain erosion, hot gas ingestion, adverse ground effects, and telltale "signature" generated by military activity.

The present research study to develop a design concept for a full-scale portable modular platform included thermodynamic considerations, establishment of design criteria, a materials survey, and structural analyses. In the development of the design concept, ease of handling and field erection of the platform, minimization of special tooling, use of simplest manufacturing procedures, and cost savings in all areas were also considered.

The study demonstrates that this type of modular platform can be designed for use with aircraft of various weights and engine exhaust characteristics.

TABLE OF CONTENTS

TABLE OF CONTENTS (CONT'D)

ILLUSTRATIONS

TABLES

LIST OF SYMBOLS AND ABBREVIATIONS

THERMODYNAMICS

A = required platform discharge area, ft^2

A_j = cross sectional area of the jet, ft^2

A_s = platform surface heat transfer area, ft^2

A_t = total attenuation of sound between source and receiver, the algebraic sum of the attenuation values resulting from a number of factors, A_1, A_2, A_3, and A_4, db.

A_1 = attenuation due to distance, db

A_2 = attenuation due to interaction with the atmosphere, db

A_3 = attenuation due to shielding, db

A_4 = attenuation due to building enclosure, db

C_a = ambient sound velocity, ft/sec

C_p = specific heat of the platform, Btu/lb °F

DI_s = directivity index, db

d = diameter of exhaust nozzle, ft

d_a = distance from source to receiver

F = net thrust, lb

g = acceleration due to gravity, ft/sec^2

h = platform surface heat transfer coefficient, Btu/hr °F ft^2

M = mass of platform, lb

p = platform discharge static pressure, psia

P_A = acoustic power, watts

P_{A_o} = reference power, 10^{-13} watts

LIST OF SYMBOLS AND ABBREVIATIONS (Cont'd)

P_j	=	kinetic energy per unit time of the jet stream, watts
PWL	=	acoustic power level of the source, db reference 10^{-13} watts
Q_j	=	dynamic pressure at nozzle, lb/ft^2
SPL_R	=	sound pressure level at the receiver, db reference 0.0002 microbar
T	=	temperature of the platform at any time, °F
T_a	=	ambient temperature, °F
T_E	=	platform discharge static temperature, °F
T_f	=	platform exposure temperature, °F
T_j	=	jet nozzle exhaust temperature, °F
T_o	=	temperature of the platform at time $\tau = 0$, °F
ΔT	=	$T - T_o$, °F
V	=	velocity of gas at platform discharge, ft/sec
V_j	=	expanded jet velocity, ft/sec
W	=	gas flow, lb/sec
x	=	height of nozzle above ground, ft
η	=	acoustic efficiency
ρ	=	density of gas at platform discharge, lb/ft^3
ρ_a	=	ambient density, lb/ft^3
ρ_j	=	density of the jet stream, lb/ft^3

τ = time, hr

τ_c = MC_p/hA_s, hr

θ = $(T_f - T_a) / (T_j - T_a)$

STRUCTURES

A = area, $in.^2$

A_{br} = area in bearing, $in.^2$

A_s = area in shear, $in.^2$

A_t = area in tension, $in.^2$

b = base of element, in.

c = distance from neutral axis to extreme fiber, in.

c = end fixity coefficient for columns

D = diameter, in.

E = modulus of elasticity in tension, psi

e = edge distance from center of hole, in.

F_b = bending stress, psi

F_{br} = bearing stress, psi

F_{bru} = ultimate bearing stress, psi

F_c = compression stress, psi

F_{cy} = compression yield stress, psi

F_s = shear stress, psi

F_{su} = ultimate shear stress, psi

F_t = tensile stress, psi

F_{tu} = ultimate tensile stress, psi

F_{ty}	=	yield tensile stress, psi
h	=	height of element, in.
I	=	moment of inertia, in.^{4}
K_t	=	tension efficiency factor for lugs
K_{br}	=	bearing efficiency factor for lugs
K_{bry}	=	yield factor for lugs
L	=	length, in.
L'	=	effective length, in.
M	=	bending moment, in. lb
M.S.	=	margin of safety
P	=	concentrated load, lb
P_{bru}	=	ultimate bearing load, lb
P_{tu}	=	ultimate tensile load lb
P_{ty}	=	yield tensile load, lb
P_y	=	limit load, lb
p	=	pressure, psi
R	=	reaction, lb
R_b	=	bending stress ratio
R_s	=	shear stress ratio
r	=	radius, in.
T	=	tension, lb
t	=	thickness of material, in.
V	=	shear
W	=	width of lug, in.

w	=	uniformly distributed load, lb/in.
y	=	distance from neutral axis to given fiber, in.
$\bar{y}$	=	distance from neutral axis to reference axis, in.
α	=	angle, degrees
ρ	=	radius of gyration, in.
θ	=	angle, degrees
$\frac{L'}{\rho}$	=	slenderness ratio
Δ	=	deflection, in.

Subscripts

L	=	left
R	=	right
all	=	allowable
max	=	maximum
min	=	minimum

MATERIALS

A-286	=	An industry designation for an iron-base superalloy.
AMS	=	Aeronautical Material Specification. Specifications for aircraft use published by the Society of Automotive Engineers.
F_{tu}	=	Ultimate tensile stress (taken from standard tensile specimens)
F_{ty}	=	Tensile yield stress at a permanent strain equal to 0.002 in. (0.2%) taken from standard test specimen.

LIST OF SYMBOLS AND ABBREVIATIONS (Cont'd)

Elong. % in 2 in.	=	A measure of ductility of the material based on a tension test using a gage length of 2 inches on the tensile specimen.
UTS	=	ultimate tensile strength
0.2% YS	=	The yield strength in ksi taken from the stress-strain curve at an offset of 0.002 in. or 0.2%.
Consutrode	=	electric vacuum (refining) melting process.
α	=	coefficient of linear thermal expansion, in./in./°F $\times 10^{-6}$
Charpy V-Notch	=	An impact test specimen incorporating a V-notch used to establish the energy in foot pounds to fracture a material (see Federal Test Methods No. 151).

SECTION I

INTRODUCTION

A concept was developed for a portable blast-diverting platform for vertical takeoff and landing (VTOL) aircraft which would divert the aircraft exhaust blast away from the aircraft and direct it into the air and thus avoid terrain erosion, hot gas ingestion, adverse ground effects, and enemy detection. The platform would be assembled in the field from modular sections, each section containing deflector vanes and being topped by a load-bearing grid.

Primarily, this concept is based on the operation of VTOL aircraft from the same ground environment as that of the combat units to which the aircraft is attached. The modular construction of the platform makes deployment by parachute, helicopter, or truck feasible, and erection can be accomplished rapidly with a minimum of equipment.

Logistically, the blast-diverting platform creates a mobile VTOL base that can be moved to new sites along with the troop support equipment. Several nondirective modules along the perimeter of the platform, in nonexhaust areas, can be used to store aircraft maintenance tools and support equipment.

The feasibility of this concept was previously demonstrated through scale-model testing by Republic Aviation Corporation.*

The purpose of the present research study is to develop a design concept for a full-scale portable modular platform.

*See Feasibility Study on the Design and Development of a VTOL Blast Controlling Platform, Report No. 3-123, August 1965, sponsored by the U.S. Army Materiel Command.

SECTION II

DEVELOPMENT OF DESIGN CONCEPT

To establish platform characteristics and functional effectiveness which will result, after future detail design, in the production of platforms which approach the optimum satisfaction of their requirements, several related factors must be considered. Existing and proposed VTOL aircraft vary in configuration; weight; type of thrust components; temperature, velocity, and volume of exhaust blast; and location and size of engine exhaust blast areas. These factors, when combined, affect the platform size, structural requirements, material, configuration of deflecting vanes, and platform exhaust area. Additional evaluations must be made with regard to the size and weight of the basic module, the ease of fabrication, the simplification of tooling, the minimization of material and manufacturing costs, transportation, the ease of site preparation and platform assembly in the field, as well as the thermodynamic, aerodynamic, and structural aspects of design.

All of the above factors have been considered in the development of the platform design concept. Thermodynamically, engine exhaust characteristics for various types of VTOL aircraft, maximum platform exposure temperatures during takeoff and hovering, platform transient heating, platform exhaust gas discharge areas, and acoustic effects were considered to be pertinent to design. Design criteria were established with respect to module size, module weight, aircraft landing weight and load factor, tire footprint, drag loads, drift loads, platform temperature, and service life. The materials survey was conducted with regard to their suitability from a mechanical, physical property, cost, and fabrication standpoint for platform construction.

The physical design concept was based on several factors of prime importance. All modules were to be the same in construction for any particular platform. Fabrication, in production quantities, shall require a minimum of tooling. Structurally, the maximum strength to weight ratio consistent with other design considerations was the goal to be achieved.

The following sections of this report are presented to indicate the manner in which satisfaction of the above requirements was attempted. They also contain information from which parameters for the factors affecting design can be established.

SECTION III

THERMODYNAMIC CONSIDERATIONS

A. ENGINE EXHAUST CHARACTERISTICS

To design a VTOL blast controlling platform, the magnitude of the following parameters must be established, i.e., engine exhaust pressure, temperature, and velocity. Since there is a wide variation in these parameters for various types of engines depending on the aircraft installation, upper limits must be established in order to evaluate the overall effect on size, weight, and cost of the platform.

In addition, continuing engine design studies, necessitated by an ever increasing need for improving the overall performance of VTOL aircraft, have been in progress for some time and are still in progress. Therefore, at present, upper limits of some engine exhaust parameters have not yet been reached.

Table 1 presents data from Reference 1 (dated November 1964) which gives the disc loading, temperature of the exhaust, and exhaust velocity of various types of VTOL aircraft designs. The figures in parentheses are the best estimates for future aircraft.

Table 1 - Engine Exhaust Characteristics (Nov. 1964)

Type of Aircraft	Disc Loading lb/ft^2	Temperature of exhaust, °F	Exhaust Velocity ft/sec
Helicopter	6.0	300.0	380.0
Propeller	50.0	300.0	580.0
Ducted Prop	100.0	300.0	650.0
Lift Fan	310.0	500.0 (1000)	650.0
Turbofan	650.0	730.0 (1500)	1675.0
Jet - Non A/B	1250.0 (2700)	1500.0 (2000)	1675.0 (2200)
Jet A/B	2750.0	3000.0 (3500)	2000.0 (2700)

Since the proposed VTOL blast controlling platform is to be used at advance bases, the parameters noted in Table 1 will have full effect for only a very short duration (just prior to takeoff and while the aircraft is within five nozzle diameters above the ground, Reference 2).

B. MAXIMUM EXPOSURE TEMPERATURE - TAKEOFF

The maximum platform temperature will be attained during takeoff. After start up, the lift engines are operated at idle power for a period of time until the pilot ascertains that engine operation is normal. During this time it is assumed that the platform will reach the idle jet temperature. The throttle is then advanced to maximum power for takeoff. For the most conservative condition (longest takeoff time) maximum power operation is assumed to produce an engine lift to aircraft weight ratio of 1.05. In the absence of ground suction, lift off will start when the lift to weight ratio just exceeds 1.0 or 95% maximum thrust. The jet exhaust temperature is highest at maximum thrust and the platform will be exposed to this maximum temperature for the time it takes the aircraft to ascend a distance of five nozzle diameters above the platform.

C. MAXIMUM EXPOSURE TEMPERATURE - HOVERING

After takeoff the aircraft could possibly hover close to the ground for 120 seconds. The engine would be operating at a lift to weight ratio of 1.0 or 95% maximum thrust under this condition. During this time, if the aircraft were hovering five diameters or less above the platform, the platform would be exposed to the maximum hover temperature, which would be somewhat lower than the maximum thrust temperature. At heights over five nozzle diameters, the platform will be exposed to temperatures that are determined as a function of the nozzle height above the ground.

Figure 1 shows the temperature that the platform surface will be exposed to as a function of the ratio of height above the ground to the exhaust nozzle diameter. This figure was derived from Reference 2 which gives the generalized formula for the platform exposure temperature as

$$\theta \frac{x}{d} = 4.8 \quad \text{for} \quad \frac{x}{d} > 5 \qquad (1)$$

where θ is the dimensionless parameter equal to $(T_f - T_a)/(T_j - T_a)$

T_a = ambient temperature, °F

T_j = jet nozzle exhaust temperature, °F

T_f = platform exposure temperature, °F

x = height of nozzle above ground, ft

d = diameter of exhaust nozzle, ft

x/d is dimensionless

For x/d less than five, the platform exposure temperature is equal to the exhaust nozzle temperature.

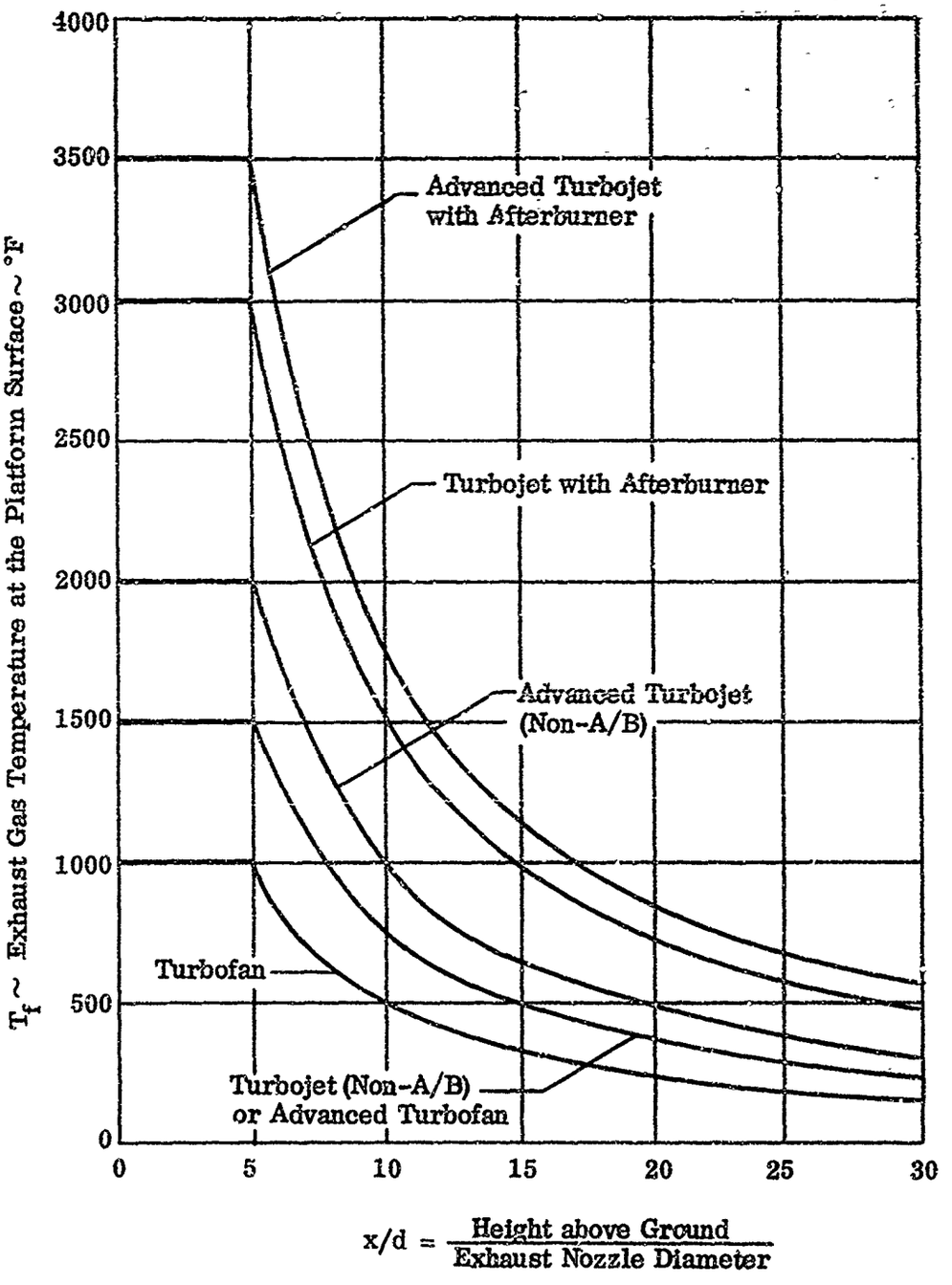

Figure 1. Exhaust Gas Temperature at the Platform Surface

D. TRANSIENT HEATING - PLATFORM MAXIMUM TEMPERATURES

To calculate the temperature rise of the platform during the start-up, lift-off, and hover conditions the platform is assumed to be heated initially to the nozzle exhaust gas temperature at idle power. On throttle advance to maximum power the platform is suddenly exposed to the maximum nozzle exhaust temperature. The platform will reach this temperature in infinite time.

Reference 3 gives the following theoretical relationship for the rate of temperature rise, ΔT applicable to this case as

$$\Delta T = T - T_o = (T_f - T_o)\,(1 - \epsilon^{\tau/\tau_c}) \qquad (2)$$

where $\tau_c = \dfrac{MC_p}{hA}$

τ = time, hr

T = temperature, °F, of the platform at any time τ

T_o = temperature, °F, of the platform at time $\tau = 0$

T_f = platform exposure temperature, °F

M = Mass of the platform, lb

C_p = specific heat of the platform, Btu/lb°F

h = platform surface heat transfer coefficient, Btu/hr°F ft^2

A_s = platform surface heat transfer area, ft^2

The assumption is made that the platform is uniform at any instant; that is, the resistance of the platform to heat flow is negligible.

Figure 2 gives the temperature rise with respect to time for various platform weights. For this typical curve the following was assumed

T_f = 2000°F

T_o = 900°F

A_s = 8 ft^2

C_p = 0.10 Btu/lb °F (steel)

h = 40 Btu/hr ft^2 °F

Figure 3 shows similar curves for afterburner (A/B) engines that give maximum platform exposure temperatures of 3000°F and 3500°F.

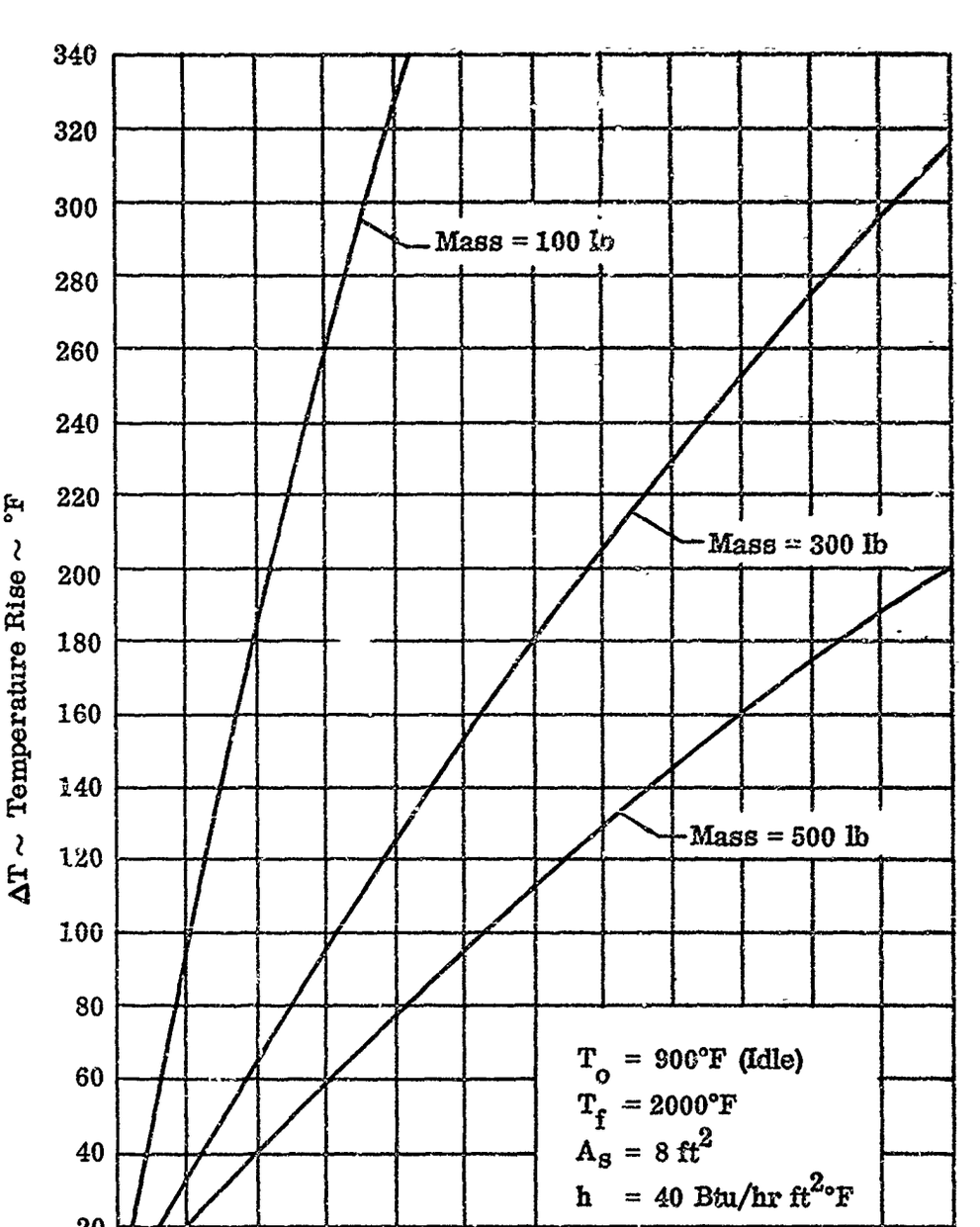

Figure 2. Platform Temperature after Idle Soak for Advanced Turbojet (Non-Afterburner)

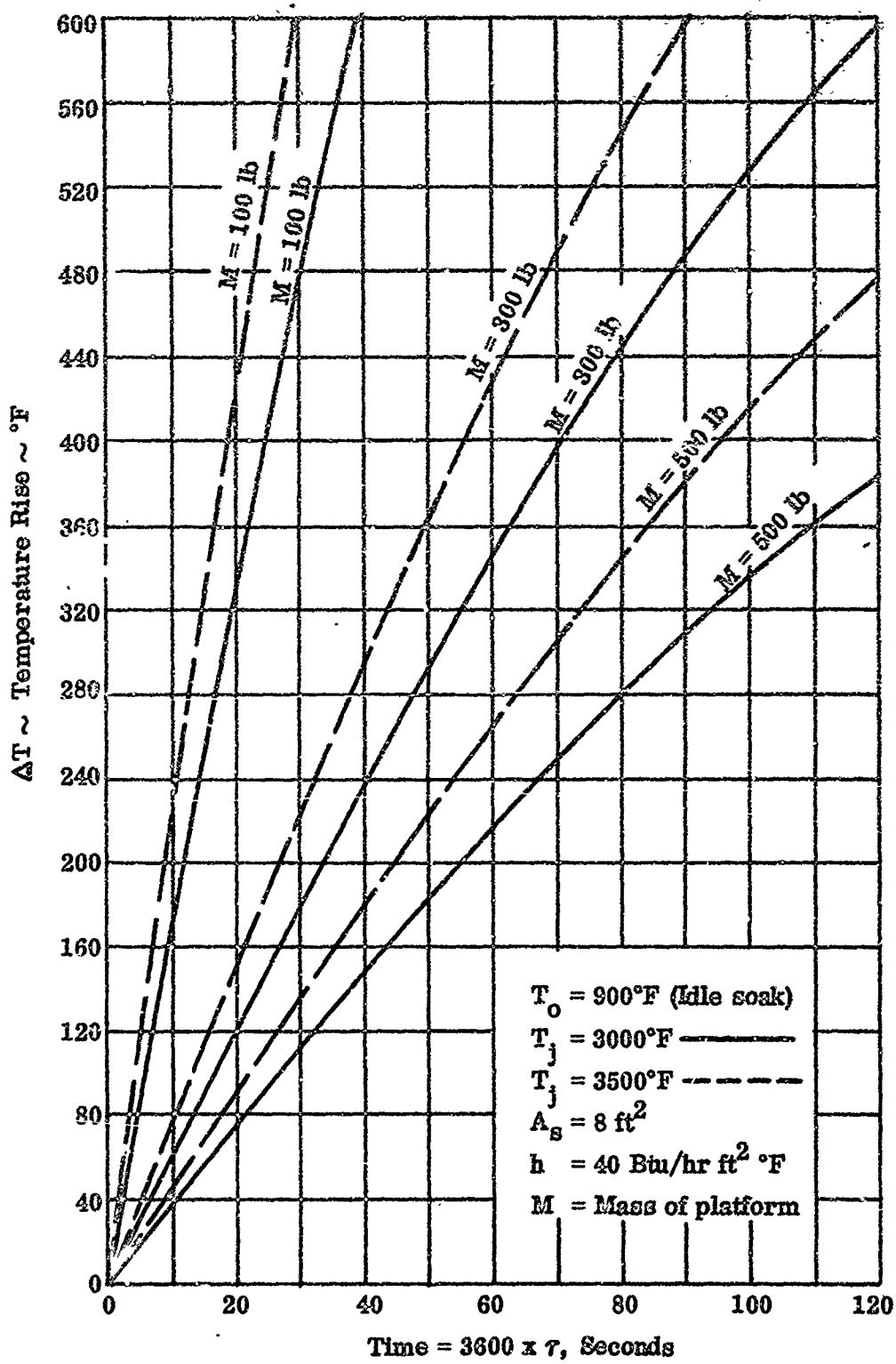

Figure 3. Platform Temperature Rise after Idle Soak for Turbojets with Afterburner

E. PLATFORM GAS DISCHARGE

Another important consideration in the design of a VTOL blast controlling platform is the discharge of the aircraft exhaust gases and entrained air from the platform. This can be accomplished by allowing the gases to discharge from the end or ends of the platform. Vanes can be used to divert the gases in any specific direction desired.

The gases must be dischared from the platform without causing ground erosion. To hold ground erosion in the vicinity of the platform to a minimum, it has been shown through experimental tests, Reference 4, that the discharge velocity should be in the order of 500 ft/sec. Therefore, the platform exhaust area should be sized to give an exit velocity not greater than 500 ft/sec.

For this flow velocity, the discharge area required is dependent on the total mass flow of aircraft jet exhaust gases combined with entrained air and the density of the gas mixture.

Figure 4 depicts the required platform discharge areas to obtain a velocity of 500 ft/sec as a function of the gas flow at constant density. For this analysis a constant exit static pressure of 15 psia was assumed. Two different exit static temperatures, T_E were chosen to show their effect on the required exit areas. The curves are based on the basic equation

$$W = \rho AV \tag{3}$$

where:

W = gas flow, lb/sec

ρ = density of gas at platform discharge, lb/ft^3

A = required platform discharge area, ft^2

V = velocity of gas at platform discharge, ft/sec

The actual area available for gas discharge is the product of the platform discharge length and the platform height. The platform length and width is determined by the aircraft size, so that only the platform height can be varied to maintain an exit velocity of not greater than 500 ft/sec.

To keep platform height to a reasonable minimum, the exit velocity, V may exceed 500 ft/sec. The effect of high discharge velocity can be controlled, if necessary, by adding diverters downstream from the platform exit to deflect the discharge gases away from the ground plane. Deflecting vanes mounted internally at the discharge end of the platform were considered. This solution was rejected because of the reduction in exit area and consequent increase in platform height required.

F. ACOUSTIC EFFECTS

In order to properly design a VTOL-blast controlling platform, the noise level derived from the aircraft must be known. The procedure used for this study has been derived from Reference 5.

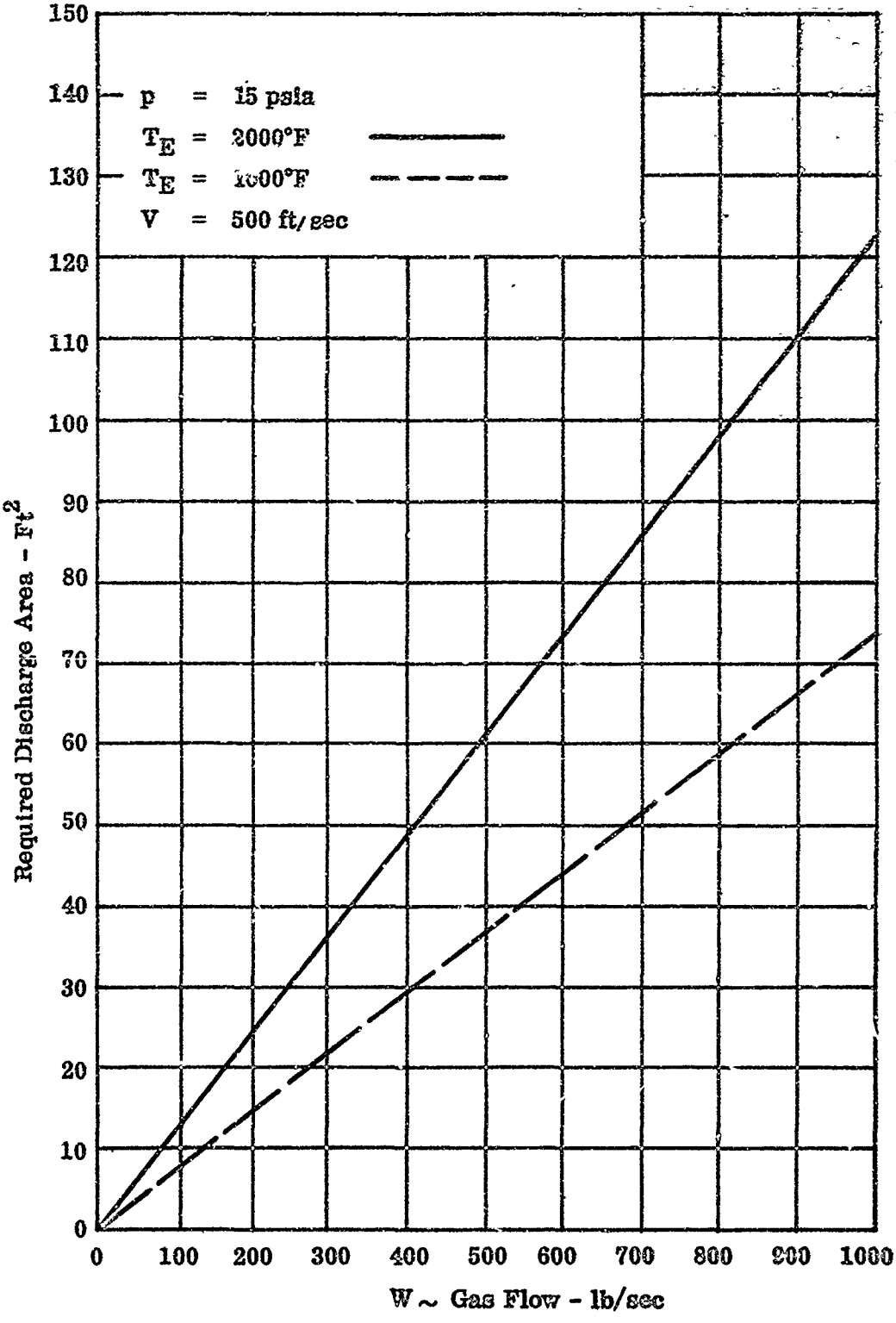

Figure 4. Platform Discharge Required Area

The amount of sound transmitted from an aircraft some distance away is governed by the sound source and its direction and by the attenuation along the sound path. The sound received may be found from the following equation:

$$SPL_R = PWL + DI_s - A_t \quad (4)$$

where

SPL_R = sound pressure level at the receiver, db reference 0.0002 microbar

PWL = acoustic power level of the source, db reference 10^{-13} watts

DI_s = directivity index of the source in the direction of propagation, db

A_t = total attenuation of sound between source and receiver, db. This total attenuation is the algebraic sum of the attenuation values resulting from a number of factors

1. Acoustic Power Level (PWL)

The acoustic power, P_A, in watts, radiated by a sound source is stated in terms of the acoustic power level (PWL) of the source:

$$PWL = 10 \log_{10} (P_A/P_{A_o}) \text{ decibels} \quad (5)$$

where P_{A_o}, the reference power, equals 10^{-13} watts. The acoustic power of a jet is related to the kinetic energy per unit of time in the jet stream by some acoustic efficiency, η

$$P_A = \eta P_j = 1/2 \eta \rho_j A_j V_j^3 (4.21 \times 10^{-2}) = 1/2 \eta F V_j (1.356)$$

where

P_j = kinetic energy per unit of time of the jet stream, watts

ρ_j = density of the jet stream, lb/ft^3

A_j = cross sectional area of the jet (usually taken as the tail pipe exit area of the jet engine), ft^2

V_j = expanded jet velocity, ft/sec

Figure 5 gives the acoustic conversion efficiency, η, plotted against the ratio of expanded jet velocity, V_j, to ambient sound velocity (outside the jet stream) C_a. The parameter of the curves is $\rho_j/\rho_a (T_j/T_a)^2$ where ρ_a and ρ_j are, respectively, the ambient and

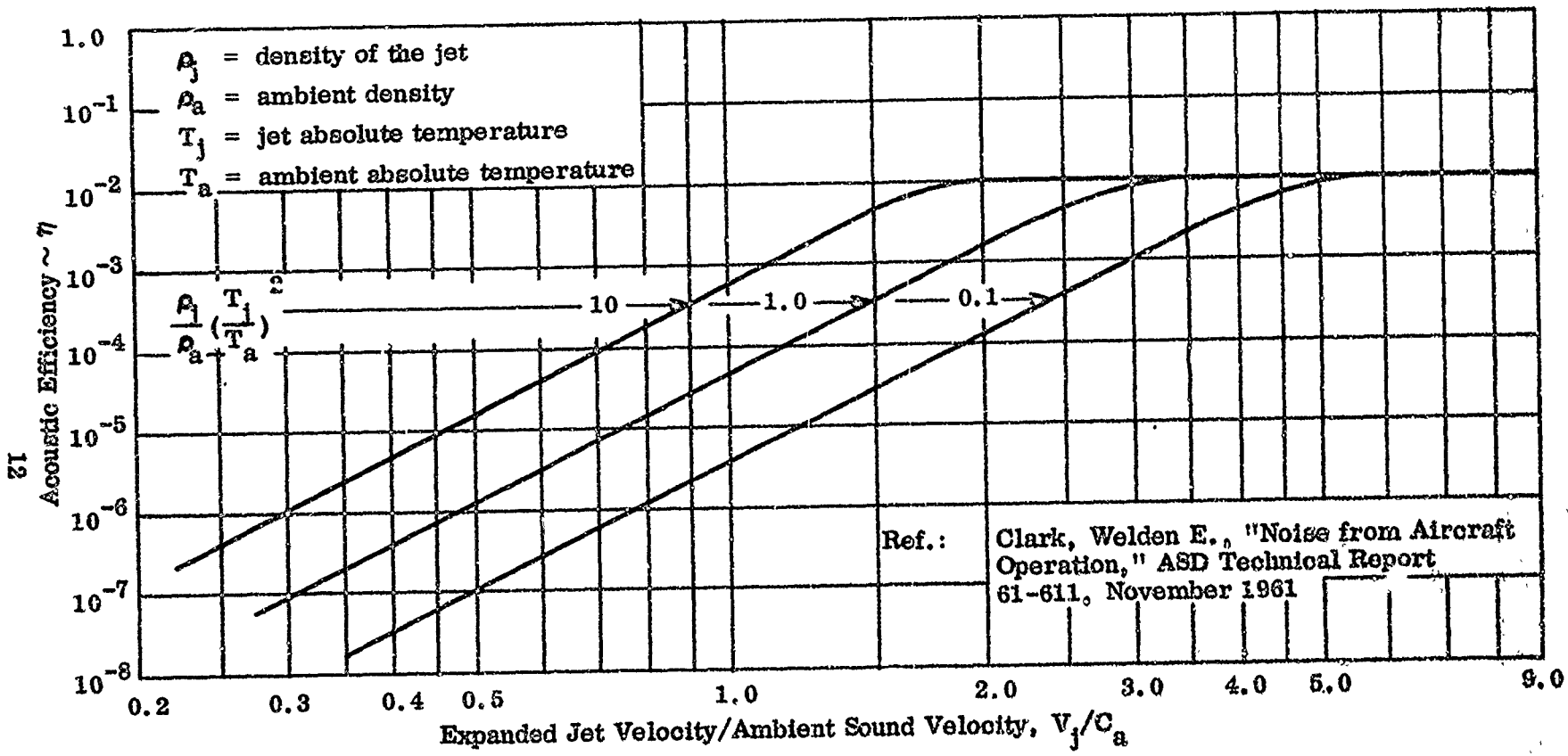

Figure 5. Acoustic Efficiency ~ η

jet densities, and T_a and T_j are, respectively, the ambient and jet absolute temperatures. The slope of the diagonal lines is determined by the Lighthill parameter (Reference 6) $\rho_j A_j V_j^8 / C_a^5$.

Within the region where the acoustic efficiency is not limited (turbojet engines operating at military power) the acoustic power is proportional to the Lighthill parameter (Reference 7).

For engineering purposes, typical values may be chosen for ρ_j and C_a so the Lighthill parameter can be used to obtain the following expression:

$$PWL = 26.6 + 20 \log_{10} d + 80 \log_{10} (F/W) \qquad (7)$$

db reference 10^{-13} watts

where

d = jet exit nozzle diameter, ft

F = net thrust, lb

W = gas flow, lb/sec

This expression is plotted in Figure 6.

Methods for predicting the acoustic power level of a jet during afterburner operation are predominantly empirical. One of the most convenient of these is illustrated on Figure 7, where the increment in acoustic power level above that of military power is plotted against the increase of thrust resulting from the afterburner. Figure 6 may be used to estimate the PWL during military power operation while Figures 6 and 7 may be used for afterburner operation. For other engine operations Equation 4 may be used.

2. Directivity Index - (DI_s)

Since the jet exhaust from the aircraft is not a simple source of sound which radiates the same amount of power in every direction but rather is "directive" in that it radiates different amounts of acoustic power in different directions, a correction factor must be utilized in estimating the sound pressure level at the receiver.

The directivity pattern of jet noise is generally assumed to be symmetrical about the axis of the jet and reaches a maximum in a cone about 40° to 50° from the jet exhaust.

From Reference 5, a series of tests were performed on several turbojet and turbojet with afterburner engines to determine the directivity patterns and the sound pressure level associated with them. Based upon this data an average value of -10 db was used for

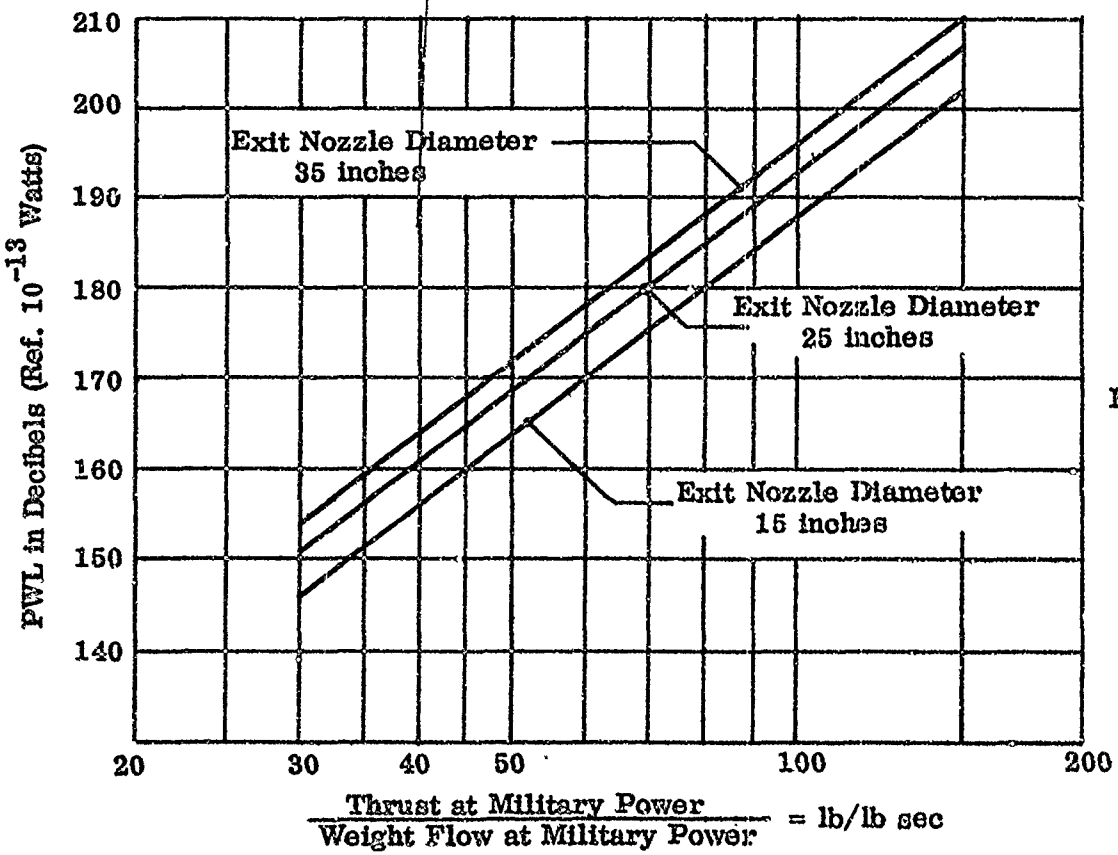

Ref.: Clark, Welden E., "Noise from Aircraft Operation," ASD Technical Report 61-611, November 1961

Figure 6. Acoustic Power Level for Turbojets at Military Power

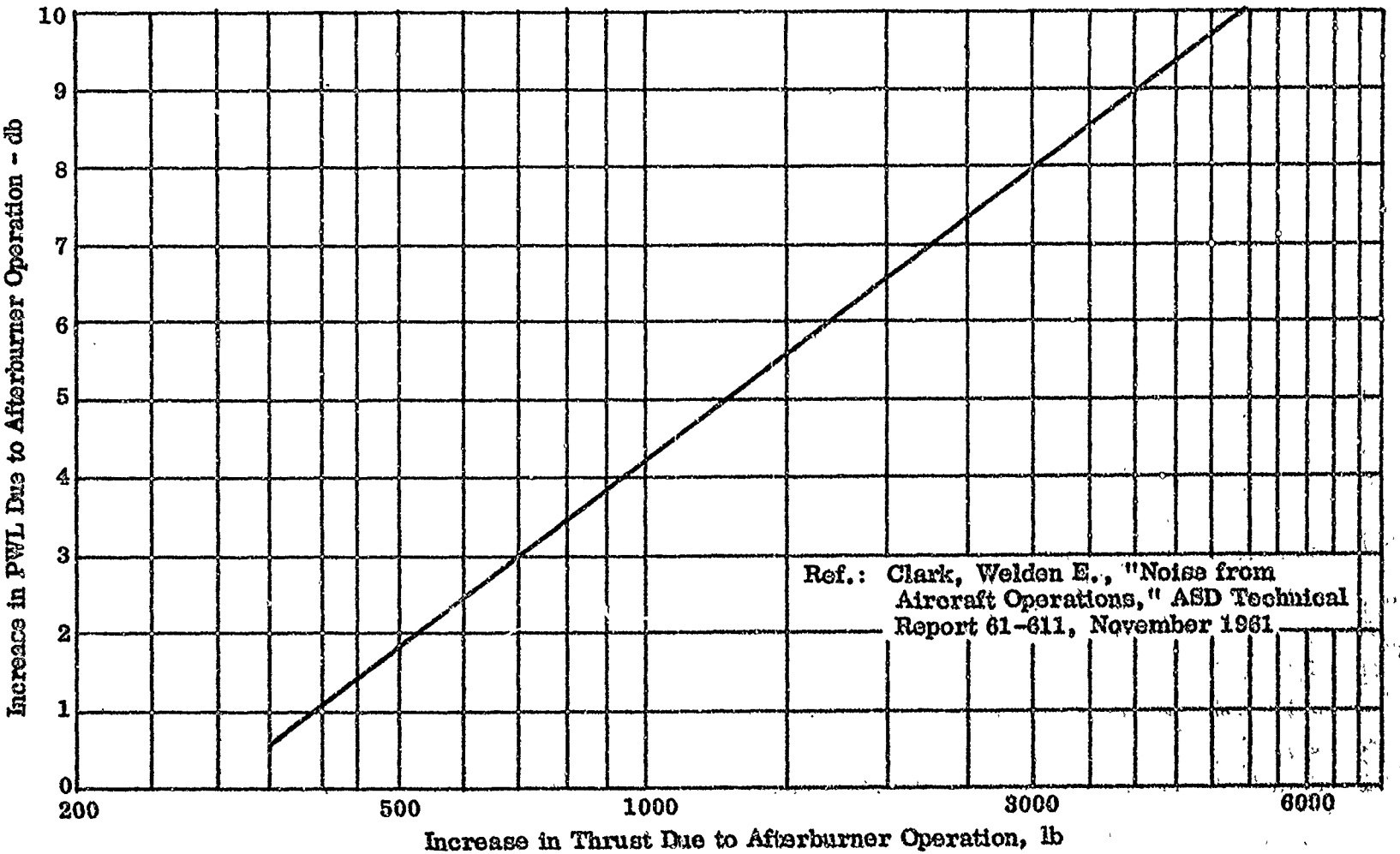

Figure 7. Acoustic Power Level Increase due to Afterburner Operation

this study since the variation in the Directivity Index was estimated to be between -15 and +8 db.

3. Total Attenuation (A_t)

The total attenuation can be considered to include attenuation from several sources:

A_1 - attenuation due to distance, db

A_2 - attenuation due to interaction with the atmosphere, db

A_3 - attenuation due to shielding, db

A_4 - attenuation due to building enclosure, db

Since the source (engine exhaust) is less than 100 ft from the receiver (the blast platform), A_2 may be neglected. Likewise since A_3 and A_4 are not under consideration for this application they are neglected.

The diminution of sound pressure level with distance when sound is radiated from a constant power point source into free space (the source is far from the ground) is called spherical divergence. Since the surface area of the sphere is proportional to the square of the radius of the sphere, the propagation loss due to distance is:

$$A_1 = 10 \log_{10} 4\pi d_a^2 \qquad (8)$$

where

d_a = distance from source to receiver, ft

For sound radiating into half space (the source is close to the ground) hemispherical divergence is found. Assuming the ground plane to be a perfect reflector the propagation loss due to distance is:

$$A_1 = 10 \log_{10} 2\pi d_a^2$$

For this application the hemispherical divergence is employed.

4. Sample Calculation

To illustrate the use of the curves and equations given in this section a sample calculation will be given.

Given:

Lift Turbojet Engine Characteristics

Thrust, F = 14,820 lb

Expanded jet velocity, V_j = 2200 ft/sec

Exhaust gas temperature, $T_j = 2000°F$

Dynamic pressure at nozzle = 2700 lb/ft^2 = 18.75 psi

Thrust/airflow = 91.8

Airflow = 162 lb/sec

Nozzle diameter = 20 in.

Calculations:

A. Acoustic efficiency (η)

$$\frac{V_j}{C_a} = \frac{2200}{1116} = 1.975$$

$$\left(\frac{T_j}{T_a}\right)^2 = \left(\frac{2460}{520}\right)^2 = 22.4$$

$$Q_j = \frac{\rho_j V_j^2}{2g} = 2700 \text{ lb/ft}^2 \text{ (dynamic pressure)}$$

$$\rho_j = \frac{2700\ (2g)}{(2200)^2} = 0.0359 \text{ lb/ft}^3$$

$$\frac{\rho_j}{\rho_a} = \frac{0.0359}{0.0765} = 0.47$$

$$\frac{\rho_j}{\rho_a}\left(\frac{T_j}{T_a}\right)^2 = 10.5$$

$\eta = 10^{-2}$ from Figure 5 for $\frac{V_j}{C_a} = 1.975$

B. Acoustic Power Level (PWL)

$$P_A = \frac{1}{2}\eta F_n V_j (1.356)$$

$$P_A = \frac{1}{2}(10^{-2})(14,820)(2200)(1.356)$$

$$P_A = 2.21 \times 10^5 \text{ watts}$$

$$PWL = 10 \log \frac{P_A}{P_{A_o}}$$

$$PWL = 10 \log \frac{2.21 \times 10^5}{10^{-13}}$$

$$PWL = 183.4 \text{ db}$$

From Figure 6 for a 20-in. exit nozzle diameter at a thrust/weight flow of 91.8 lb/(lb/sec), the above value is also obtained.

C. Sound Pressure Level at the Blast Platform

$$SPL_R = PWL + DI_s - A_t$$

For a distance of 4.25 ft between source and platform

$$A_t = A_1 = 10 \log_{10} 2\pi d_a^2$$

$$= 10 \log_{10} 2(3.14)(4.25)^2$$

$$= 10 \log_{10} 113$$

$$= 20.4 \text{ db}$$

$$SPL_R = 183.4 - 10 - 20.4$$

$$= 153 \text{ db at takeoff}$$

REFERENCES

1. Vasiloff, A., "Test Results of Research for Rapid Site Preparation for V/STOL Aircraft," APL-TDR-64-164, November 1964.

2. Squire, H.B., "Jet Flow and its Effects on Aircraft," Jet Propulsion, March 1950.

3. General Electric Co., "Design Data Heat Transfer Section G503.2," September 1943.

4. Fearon, J.P.C. and Norman, D.H., "Simple Solution to Some of the Operating Problems during Take-Off and Landing," Journal of the Royal Aeronautical Society, February 1962.

5. Clark, Welden E., "Noise from Aircraft Operations," ASD Technical Report 61-611, November 1961.

6. Lighthill, M.J., Proceeding Royal Society (London) A211, page 264, 1952, A222, page 1, 1954.

7. Frankin, P.A., "Review of Information of Jet Noise," Noise Control, May 1958.

SECTION IV

DESIGN CRITERIA

A. INTRODUCTION

This section covers the load and temperature criteria involved in the structural design of the VTOL blast controlling platform. The basic design concept is a sectional or modular type of platform in which each module measures 4 ft by 2 ft in order to be easily portable. Loads and temperatures are given for the individual module. A weight of 200 to 250 lb for each field-handled component was assigned.

B. AIRCRAFT LANDING WEIGHT AND LOAD FACTOR

An aircraft weight of 50,000 lb was initially selected for the design concept presented. The limit load factor in landing is 2.5g which is commensurate with an aircraft sink speed of 15 ft/sec and with a compatible landing gear shock strut design. For a study of module sizing for the various aircraft weights of 20,000, 30,000, and 40,000 lb the load factor of 2.5g was maintained.

The footprint (loading area under the tire) was established by using the higher level of tire pressures for the pertinent static rated tire associated with each aircraft weight. A footprint of 160 sq in. was selected for all aircraft weights.

Table 2. Tire Ratings and Footprint Pressures

Aircraft Weight lb	Static Rating of Tire lb	Tire Footprint $in.^2$	Footprint Pressure $lb/in.^2$
50,000	25,000	160	156
40,000	20,000	160	125
30,000	15,000	160	94
20,000	10,000	160	63

The above stated pressures are considered conservative from the standpoint of tire ratings and footprint pressures.

C. TWO-WHEEL LANDING

The maximum vertical reaction is combined with a drag load equal to one-quarter of the maximum vertical reaction of one gear in a two-wheel landing. For the 50 000-lb aircraft, the normal load on the gear is

$\frac{50,000\ (2,5)}{2}$ = 62,500 lb. The drag load is 62,500(0.25) = 15,600 lb.

D. DRIFT LANDING

The aircraft is assumed to be in the level attitude with only the main landing gear contacting the platform. The vertical reaction on each gear is assumed to be one-half of the maximum obtained in the two-point level landing. The inward acting load and the outward acting load are, respectively, 80% and 60% of the vertical load.

For the 50,000-lb aircraft:

$$\text{Inward acting load} = \frac{62,500}{2}(0.80) = 25,000 \text{ lb}$$

$$\text{Outward acting load} = \frac{62,500}{2}(0.60) = 18,750 \text{ lb}$$

E. PLATFORM TEMPERATURES

The maximum gas temperature at the platform occurs during takeoff. It is assumed that, after start-up, the engines are operated at idle power for a sufficient time to attain heat soak in the platform. Although the exhaust temperature is highest at maximum thrust (takeoff), the platform will be exposed to this temperature only for the short period that it takes the aircraft to ascend a distance of five exhaust nozzle diameters above the platform. Figure 1 in Section III shows that the temperature to which the platform surface will be exposed will be a function of the ratio of height above the ground to the exhaust nozzle diameter for various engines.

Maximum exposure time will occur at hovering. For determination of design temperature, the platform will initially be considered heat soaked at 900°F (idle power) with the increase in temperature, Δt, resulting from the time of hovering. As regards load and temperature, for the purpose of design, it is assumed that subsequent to hovering, the aircraft will slip sufficiently to have its landing gear contact the heated module. A structural temperature of 1000°F was assigned to act in conjunction with the landing loads of the 20,000-, 30,000-, 40,000-, and 50,000-lb aircraft considered in development of the design concept.

Figure 2 in Section III gives the temperature rise with respect to time for various platform weights for non-afterburner power. For a total module weight, including grid, of 400 lb a temperature rise of 100°F above the 900°F heat soak would require 42 seconds of hovering at a height of five exhaust nozzle diameters or less. Figure 3 in Section III shows similar curves for afterburner engines that give maximum platform exposure temperatures of 3000°F to 3500°F.

F. ACOUSTICS

Sound pressure levels (SPL) and their derivations are presented in Section III.

SECTION V

MATERIALS SURVEY

A. INTRODUCTION

As a prelude to the formulation of the platform design concept, a survey of materials available for construction was required. This was to assure that the materials used are those best suited to the design requirements. Factors considered in the selection of these materials are the ability to withstand the temperature of exhaust blast, minimum weight without sacrifice of structural integrity, ease of fabrication, ability to withstand environmental conditions, and cost as related to the advantages and disadvantages of the other factors.

B. MATERIAL REQUIREMENTS

The materials of construction should, in addition to meeting design requirements, be readily fabricated and moderate in cost. The base structure will be assembled with mechanical fasteners, therefore welding will not be required. The material or assembly must be corrosion and oxidation resistant, either through the inherent nature of the material or through the use of auxiliary coatings.

C. MATERIAL SELECTION

The method used for selection of material is presented by analysis of material requirements for three types of engine exhaust characteristics, those of advanced turbojet engines with exhaust nozzle temperatures of 2000°F and those of turbojet and advanced turbojet engines with afterburner with exhaust nozzle temperatures of 3000°F and 3500°F, respectively. Using the information from Section III-A regarding exhaust blast temperatures for other types of aircraft and engines, formulae for calculation of platform exposure temperatures, and applying appropriate design loads, material selection can be made.

D. ADVANCED TURBOJET AIRCRAFT

1. Design Load Requirements

The material for platform construction should have a minimum short time ultimate tensile strength (uts) of 100,000 psi at 1000°F. It shall also be capable of being exposed to 1200°F under no load conditions for 600 hours without degradation of subsequent ambient and 1000°F properties. The material shall, in addition, be capable of being temperature cycled from room temperature (RT) to 1200°F for at least 10,000 times without mechanical property degradation. Each temperature cycle will impose design loads of 1 minute duration at 1000°F, and up to 3 minutes at 900°F. In addition, the material should have a low coefficient of thermal expansion in order to minimize thermal stresses.

2. Material Selection

(a) Approach. Two divergent approaches were undertaken in the selection of the candidate material. The first was the evaluation of a stainless and heat resistant alloy which could meet the design load requirements without supplementary heat and corrosion resistant coatings.

The second approach was the use of heat resistant, but not corrosion resistant, alloy steel with a supplementary low thermal conductivity and corrosion resistant coating.

(b) Costs. Heat and corrosion resistant alloy are more expensive than alloy steels, depending on the alloy content and fabrication procedures. However, the basic heat and corrosion resistant alloy chosen (A-286) is only about twice as expensive as the alloy steel, since its alloy content is just sufficient to make it useful in the temperature range under consideration.

The use of coatings will, however, increase the price of the part made of alloy steel, the amount of which is dependent on the type of coating and method of attachment or application. It is estimated that use of a plastic laminate coating will make the part price equivalent to one made of the heat and corrosion resistant steel. Coating costs are discussed additionally in paragraph 5 below.

3. Material Properties - Steel

(a) Alloy A-286. The heat and corrosion resistant alloy A-286 is an iron-base precipitation hardening steel, which is available in bar, sheet, tubing and forgings, with appropriate AMS specifications. Its mechanical properties are detailed in MIL-HDBK-5, unless otherwise stated. Its approximate price per pound for sheet is $2.15.

The minimum room temperature mechanical and physical properties are (bar, forging, tubing; consutrode melted):

F_{tu} = 140,000 psi

F_{ty} = 95,000 psi

Elong % in 2 inches = 12

Density = 0.287 lb/in.^{3}

NOTE: The mechanical properties of air-melted A-286, are 10 ksi lower in UTS and 0.2% YS

Mean coefficient of thermal expansion α = in./in./°F x 10^{-6}

RT-200°F = 9.2

RT-800°F = 9.6

RT-1200°F = 9.8

The elevated temperature strength - after exposure to the temperature cited for 1000 hours and no load - is as follows:

	Strength at				
	Room Temp.	800°F	900°F	1000°F	1200°F
F_{tu} (psi)	140,000	123,200	120,400	114,800	95,200
F_{ty} (psi)	95,000	79,800	79,000	76,950	62,700

Data from Battelle Memorial Institute Report DMIC 112, dated May 1, 1959 "Physical and Mechanical Properties of Nine Commercial Precipitation-Hardenable Stainless Steels," gives the typical 600 hour rupture strength for A-286 at 1000°F as 87,000 psi. However, since our application is one of cyclic loading, stress-rupture cannot be used directly. Data on cyclic rupture strength is not available for A-286, however it has been postulated that the cyclic rupture strength is intermediate between the rupture and short time tensile strength. On this basis the cyclic rupture strength of A-286 at 1000°F (room temperature to 1000°F) is assumed to be 102,000 psi.

(b) Alloy Ladish D-6A. The mechanical properties of a heat resistant non-corrosion alloy steel were examined at the design load requirements. The alloy selected was Ladish D-6A, a hot-work die steel which has been extensively used for missile motor cases because of its high strength and good fracture toughness. This steel has a nominal chemical composition of C=0.46%; Ni= 0.55%, chromium=1.00% molybdenum 1.00%, and iron remainder. It can be hardened and tempered at 1000°F to the following typical room temperature properties.

F_{tu} = 210,000 psi

0.2% yield strength (YS) = 204,000 psi

Elong % in 2 inches = 13

Charpy V-notch = 18.0 ft-lb

The steel when heat treated as above has the following typical properties (short time (1/2 hr)) at 1000°F.

F_{tu} = 138,800 psi

0.2% YS = 120,620 psi

Elong % in 2 inches = 19.8

However, exposure of the steel to tempering temperatures of 1250°F will reduce the room temperature strength to

F_{tu} = 133,000 psi (typ.)

0.2% YS = 126,250 psi

Elong % in 2 inches = 20

The mechanical properties of the steel tempered at 1250°F and tested at 1000°F are as follows:

F_{tu} = 56,000 psi

0.2% YS = 49,000 psi

It can thus be seen that the alloy steel when exposed to a temperature of 1250°F (approximately) will suffer a permanent degradation of mechanical properties. For this reason, a coating with low thermal conductivity is required to reduce the temperature below 1000°F when in use.

4. Material Properties Coatings

(a) Plastic Laminate and Rubber Coatings. Two different corrosion resistant organic materials, plastic laminates and rubber, were considered for use as low thermal conductivity materials. The temperature induced in the module structure due to exhaust gas heating is too low to permit ablative cooling from these materials. Phenolics, in general, vaporize at approximately 2000°F and above and silicones vaporize at temperatures in excess of 3000°F. Mechanical properties of plastic laminates vary considerably with materials of construction, resin system, and cure; however, we will breifly discuss the properties of a typical heat-resistant laminate - namely phenolic glass. The properties are taken from MIL-HDBK-17, "Plastics for Flight Vehicles." Data contained therein indicate that the tensile strength at 1000°F (by extrapolation) is less than 1000 psi. The handbook also states that several hours exposure at 1000°F will permanently destroy the laminates' mechanical and physical properties. Silicone rubbers suffer the same order of loss of physical properties at that temperature as does the phenolic glass. However, the low thermal conductivity of both materials (approximately 1.4 Btu/hr/sq ft/°F/in. at 700°F) makes it possible to use these materials for short time protection or for temporary repairing.

(b) Ceramic Coating. Another thermal barrier coating considered is ceramic in nature. The coating is stabilized zirconium oxide, whose high melting point (> 4000°F), low thermal conductivity (1.2 Btu/hr/sq ft/°F/in.), and low thermal expansion (5 x 10^{-6}/in./in./°F) make it potentially attractive. In addition, the material can be applied rather easily with an oxyacetylene type gun and is commerically available (Rokide Z, Norton Co., Worcester, Mass.). However,

because of its inherent brittleness, it can withstand little or no tensile loading, and because it is mechanically attached to the steel, i.e., imbedded in a roughened surface, its resistance to removal by mechanical abrasion is low.

It also could be considered as a temporary or repair coating to protect from "hot spots."

5. Cost

To review the cost factors again, it is estimated that a plastic laminate coated steel would give a part price the same as a heat and corrosion resistant steel, while a rubber coated or ceramic coated steel would be somewhat cheaper than a comparable part in A-286.

6. Alternate Heat and Corrosion Resistant Steels

(a) Due to the current "spotty" difficulty in procurement of nickel and molybdenum containing heat and corrosion resistant materials, the following materials are suggested as alternates to A-286 if necessary. Both materials have superior properties at room and elevated temperature to A-286.

(b) The first selection is Alloy 901 whose nominal composition is:

Nickel - 42%

Molybdenum - 5%

Titanium - 2.8%

Iron - balance

This alloy is covered by AMS specification 5660 for bar and rod. It is also available in sheet form. The alloy requires a precipitation heat treatment to attain its strength (as does A-286).

Its typical mechanical properties are (except as noted):

	* RT	1000°F	1200°F
UTS, ksi	150	124	114
0.2% YS ksi	100	83	83
Elong. % in 2 inches	12	12	13

* These properties are minimum.

The alloy cost is approximately $4 to $5 per pound depending on form and amount ordered.

(c) The second alternate material is the nickel base alloy Inconel X-750 (formerly Inconel X). This alloy is covered by Federal, AMS, and Republic RE-N-2A specifications.

AMS 5542, MIL-N-7786 - sheet and plate

AMS 5667, 5668, MIL-N-8550 - bar, rod, and forging

Its nominal chemical composition is:

Chromium - 15%
Iron - 7%
Titanium - 2.5%
Aluminum - 0.8%
Nickel - balance

Its typical mechanical properties are (except as noted):

	* RT	1000°F	1200°F
UTS ksi	165	143	125
0.2% YS ksi	105	97	95
Elong. % in 2 inches	15	13	5

* These properties are minimum.

Its approximate cost is $7 to $8 per pound depending on form and amount ordered.

7. Conclusion

It is concluded that the heat and corrosion resistant steels A-286, Alloy 901, or Inconel X-750 would be the best choice for construction since, unlike the heat resistant steel (D6A) they do not rely on plastic or ceramic coatings which either degrade on temperature exposure or are subject to undesirable brittleness.

The A-286 alloy being the cheapest and usually the most readily available alloy is the first choice among the heat and corrosion resistant alloys.

E. TURBOJET AND ADVANCED TURBOJET AIRCRAFT WITH AFTERBURNER

1. Design Load Requirements

The design load requirements are similar to those noted in paragraph D1 above. The material shall have an ultimate tensile strength (minimum) of 100,000 psi at 1250°F. The duration of load at 1250°F is one minute per cycle. The metal or module shall be capable of being cycled 10,000

times to 1250°F. Therefore, the total life at temperature shall be 600 hours. The metals shall be capable of being exposed to 1450°F maximum temperature without loss of subsequent 1250°F load strength requirements. The above is based on platform exposure temperatures for advanced turbojet engines with afterburner. The lower platform exposure temperatures of turbojet engines with afterburner, 50°F in both conditions, do not warrant separate consideration in the selection of materials.

2. Material Selection Approach

(a) Non-corrosion heat resistant alloy steels (Ladish D-6A) with supplementary low conductivity coatings cannot be used in this application for the same reasons as those noted in consideration of advanced turbojet engines.

(b) Heat and corrosion resistant alloy A-286 cannot be used in this application since, as noted previously, it will not meet the strength requirements at temperature, particularly if subjected to the overaging effect of 1450°F on extended exposure.

(c) The materials selected for use with turbojet and advanced turbojet engines with afterburner, in accordance with design requirements, are the two alternate materials specified in D6 above, Alloy 901 and Inconel X(X750).

(d) The typical short time elevated temperature properties of Alloy 901 are as follows:

	RT	1000°F	1200°F	1250°F
UTS, ksi	150	124	114	106
0.2% YS ksi	100	83	83	83
Elong % in 2 inches	12	12	13	13

(e) Alloys 901 and X-750 will not be affected by prolonged no-load exposure up to 1450°F. This will, in effect, lengthen their normal aging time for precipitation heat treatment which will not degrade tensile properties.

(f) From the data supplied by the International Nickel Company's bulletin (Nickel-Base Alloys, 1966) the 600 hour cyclic rupture life at 1250°F is 92 ksi in accordance with the postulate in D3 above.

(g) The guaranteed room temperature and 1200°F short time tensile properties for sheet (0.251 in.) are given in Republic Specification RE-N-2A as follows:

	RT	1200°F
UTS ksi	165	110
0.2% YS ksi	110	80
Elong % in 2 inches	15	*

* Not required but estimated at 5% minimum.

Data from the International Nickel Company indicate the following properties at 1250°F, using RE-N-2A material.

	1250°F
UTS ksi	100
0.2% YS ksi	70
Elong % in 2 inches	*

* Not required but estimated at 5% minimum.

The postulated 600 hour cyclic rupture life of Inconel X(X-750) at 1250°F is 86 ksi.

3. Conclusion

The short time properties at 1250°F of both materials are adequate although the properties of Inconel X are slightly higher. The rupture life of 901 at 1250°F is somewhat better than Inconel X. The ductility of Inconel X drops at 1200-1250°F which is typical of high nickel alloys and requires that applications involving sharp radii be given careful consideration. The higher nickel content of Inconel X makes it somewhat more prone to sulfur embrittlement from fuel exhaust than Alloy 901.

The possibility exists that the nozzle temperature (3500°F) of the afterburner may impose high skin temperatures (in excess of 2000°F) on the module. Temperatures of this magnitude will degrade the elevated temperature properties permanently. If overheating such as this is observed during prototype testing, consideration will be given to the use of ceramic low thermal conductivity barrier coatings (Rokide Z) as a means of reducing these transient temperatures to design levels.

(a) Consideration has also been given to the use of a higher strength nickel-base alloy in the event that the increased cost of the material is justified by the weight saving. An alloy considered is Inconel 718 whose approximate cost is $10/lb. The typical short time tensile properties are as follows:

	RT	600°F	1200°F	1300°F
UTS ksi	200	195	170	145
0.2% YS ksi	175	160	150	135
Elong % in 2 inches	20	20	20	20

SECTION VI

DESIGN CONCEPT ANALYSIS

A. INTRODUCTION

As previously outlined in Section II of this report, there are many variable factors and many combinations of these factors affecting design of platforms and modules. The design concept presented was based on the application of all factors affecting design. The methods of applying these factors have been established in the thermodynamic, design criteria, materials, and structural analysis considerations.

B. PLATFORM CHARACTERISTICS

The most important aspect of platform characteristics is the satisfaction of its requirements for field use. Ease of handling and erection are of prime importance and have been demonstrated in this design. (See Figures 8 through 15.)

All modules for a particular platform are exactly the same in configuration. This eliminates the task of selecting a certain module for a particular position. All ties between modules are alike and can be made up with a standard wrench (reference Figure 13). The side plates which prevent escape of exhaust gases (reference Figure 14) are simply inserted into the modules and locked into place by rotation of a latch. The end plates (for the same purpose) are installed by hooking on to the module tie fittings of the end modules and inserting two quick-disconnect type pins. The diverters at the exhaust end of the platform are tied to the modules with the same tie fittings as those used to tie the modules (reference Figure 8). The platform size may be varied by merely adding or subtracting quantities of the above components.

In the event that exhaust gas discharge from both ends of the platform is desired, several of the modules can be rotated 180° in the horizontal plane and the end plates replaced by diverters.

Of thermodynamic importance as a platform characteristic is the ability of exhaust gases to spread out laterally between modules and not be restricted to longitudinal flow. This serves to make maximum use of the exhaust area and therefore keeps the platform height to a minimum. The use of tubes as truss members provides maximum interflow area between modules.

C. MODULE CHARACTERISTICS

1. Structural Requirements

The structural requirements for the various components of the modules and substantiation of the selection of the type of components used in the design concept are presented in the structural analysis (Section VII).

2. Size and Weight

A module size smaller than that of the 2 by 4 ft (in planform) established by design criteria was considered unsatisfactory from the standpoint of height to width ratio and also with respect to the number of modules required to assemble a platform.

Inspection of the weight calculations for the modules analyzed in Section VII indicates that, except for the module base supporting the 50,000-lb aircraft (at 1000°F), the module base assemblies and grids are within the 150- to 260-lb weight range. All of these components are considered as being capable of manual field handling.

When the module base used to support the 50,000 pound aircraft at room temperature was inspected with respect to the thickness of its components, the following was noted. These members are of a size that, for two reasons, is considered to be the minimum allowable. First, lighter members in some cases would not be structurally adequate even for lighter-weight aircraft and, second, they would not be rugged enough to sustain the type of field handling anticipated. Therefore, it appears that modules for lighter-weight aircraft would not weigh less.

The above analysis indicates that most of the field-handled components will be in the weight range selected by the design criteria and that a one-piece module (base and grid) is not practical from a weight aspect.

However, in order not to limit the utility of the blast controlling platform because of weight considerations, another method of handling should be considered. This is the use of a lightweight, knockdown, two-wheeled, "A"-frame trundling dolly such as that shown in Figure 16. This could be delivered with the modules, rapidly assembled, and would allow for handling of the heavier components and of one-piece modules (base and grid combined) if so desired. This is presented as a logistic problem to be considered by the using command.

3. Configuration of Air Deflecting Vanes

The vanes shown in the design (reference Figure 12) were analyzed structurally with respect to exhaust gas pressures. The curved vane was chosen because it has greater beam strength. The proper angle and size of vane can only be determined by testing of full size components using various exhaust mass flow quantities.

4. Manufacturing

Ease of manufacturing with a minimum of special tooling and a minimum of shop operations was considered next to structural integrity in design evaluation. Examination of the various members of the module shows that shop manufacturing procedures are not complicated. The drawings indicate formed sections to demonstrate the feasibility of their use. However, in large production quantities

where mill runs of material are required, the cost of extruded shapes cut to length versus the cost of cutting and forming of sheet and plate should be analyzed. Forgings should be used in place of machined bar stock for fittings and tension bars when cost savings can be realized (reference Figures 11 and 12).

In the determination of grid design, manufacturers of this type of equipment are best equipped to satisfy the requirements. They also have the necessary tooling and manufacturing capabilities which are generally not a part of other manufacturing facilities (reference Figure 10).

5. Materials

Section V of this report presents the method to be used in material selection for the various conditions of temperature and loading and shows the use of balancing costs against other factors. It should be further noted that the use of commercial specifications for materials should be evaluated as a cost saving factor. This should only be done where these commercial materials satisfy all design requirements and when their use is approved by the procuring agency.

In the selection of hardware (fasteners, etc.) the various conditions of loading and temperature must be considered so that it is compatible with the other materials used.

D. SUMMARY

The above analysis has been presented in order to coordinate sections of the report and to present an evaluation of the various aspects of the design concept in relation to design and manufacturing requirements.

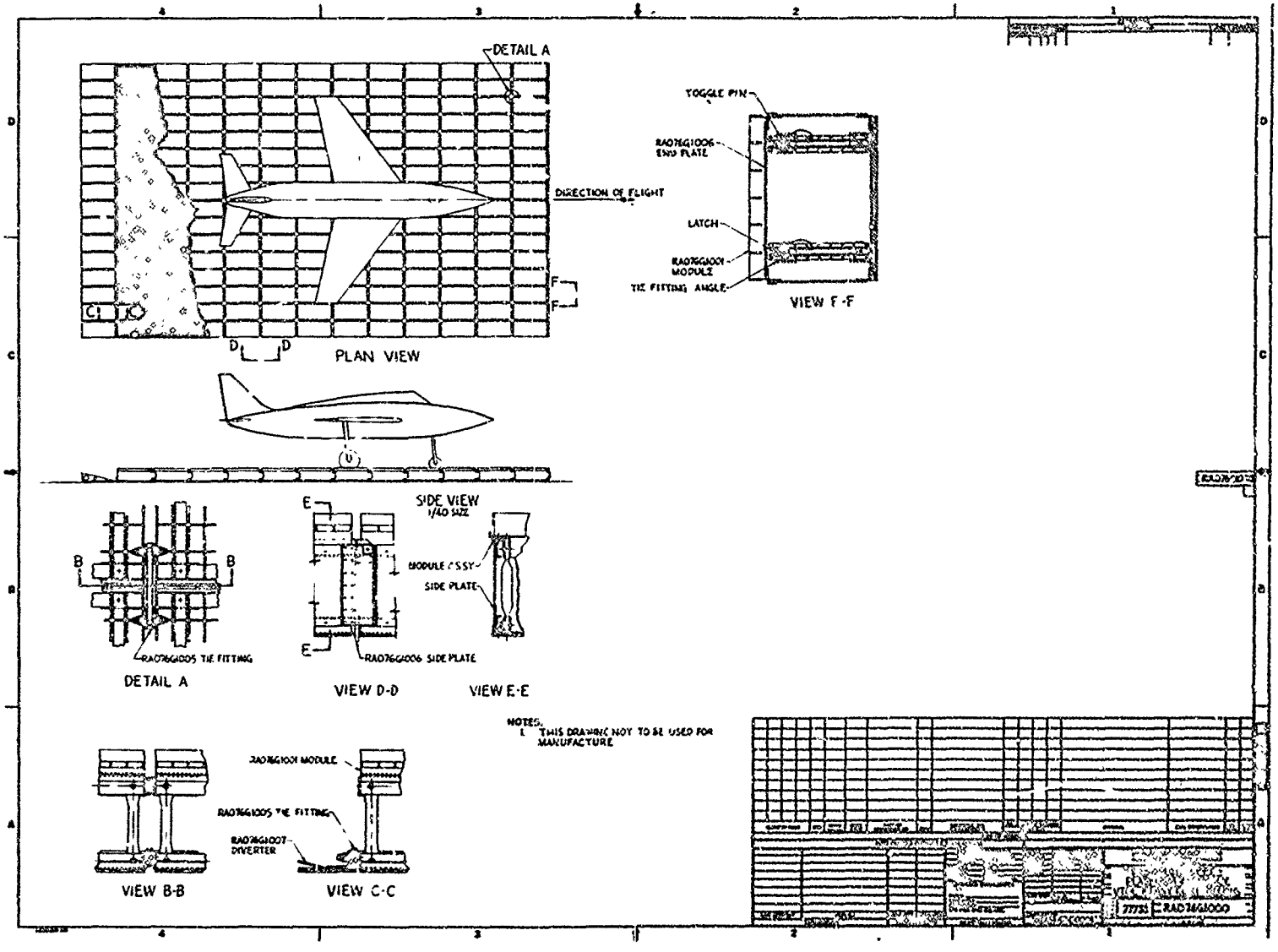

Figure 8. Design concept, platform assembly

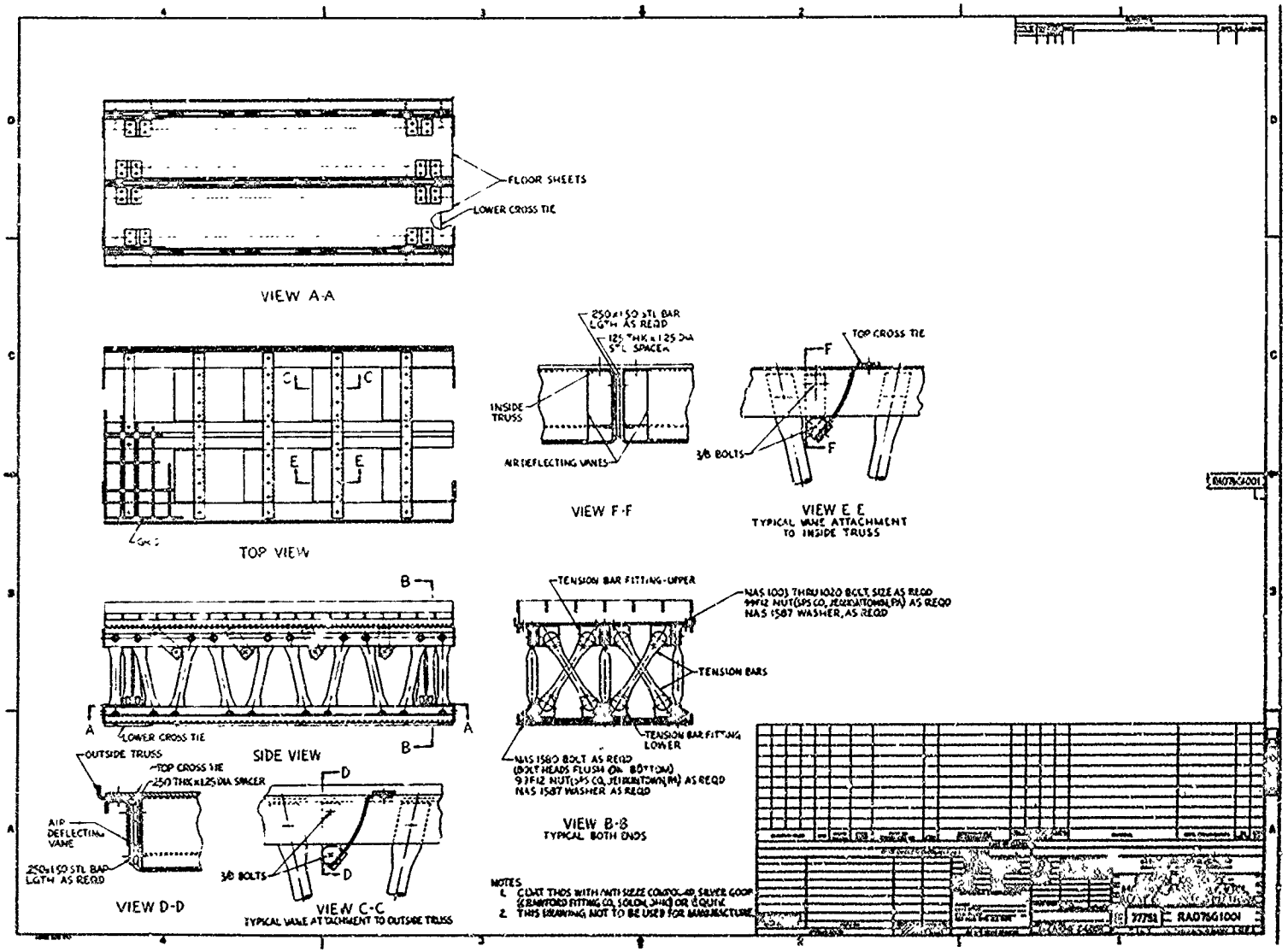

Figure 9. Design concept, module assembly

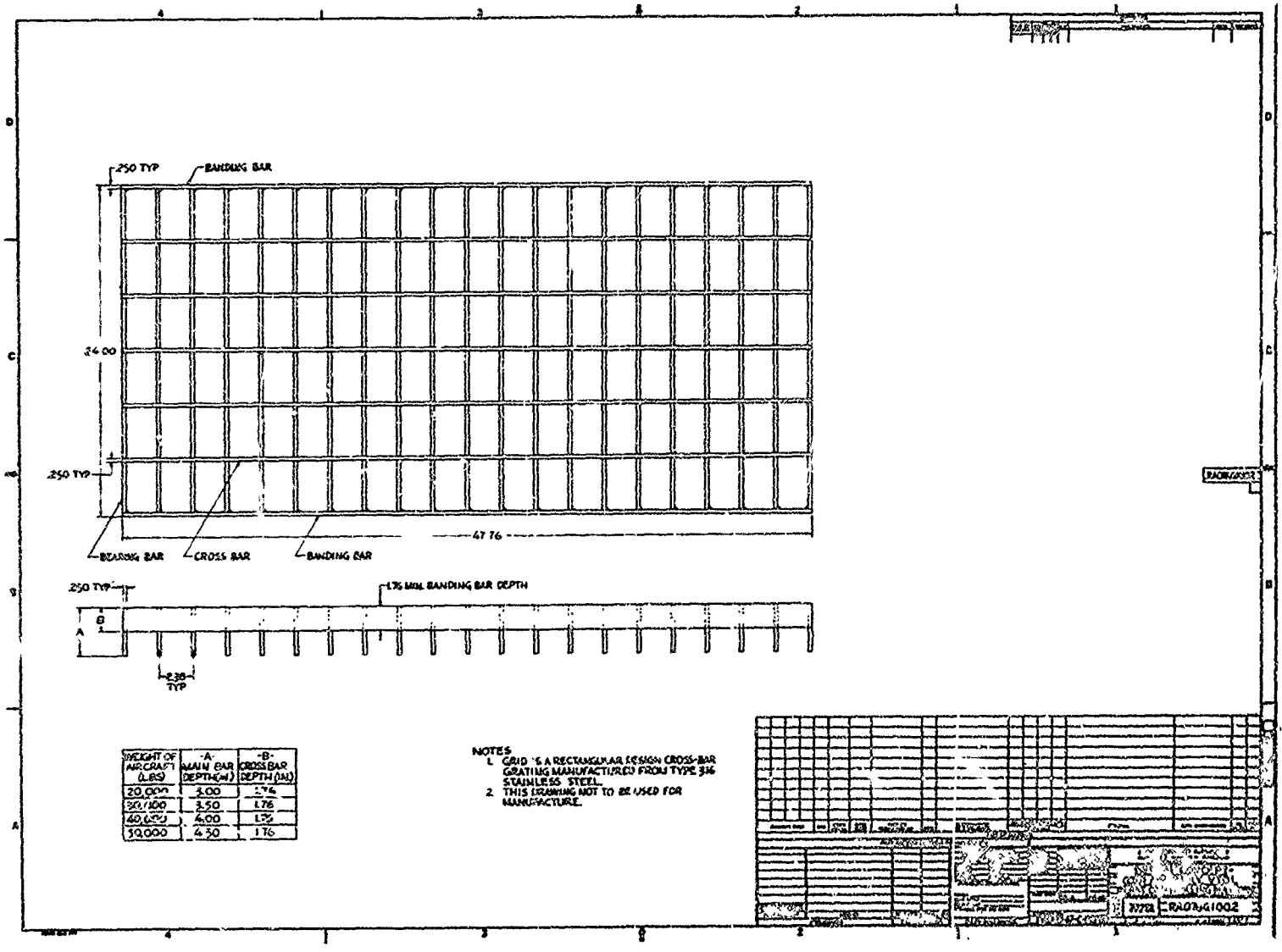

Figure 10. Design concept, grid assembly

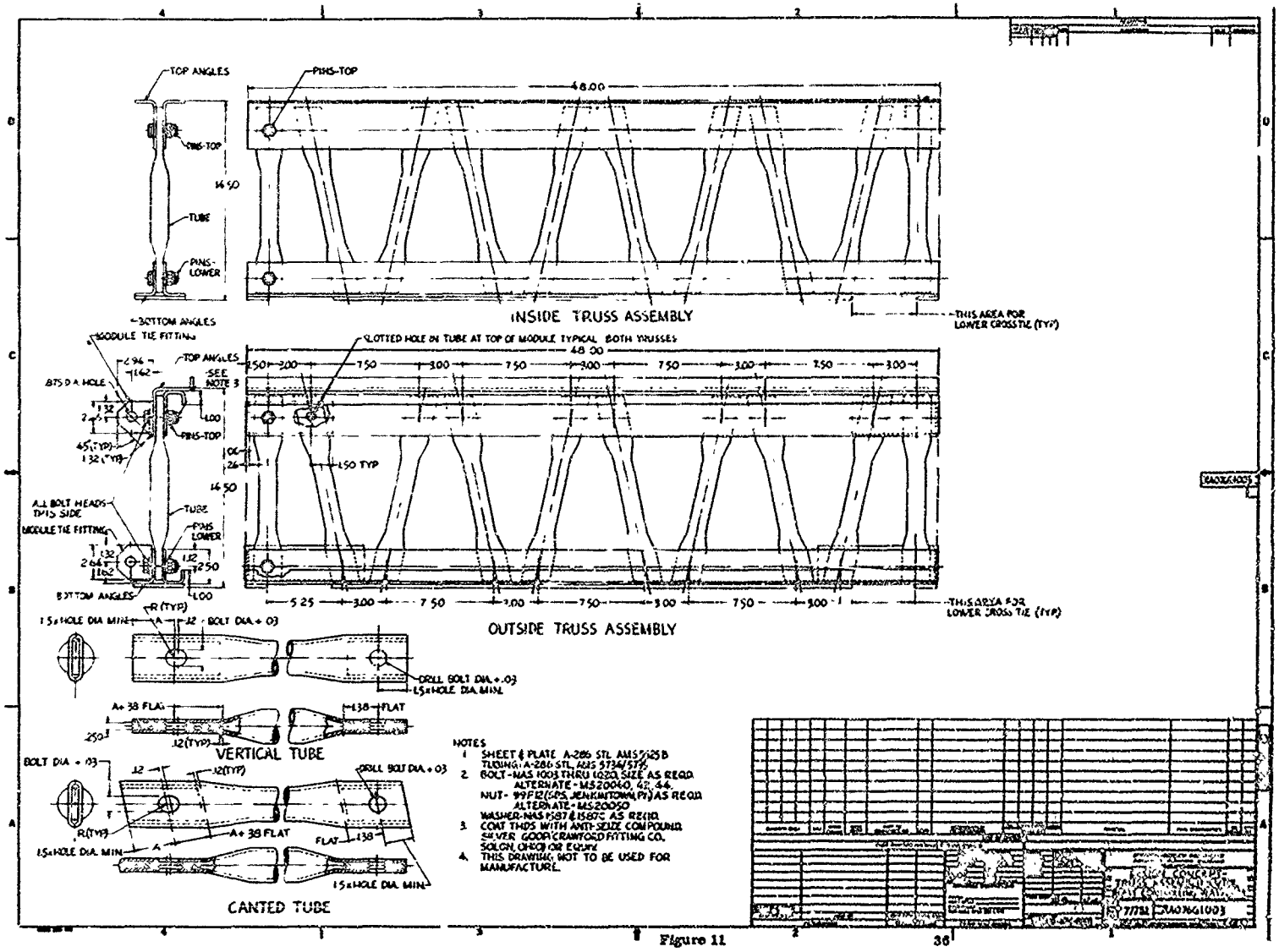

Figure 11

Figure 11. Design concept, truss assemblies

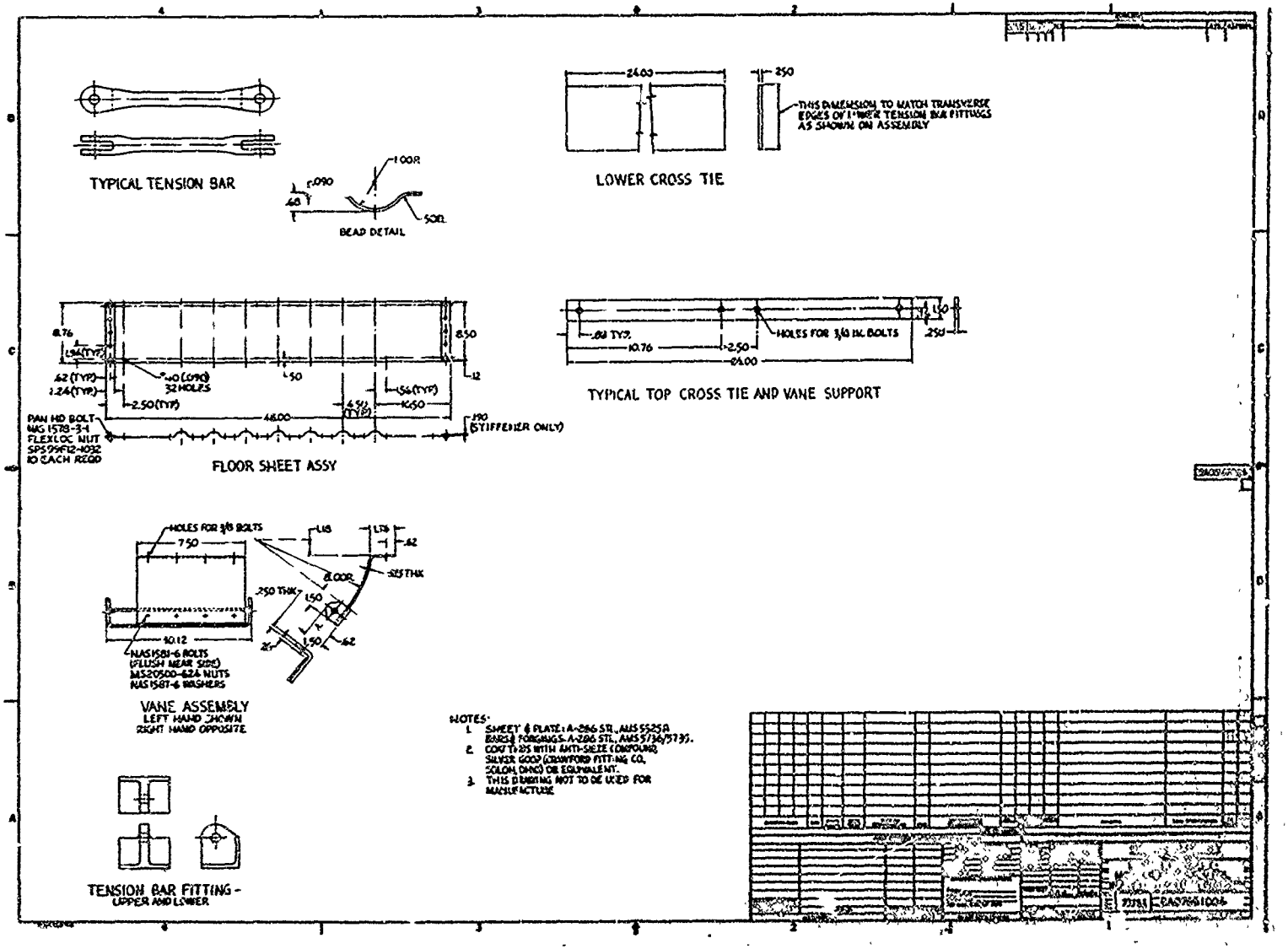

Figure 12. Design concept, module details

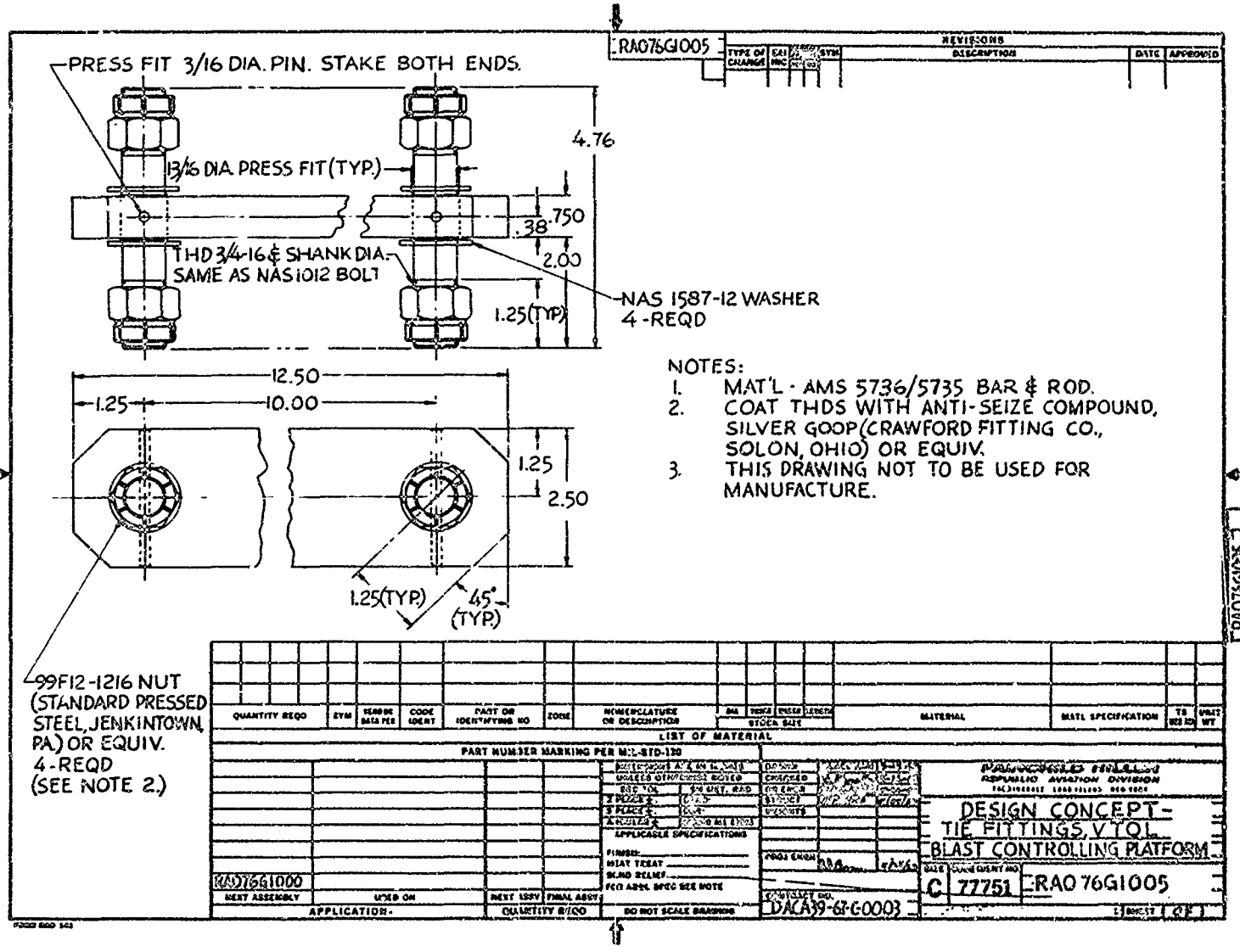

Figure 13. Design concept, tie fittings

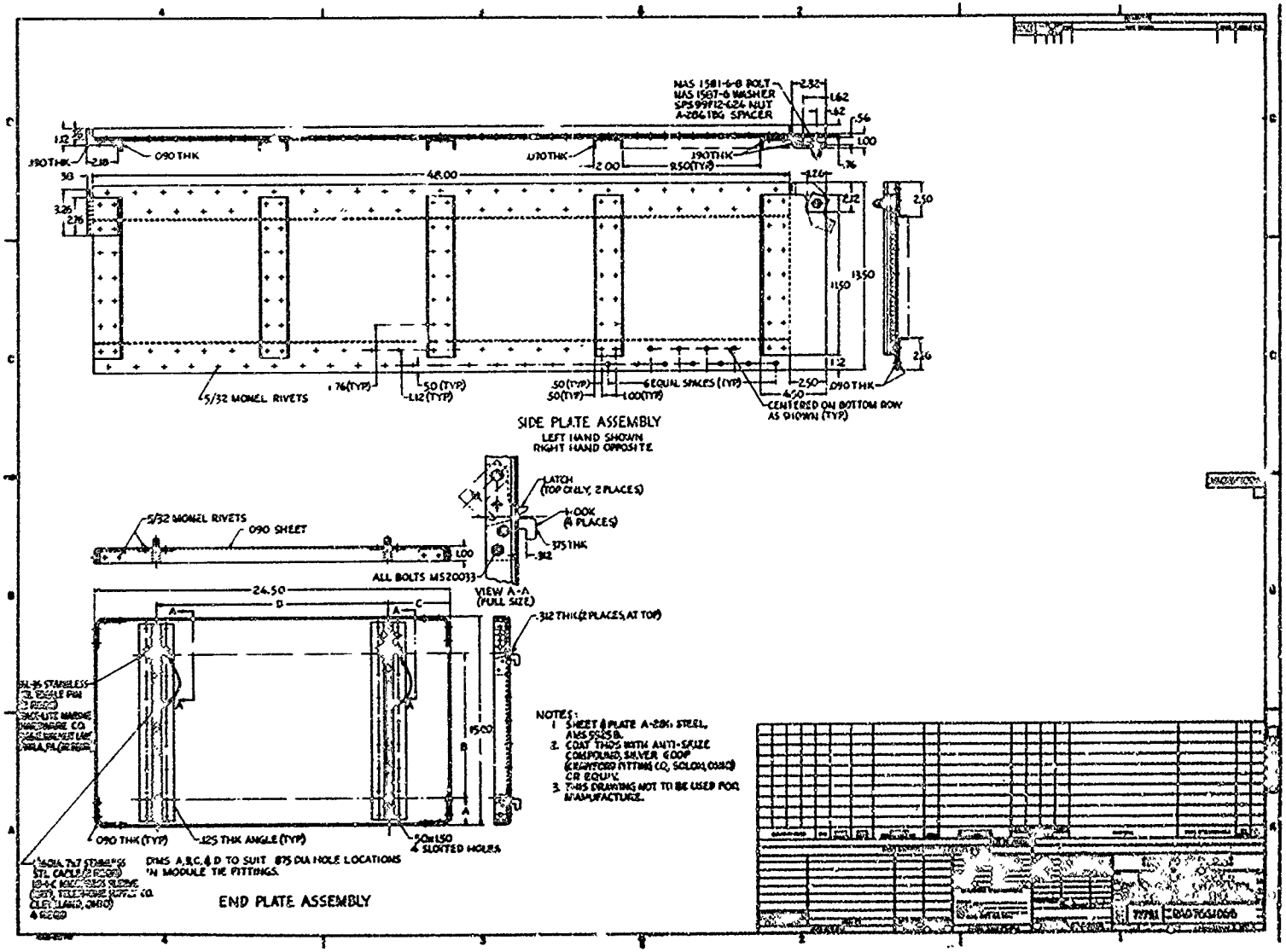

Figure 14. Design concept, end plate and side plate

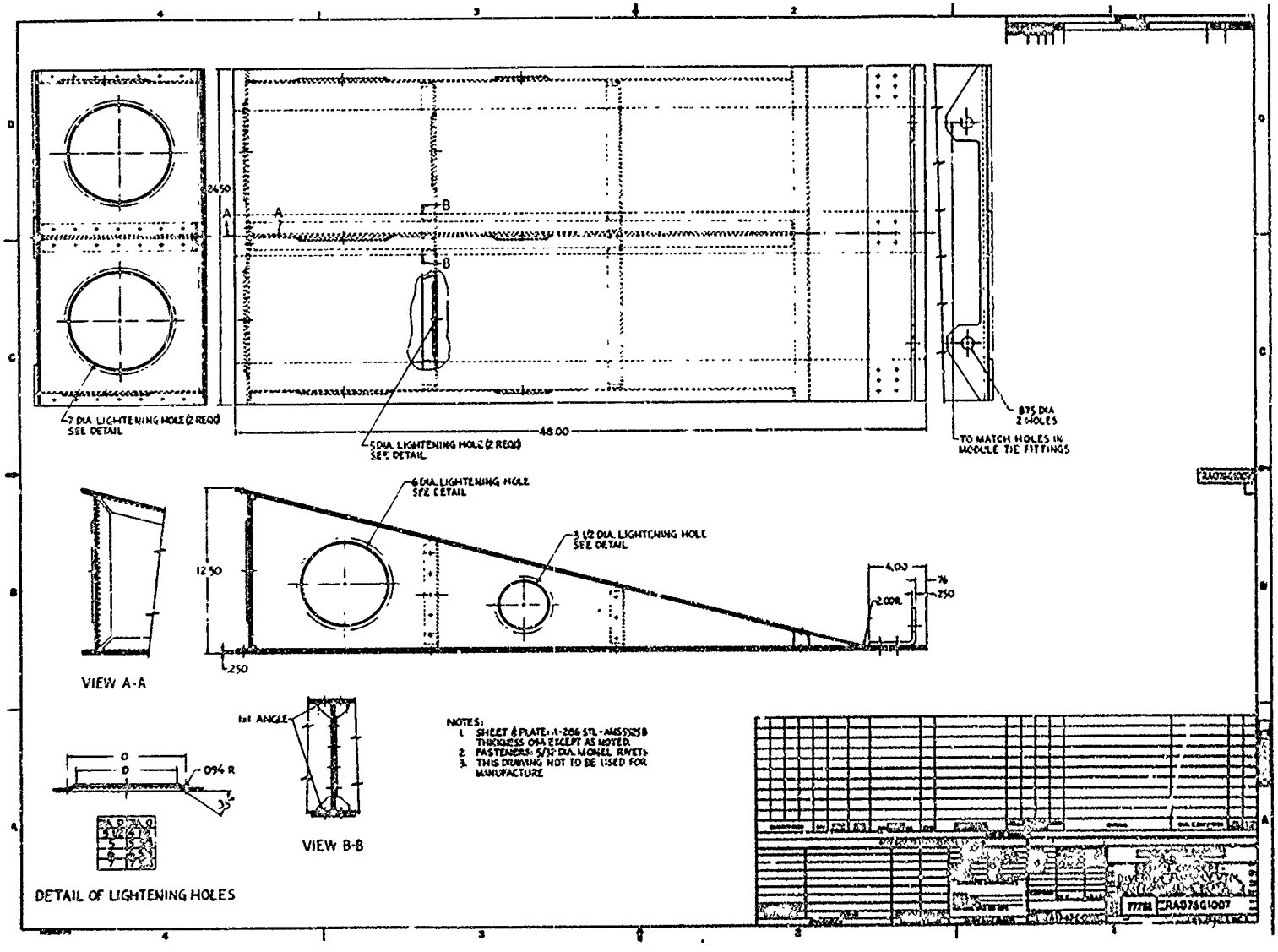

Figure 15. Design concept, diverter assembly

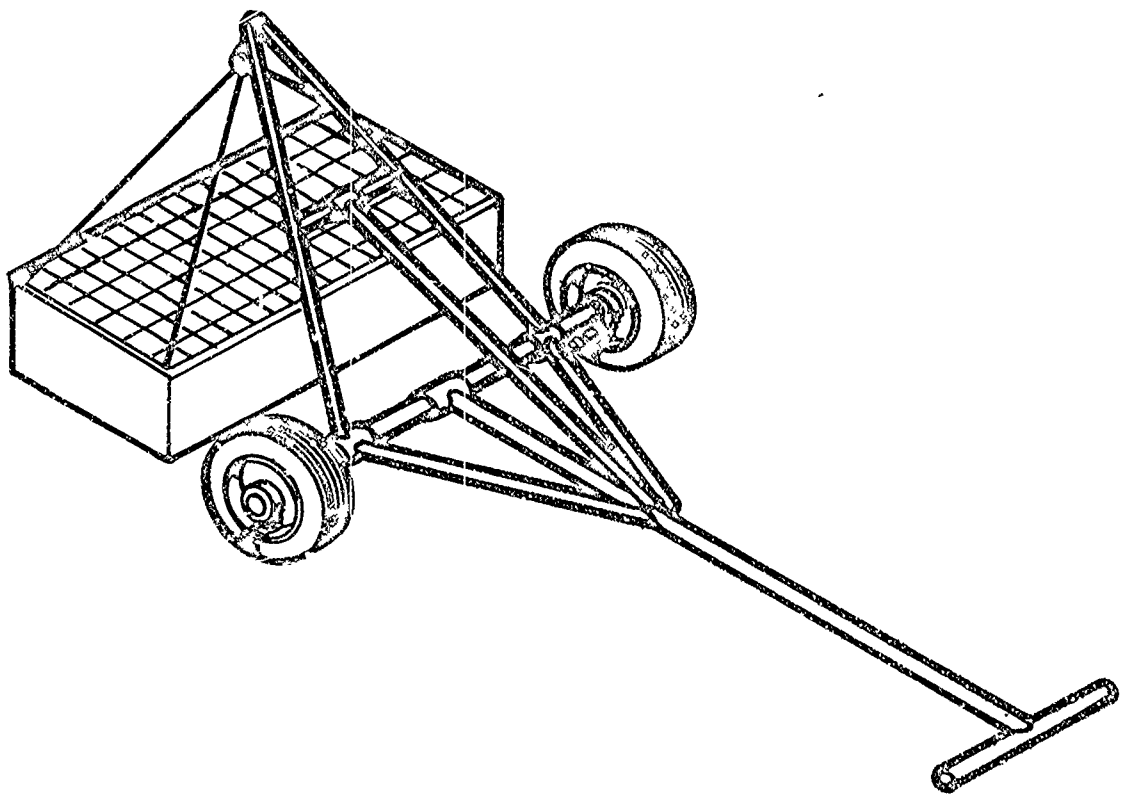

Figure 16. "A"-Frame Trundling Dolly

SECTION VII

STRUCTURAL ANALYSIS

A. INTRODUCTION

In the design of a blast controlling platform for VTOL aircraft, the structures department was given the task of aiding the design group in determining the basic type of construction and configuration that would best meet the requirements of load, temperature, and portability (meaning lightness of weight). In order to evaluate this problem, two separate studies were undertaken. In the first study a general survey of various types of construction was made. In the second study, the type of structure finally decided upon in the general survey is analyzed, in detail, for the various loading conditions.

B. GENERAL SURVEY

The basic purpose of this survey was to consider various types and configurations of structure and determine which would best meet the requirements of load, temperature, and portability.

Since the platform is to be portable, the weight factor is critical. In order to insure the ease of portability, it was decided to make the platform of a number of small individual modules, each light enough to be easily moved.

Each module in the platform will be under different loading conditions. The two most critical modules will be one directly under the tire and one directly under the exhaust nozzle of the lift engines. The module under the tire will be subject to load while the module under the exhaust nozzle will be subject to the extremely high temperature of the exhaust gases. Since it is impossible to determine exactly which module will be under tire loads and which modules will be under high temperature a module must be designed to satisfy both requirements.

One of the intentions of the platform is to direct the exhaust gases out of one end of the platform. This is best accomplished by using curved vanes in the individual modules to divert the gases in the direction required. A floor sheet should be used to eliminate the entrainment of dirt, sand, etc.

The upper surface of the module must allow the exhaust gases to enter the module. It must also provide a surface on which the aircraft can land and maintenance personnel can walk. For this surface a grid type of structure best satisfies the requirements.

A truss type of structure is the best method of supporting the grid due to its high strength-to-weight ratio. The type of truss recommended is shown in Figure 11. The reasons for choosing the various members as shown are as follows:

1) Top Angles - The top angles were selected because they must resist bending and the long vertical flanges provide a large moment of inertia to resist the bending stress. The short horizontal flanges provide a surface for the bearing bars of the grid to rest on. The angles are separated to permit the tubing to fit between the long flanges. This also puts the attachments in double shear which is necessary for heavy aircraft. The horizontal flanges on the top angles of the outside truss members of a module are both faced in the same direction, thereby maximizing the area allowing exhaust gases to enter the module. The extra vertical flange on these angles acts as a guide for the grid.

2) Bottom Angles and Plate - The bottom angles were selected because they must resist bending and the vertical flanges provide a large moment of inertia which resists the bending. The horizontal flanges and the plate provide a large, stiff area for bearing on the soil. The angles are separated to permit the tubing to fit between the vertical flanges. This also puts the attachments in double shear.

3) Pins - The use of pins (single-pin joint) in a truss member limits the type of load carried by the vertical members to axial loads. This will limit the type of failure to buckling or column failure.

4) Tubes - Tubes were recommended because these members are subjected to axial loads only (pinned at both ends) and a circular section is most efficient for this type of loading. Hollow tubing was recommended to save weight. Slotted holes in the tubes (top only) eliminate any thermal stresses induced by differential expansion of various members.

The best method of stabilizing the truss members is to use two sets of tension bars at both ends of each module. At intermediate points crossties attaching the tops of the trusses will also aid in stabilizing the module.

Summarizing, it appears that the type of structure that best meets the requirements of load, temperature, and portability is a grid type structure supported by pinned member trusses with tension bars and crossties supplying lateral stability (Ref. Figure 9).

C. DETAILED ANALYSIS

In the detailed analysis the basic type of structure decided upon in the general survey was analyzed for 20,000-, 30,000-, 40,000-, and 50,000-lb aircraft at 1000°F and for 50,000-lb aircraft at room temperature in order to determine how the weight of the typical module varies with the weight of the aircraft it is to support. A type of parametric study was performed. The only variable in this study, however, was the size of the individual members. The

configuration and the overall size of the module remained identical. It is worthy to note, however, that the typical module analysed is the best configuration for the 50,000-lb aircraft at 1000°F under load but, it might not be the best configuration for a 20,000-lb aircraft at 1000°F. For example, fewer vertical supports might be required in the truss members for the 20,000-lb aircraft.

For each of the analyses, the following information was supplied by the thermodynamics group, the design requirements group, and the materials group.

1) Use of A-286 steel

2) Load factor of 2.5g (1.25g for drift landing side load only)

3) Maximum temperature of module under load is 1000°F (1200°F under no load conditions)

4) Tire print of 160 $in.^2$

5) Noise level pressure of 0.16 psi (155 db)

6) Pressure due to exhaust gases of 18 psi

7) The given loads are applied to a 1.5 factor of safety (in order to keep the weight at a minimum). This 1.5 factor of safety is multiplied by the given loads and, using these values, the structure is designed to ultimate load allowables as obtained from MIL-HDBK 5-A.

8) The entire weight of the airplane is on two landing gear.

Using the above information and a 50,000-lb aircraft, a preliminary analysis was conducted to provide the tentative size of an individual module. The ideal weight of each module was estimated to be about 200 to 250-lb. The most efficient size in this weight range was found to be 4 ft by 2 ft with three truss members.

For design purposes, various assumptions were made which led to a conservative type of structure. These assumptions are:

1) The entire wheel load is completely reacted by one truss member of one module.

2) The entire wheel load is reacted by one span of the top angles rather than by the entire length of the angle.

At the same time, an assumption was made that was not conservative. This assumption was that the ground under the module was relatively flat and that,

when subjected to load, the ground would settle under the bottom plate of the truss until there was a uniform pressure exerted on the surface of the plate. This assumption limits the surface conditions of the soil directly under the individual modules.

For the design of a grid, manufacturers of this type of equiment were called on. Design information obtained was as follows:

> Based on sustaining aircraft tire loads of 25 kips, 37 kips, 50 kips, and 62 kips, on a tire print area of 9" x 18", with the grating bearing bars spanning 10" center to center of supports, a rectangular design cross-bar grating having bearing bars spaced 2-3/8" on centers with cross bars 4" on centers was recommended. For intermittent elevated temperature service of 1000°F the material was to be type 316 stainless steel.
>
> The recommended bearing bar sizes in corresponding order to the above indicated tire loads, are 3" x 1/4", 3-1/2" x 1/4", 4" x 1/4", and 4-1/2 x 1/4". The cross bar size in all cases will be 1-3/4" x 1/4". A banding bar shall be welded to the ends of the bearing bars, continuous for the panel width, and shall have a depth not less than 1-3/4".

The top and bottom angles of the truss members were checked for tension, compression or crippling, shear, and bearing. For the module to support 20,000-, 30,000-, and 40,000-lb aircraft, the thickness used was 0.125 inch. For the module to support a 50,000-lb aircraft, the thickness used was 0.19 inch (the additional thickness was needed for bearing area). In most cases the length of the vertical (long) flange was governed by edge distance requirements of pins attaching the angles of the tubes.

The tubes were checked for bearing and column failure. For the module supporting 20,000-, 30,000-, and 40,000-lb aircraft the thickness was 0.125 inch. For the module supporting a 50,000 pound aircraft, the thickness was 0.19 inch (again the additional thickness was needed for bearing area). In order to increase the load carrying ability of the tubes, the inside diameter and outside diameter were varied to decrease L'/ρ and increase $F_{c_{all}}$.

The pins attaching the bottom angles to the tubes were checked for double shear. The pins attaching the top angles to the tubes were checked for a combined loading condition (bending and shear) due to the effect of the slotted holes in the tubes.

The tension bars were checked for tension and compression, and the lugs were checked for bearing and shear-out. The tension bars are the same for all modules. The tension bar fittings were checked for bearing and shear out (lug analysis).

The vanes and floor sheet were checked for failure as simple beams under a uniform pressure. The deflection of the floor sheet was checked to determine if, under load, it would come in contact with the ground. The vanes and floor

sheet will be the same for all modules.

Since there are two different loading conditions (wheel load and exhaust gas pressure), various parts of the module will be subject to different loads. There is also a load caused by the engine noise level. This load is calculated as 0.16 psi and was considered negligible in this analysis. Therefore, the total design loads on the structure were (1) wheel load (weight of aircraft) for the top and bottom angles, pins, and tubes, (2) exhaust gas pressure load for the vanes and floor sheet at 1200°F.

An analysis was also performed on the typical module for support of a 50,000-lb aircraft at room temperature using a common grade of steel such as 4130, HT 180-220. This module was analyzed in an identical manner except that different allowables were used. This analysis showed that the high temperatures caused the weight of the module to increase by 40 percent.

D. ANALYSIS OF LOADS AT 1000°F, USING A-286 STEEL - 20,000-lb AIRCRAFT

1. Design Specifications

1) 20,000-lb aircraft at 2-1/2g (limit value)

2) All load on two gears

3) Maximum temperature under wheel = 1000°F

4) Maximum temperature under engine (no load) = 1200°F

5) Load/Gear = $\frac{20,000\ (2.5)}{2}$ = 25,000-lb (limit)

= 25,000 (1.5) = 37,500-lb (ultimate)

6) Use tire print of 160 in.^{2}

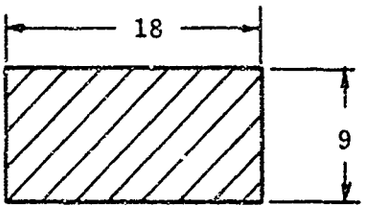

Tire Print

Note: Dimensions on sketches are in inches unless otherwise noted.

2. Top Angles of Outside Trusses (Reference Figure 11)

Assume entire load acting on one truss

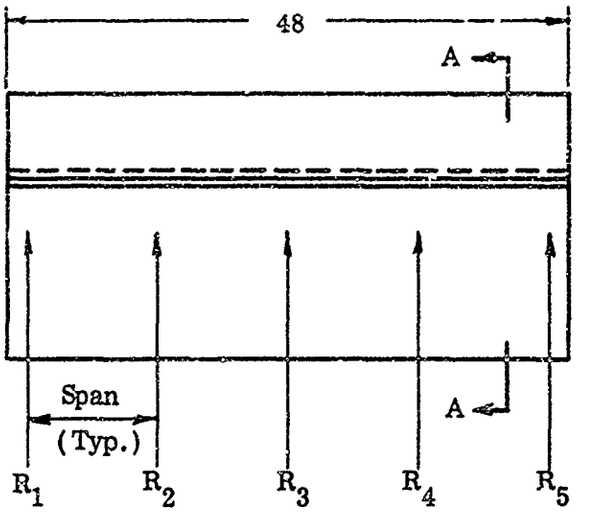

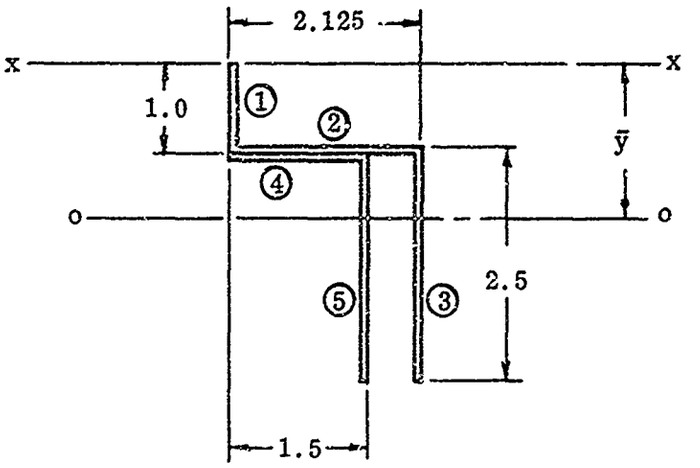

Section AA

Maximum reaction = 37,500 lb (entire load)

For maximum bending moment assume entire load acting on one span

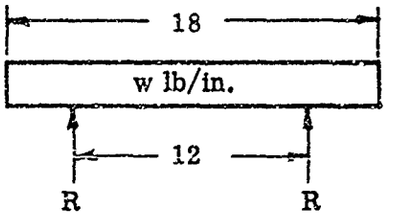

$$w = \frac{37,500}{18} = 2080 \text{ lb/in.}$$

$$M_{max} = 6\left(\frac{37,500}{2}\right) - 9(2080)(9/2) \text{ at center}$$

$$= 112,500 - 84,400 = 28,100 \text{ in. lb}$$

$$= 28.1 \text{ in. kips}$$

$$F_b = \frac{Mc}{I} \qquad \text{use } t = 0.125$$

Section	b	h	A	y	A_y	A_y^2	I
1	0.125	1.00	0.125	0.50	0.0625	0.0313	0.0104
2	1.875	0.125	0.234	0.94	0.2200	0.2068	0.0003
3	0.125	2.50	0.313	2.125	0.6641	1.4112	0.1628
4	1.375	0.125	0.1719	1.06	0.1822	0.1931	0.0002
5	0.125	2.375	0.2969	2.19	0.6502	1.4239	0.1395
$\sum$			1.1408		1.7790	3.2663	.3132

$$\bar{y} = \frac{\sum Ay}{\sum A} = \frac{1.7790}{1.1408} = 1.559 \text{ in.}$$

$$I = \sum I + \sum Ay^2 - \bar{y}^2 \sum A = 0.804 \text{ in.}^4$$

$$F_b = \frac{Mc}{I} = \frac{(28.1)(1.81)}{0.804} = 63.3 \text{ ksi tension}$$

$$F_b = \frac{M\bar{y}}{I} = \frac{(28.1)(1.56)}{0.804} = 54.5 \text{ ksi compression}$$

At 1000°F $F_{tu} = 103.5$ ksi (Fict.)

$F_{cy} = 72$ ksi

$F_{bru} = 198$ ksi

$F_{su} = 68$ ksi

$$\text{M.S.} = \frac{103.5}{63.3} - 1 = 0.64 \text{ tension}$$

$$\text{M.S.} = \frac{72.0}{54.5} - 1 = 0.32 \text{ compression}$$

Bearing (of Truss Tube Pins on Angles)

$A_{br} = Dt = (0.625)(0.125) = 0.0781 \text{ in.}^2$ (for one angle and one pin)

$$P = \frac{38,500}{4} = 9600 \text{ lb (for one angle and one pin)}$$

$$F_{br} = \frac{P}{A} = \frac{9600}{0.0781} = 123 \text{ ksi} \qquad F_{bru} = 198 \text{ ksi}$$

$$M.S. = \frac{198}{123} - 1 = 0.63$$

Shear

Maximum shear across angles = $\frac{R_{max}}{2} = \frac{37,500}{2} = 18,750$ lb

A_s = area of section - 2Dt = 1.141 - 2(0.125)(0.625)

A_s = 1.141 - 0.156 = 0.985 in.^{2}

$$F_s = \frac{P}{A_s} = \frac{18,750}{0.985} = 19 \text{ ksi}$$

F_{su} = 68 ksi

M.S. = ample

3. Top Angles on Inside Truss (Reference Figure 11)

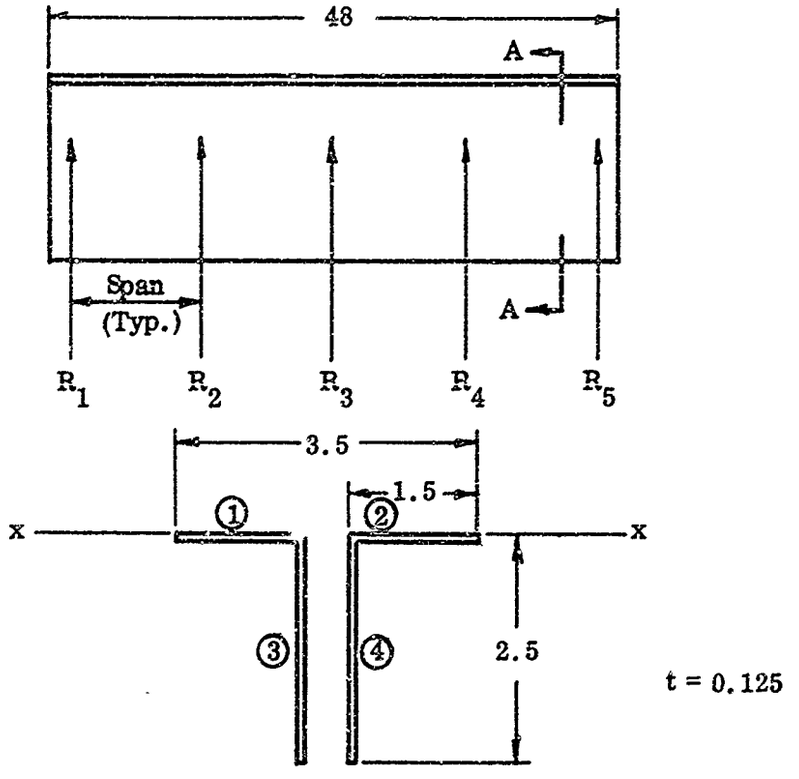

Section AA

Maximum reaction = 37,500 lb (entire load)

For maximum bending moment assume entire load acting on one span:

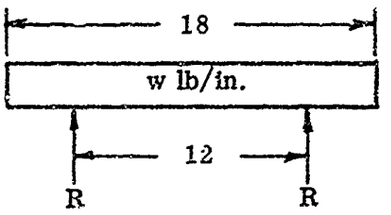

$$w = \frac{37,500}{18} = 2080 \text{ lb/in.}$$

$$M_{max} = 6\left(\frac{37,500}{2}\right) - 9\,(2080)\,(9/2)$$

$$= 112,500 - 84,400 = 28,100 \text{ in. lb}$$

$$= 28.1 \text{ in kips}$$

$$F_b = \frac{Mc}{I} \qquad \text{use } t = 0.125$$

Section	b	h	A	y	A_y	A_y^2	I
1	1.375	0.125	0.1719	0.0625	0.0107	0.00069	0.00022
2	1.375	0.125	0.1719	0.0625	0.0107	0.00069	0.00022
3	0.125	2.50	0.3125	1.250	0.3906	0.48825	0.16276
4	0.125	2.50	0.3125	1.250	0.3906	0.48825	0.16276
$\sum$			0.9688		0.8026	0.97788	0.32596

$$\bar{y} = \frac{\sum Ay}{\sum A} = \frac{0.8026}{0.9688} = 0.82844 \text{ in.}$$

$$I = \sum I + \sum Ay^2 - \bar{y}^2 \sum A = 0.63914 \text{ in.}^4$$

$$I = 0.639 \text{ in.}^4$$

$$F_b = \frac{Mc}{I} = \frac{(28.1)(1.67)}{0.639} = 73.5 \text{ ksi tension}$$

$$F_{tu} = 103.5 \text{ ksi}$$

$$M.S. = \frac{103.5}{73.5} - 1 = 0.41$$

$$F_b = \frac{My}{I} = \frac{(28.1)(.83)}{0.639} = 36.5 \text{ ksi compression}$$

$F_{cy} = 72$ ksi

$$M.S. = \frac{72}{36.5} - 1 = 0.97$$

Bearing (of Truss Tube Pins on Angles)

$A_{br} = Dt = (0.625)(0.125) = 0.0781 \text{ in.}^2$ (for one angle and one pin)

$P = \frac{38,500}{4} = 9600$ lb (for one angle and one pin)

$F_{br} = \frac{P}{A_{br}} = \frac{3600}{0.0781} = 123$ ksi

$F_{bru} = 198$ ksi

$$M.S. = \frac{198}{123} - 1 = 0.63$$

Maximum Shear - Across Angles

Maximum shear $= \frac{R_{max}}{2} = \frac{37,500}{2} = 18,750$-lb

A_s = area of section - 2 Dt = 0.9688 - 0.156
= 0.813 in.^2

$F_s = \frac{P}{A_s} = \frac{18,750}{0.813} = 23.1$ ksi

$F_{su} = 68$ ksi

M.S. = ample

4. Pins (Attaching Truss Tubes to Top Angles) (Reference Figure 11)

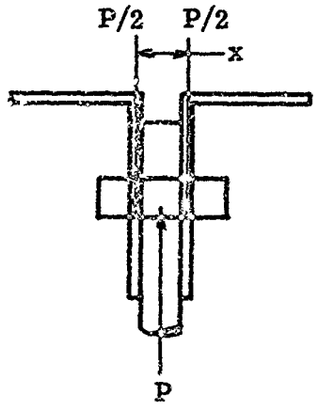

Slotted holes in tubes
(Top only)

Due to the slotted holes in the truss tubes a bending moment (M) is induced in the pin

$$M = \left(\frac{P}{2}\right)\left(\frac{x}{2}\right)$$

$$P = \frac{37,500}{2 \cos 12.5^\circ} = 19.2 \text{ kips}$$

$$x = 1/2 + 2(0.125/2) = 0.625 \text{ in.}$$

$$M = \left(\frac{19.2}{2}\right)\left(\frac{0.625}{2}\right) = 2.98 \text{ in. kips}$$

For 5/8-in. Diameter Pin

$I = 0.0075 \text{ in.}^4$ $c = 0.3125$ in. $A = 0.307 \text{ in.}^2$

$$F_b = \frac{Mc}{I} = \frac{(2.98)(0.3125)}{0.0075} = 124 \text{ ksi}$$

$F_{b_{all}} = 175$ ksi (Reference 3, page 211)

$$R_b = \frac{F_b}{F_{b_{all}}} = \frac{124}{175} = 0.71$$

Double Shear

$$F_s = \frac{P/2}{A} = \frac{19.2/2}{0.307} = 31.3 \text{ ksi}$$

$F_{su} = 68$ ksi

$$R_s = \frac{F_s}{F_{su}} = \frac{31.3}{68} = 0.46$$

$$M.S. = \frac{1}{\sqrt{(.71)^2 + (.46)^2}} - 1 = 0.09$$

Use 5/8-in. diameter pin

5. Tubing (Reference Figure 11)

Assume entire load is reacted at one joint

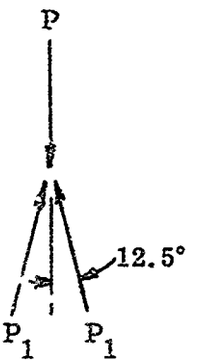

Each pin carries
1/2 the load

$$P_1 = \frac{P}{2 \cos 12.5} = 19.2 \text{ lb}$$

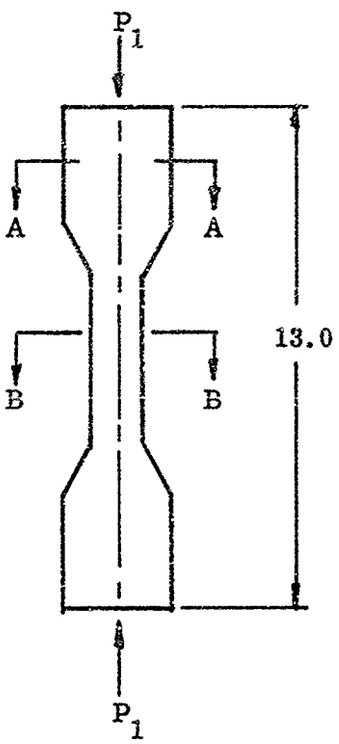

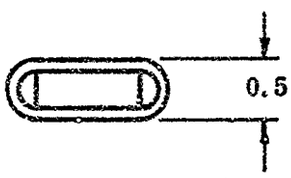

Section AA

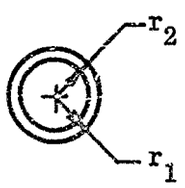

Section BB

For 1.25 in. O.D. x 0.125 in. tube

Bearing

$A_{br} = 2Dt = 2(0.438)\ (0.125) = 0.110 \text{ in.}^2$

P = 19.2 kips

$$F_{br} = \frac{P}{A_{br}} = \frac{19.2}{0.110} = 175 \text{ ksi}$$

$F_{bru} = 198$ ksi

$$M.S. = \frac{198}{175} - 1 = 0.13$$

Column Action

$$I = \frac{1}{4}\pi (r_1^4 - r_2^4) = 0.1198 - 0.0491 = 0.071 \text{ in.}^4$$

Tube is pinned at both ends, therefore c = 1 and L′ = L

$$\rho = \sqrt{\frac{I}{A}}$$

$$A = \pi (r_1^2 - r_2^2) = 0.443 \text{ in.}^2$$

$$\rho = \sqrt{\frac{0.071}{0.443}} = 0.4 \text{ in.}$$

$$\frac{L'}{\rho} = \frac{13}{0.4} = 32.5$$

$F_{c_{all}} = 80$ ksi (Reference 1, page 1.1630-4)

$$F_c = \frac{P}{A} = \frac{19.2}{0.443} = 43.3 \text{ ksi}$$

$$M.S. = \frac{80}{43.3} - 1 = 0.85$$

Use 1.25 in. O.D. x 0.125 in. tube

6. Pins (Attaching Truss Tubes to Lower Angles) (Reference Figure 11

Shear is only factor (no slotted holes)
Double shear = 19.2 kips
Single shear = 9.6 kips

Use 7/16-in. Pin

Area = 0.150

$$F_s = \frac{9.6}{0.150} = 64 \text{ ksi}$$

$F_{su} = 68$ ksi

$$M.S. = \frac{68}{64} - 1 = 0.06$$

7. Bottom Angles on Trusses (Reference Figure 11)

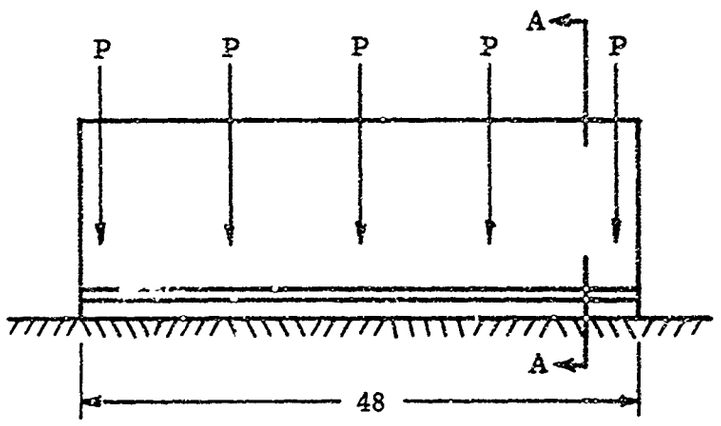

t= 0.125 (angles)

t= 0.250 (plate)

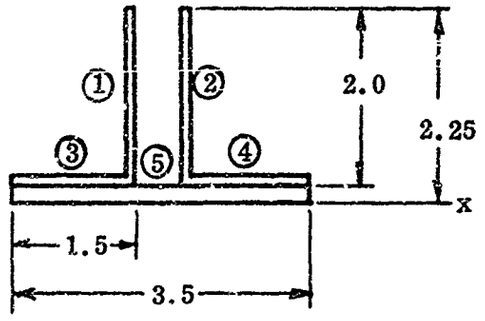

Section AA

Section	b	h	A	y	A_y	A_y^2	I
1	0.125	2.00	0.250	1.25	0.3125	0.3910	0.0833
2	0.125	2.00	0.250	1.25	0.3125	0.3910	0.0833
3	1.375	0.125	0.172	0.31	0.0533	0.0165	0.0002
4	1.375	0.125	0.172	0.31	0.0533	0.0165	0.0002
5	3.5	0.25	0.875	0.125	0.1095	0.0137	0.0037
$\sum$			1.719		0.8411	0.8287	0.1707

$$\bar{y} = \frac{\sum Ay}{\sum A} = \frac{0.8411}{1.719} = 0.48 \text{ in.}$$

$$I = \sum I + \sum Ay^2 - \bar{y}^2 \sum A = 0.1707 + 0.8287 - 0.3950$$

$$I = 0.588 \text{ in.}^4$$

Assume that under loading conditions the ground under the plate will settle until the load is evenly distributed over the surface of the plate.

Maximum moment occurs under 2nd load

$M_{max} = 0.1071\ wL^2$ (Reference 2, page 2-133)

$M_{max} = 0.1071 \left(\frac{37,500}{48}\right) (12)^2 = 12.2$ in. kips

$F_b = \frac{Mc}{I} = \frac{(12.2)(1.77)}{0.588} = 36.7$ ksi tension

$F_{tu} = 103.5$ ksi

M.S. = ample

$F_b = \frac{My}{I} = \frac{(12.2)(.48)}{0.588} = 10$ ksi compression

$F_{cy} = 72$ ksi

M.S. = ample

Bearing (of Truss Tube Pins on Angles)

$A_{br} = Dt = (0.437)(0.125) = 0.0545 \text{ in.}^2$ (for one angle and one pin)

$P = 9.600$ kips (for one pin and one angle)

$F_{br} = \frac{P}{A_{br}} = \frac{9.6}{0.0545} = 176$ ksi

$F_{bru} = 198$ ksi

M.S. $= \frac{198}{176} - 1 = 0.12$

Shear

Maximum shear $= \frac{37,500}{2} = 18,750$ lb

A_s = area of section $- 2Dt = 1.719 - 2(0.437)(0.125)$

$A_s = 1.61$

$F_s = \frac{P}{A} = \frac{18,750}{1.61} = 11.7$

$F_{su} = 68$ ksi

M.S. = ample

8. Tension Bars (Reference Figure 9)

Assume 1) 20,000-lb aircraft

2) Load factor of 1.25 (drift landing only)

3) Side load = 0.8 x maximum gear load

$$= \frac{(0.8)(20,000)(1.25)(1.5)}{2}$$

= 15,000 lb ultimate (for each gear)

4) For design purposes assume that all side load is taken out in two bars, either tension or compression

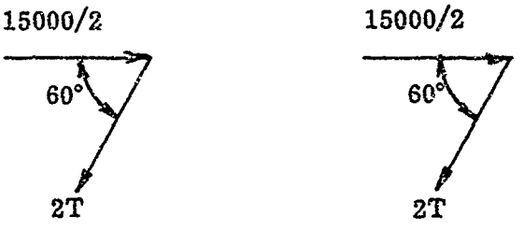

$$2T = \frac{15,000}{2 \cos 60^{\circ}} = 15,000 \text{ lb ultimate (7500 lb/lug)}$$

Tension (for Method of Analysis see Reference 1, Section 1.6200)

P = 7500 lb (ult) P_y = 5000 lb (limit)

$\frac{e}{D} = 1.6$ $\frac{W}{D} = 3.2$ $\frac{D}{t} = 1.67$

$A_t = (W - D)t = 0.516$ in.^{2}

$A_{br} = Dt = 0.234$ in.^{2}

Bearing

$P_{bru} = (K_{br})(F_{tu})(A_{br})$

$K_{br} = 1.55$ (Reference 1, page 1.6200-13)

$F_{tu} = 103.5$ ksi

$P_{bru} = (1.55)(103.5)(0.234) = 27.5$ kips

M.S. = ample

P = 7.500 kips

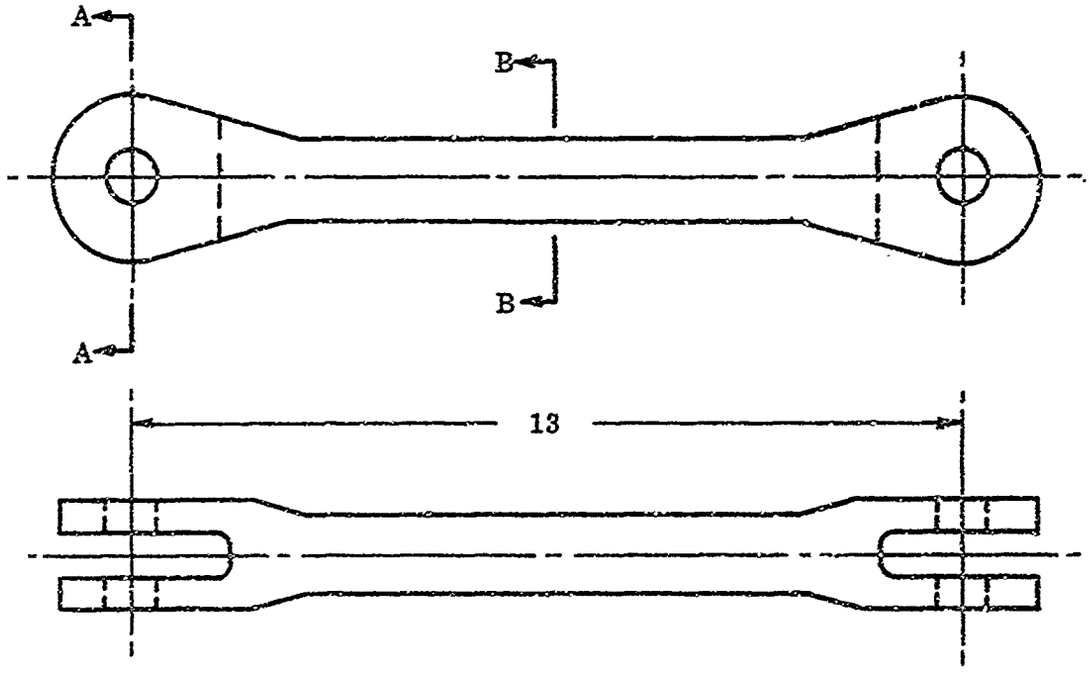

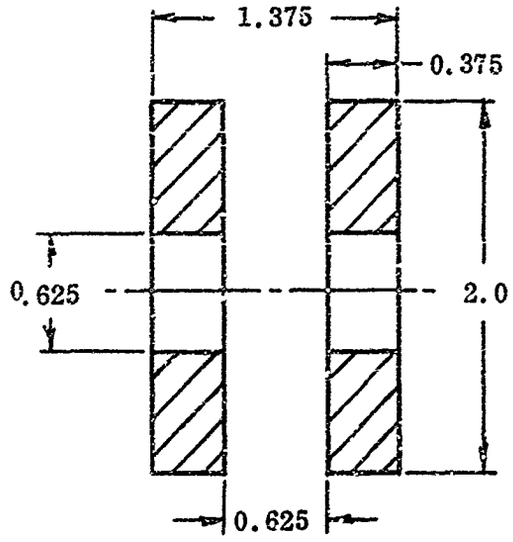

Section AA

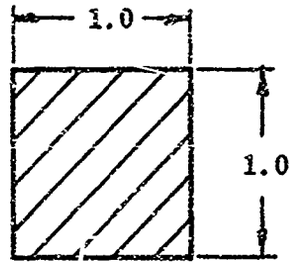

Section BB

Tension

$P_{tu} = (K_t)(F_{tu})(A_t)$

$K_t = 0.905$ (Reference 1, page 1.6200-12)

$F_{tu} = 103.5$ ksi

$P_{tu} = (0.905)(103.5)(0,516) = 48.5$ kips

$P = 7.50$ kips M. S. = ample

Tension Yield

$P_{ty} = (K_{bry})(F_{ty})(A_{br})$

$K_{bry} = 1.55$ (Reference 1, page 1.6200-14)

$F_{ty} = 72$ ksi

$P_{ty} = (1.55)(72)(0.234) = 26.1$ kips

M.S. = ample

$P_y = 5$ kips

Compression Bearing

Bearing

$A_{br} = 2Dt = 0.468$ in.^{2}

$F_{br} = \frac{P}{A_{br}} = \frac{15.0}{0.468} = 32.2$ ksi

M.S. = ample

$F_{bru} = 198$ ksi

Column Action

$I = \frac{1}{12} bh^3 = \frac{1}{12} (1)(1)^3 = 0.0833$ in.^{4} (Section BB)

$A = 1$ in.^{2} $\qquad$ $c = 1$ and $L' = L$

$\rho = \sqrt{\frac{I}{A}} = \sqrt{0.0833} = 0.289$ in.

$\frac{L}{\rho} = \frac{13}{0.289} = 45$

$F_{c_{all}} = 50$ ksi (Reference 1, page 1.1630-4)

$F_c = \frac{P}{A} = \frac{15}{1} = 15$ ksi $\qquad$ M.S. = ample

Pins

5/8-in. pin - pins are in double shear

$A_s = (2)$ (area) $= 0.614$ in.^{2}

$$F_s = \frac{P}{A_s} = \frac{15}{0.614} = 24.8 \text{ ksi}$$

F_{su} = 68 ksi M.S. = ample

Fitting

Single lug fitting

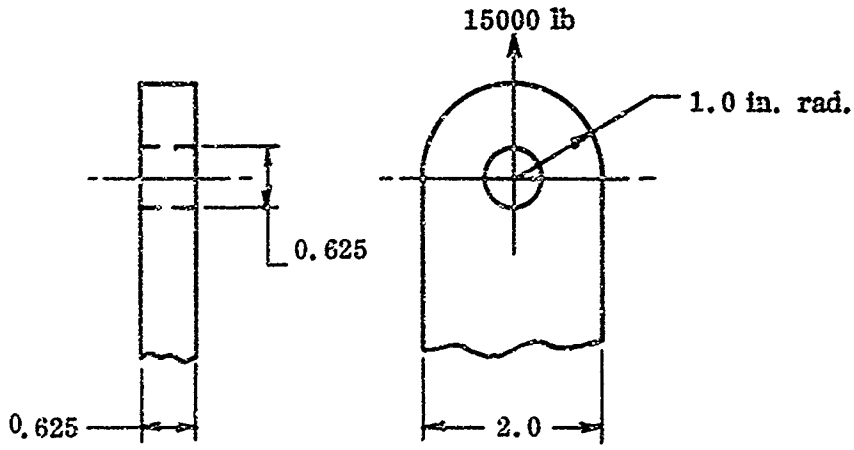

$\frac{e}{D} = 1.6$ e = 1.0 in.

$\frac{W}{D} = 3.2$ D = 0.625 in.

W = 2.0 in.

$\frac{D}{t} = 1$ t = 0.625 in.

$A_t = (W - D)t = 0.86 \text{ in.}^2$

$A_{br} = Dt = 0.39 \text{ in.}^2$

(For method of analysis see Reference 1, Section 1.6200)

Bearing

$P_{bru} = (K_{br})(F_{tu})(A_{br})$

$K_{br} = 1.47$ (Reference 1, page 1.6200-13)

$F_{tu} = 103.5$ ksi

$P_{bru} = (1.47)(103.5)(0.39) = 59.4$ kips

P = 15 kips M.S. = ample

Tension

$P_{tu} = (K_t)(F_{tu})(A_t)$

$K_t = 0.905$ (Reference 1, page 1.6200-12)

$F_{tu} = 103.5$ ksi

$P_{tu} = (0.905)(103.5)(0.86) = 80.5$ kips

$P = 15.0$ kips

M.S. = ample

Tension Yield

$P_{ty} = (K_{bry})(F_{ty})(A_{br})$

$K_{bry} = 1.47$ (Reference 1, page 1.6200-14)

$F_{ty} = 72$ ksi

$P_{ty} = (1.47)(72)(0.39) = 41.3$ kips

$P_y = 10$ kips

M.S. = ample

9. Analysis of Air Deflecting Vanes at 1200°F, Using A-286 Steel – 20,000-lb Aircraft (Reference Figure 9)

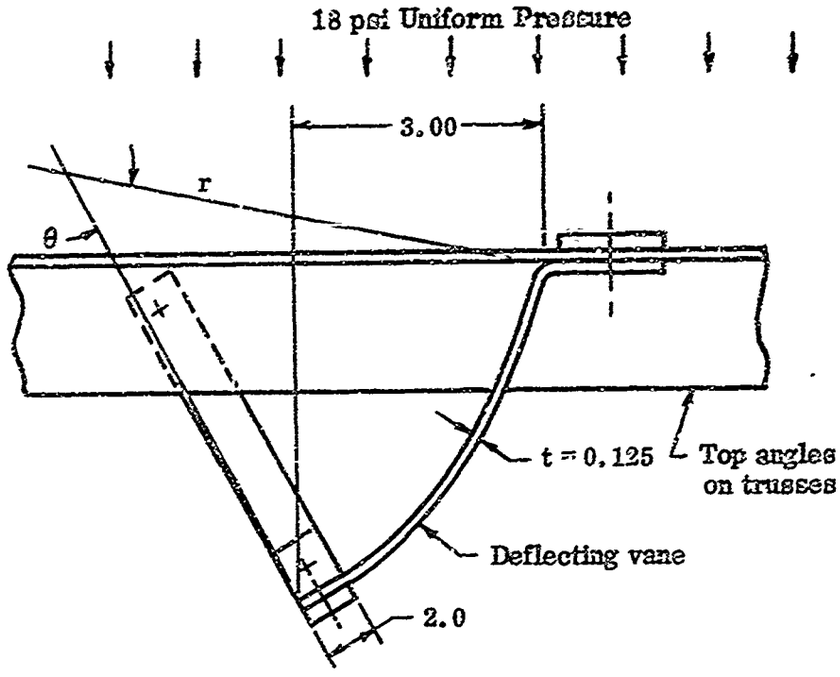

Total depth of vanes = 7.50 in.

Length of vane = θr = (0.785) (8) = 6.28 in.

For design purposes assume 1-in. wide strip simply supported at both ends with a limit load of 18 lb/in. applied uniformly. Assume strip to be flat.

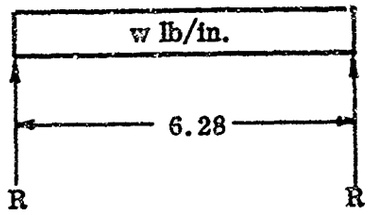

w = 18 (1.5) = 27 lb/in. (ult.)

Maximum bending moment (M) at center

$$M = \frac{wL^2}{8} = \frac{(27)(6.28)^2}{8} = 133 \text{ in. lb} = 0.133 \text{ in. kips}$$

$F_b = \frac{Mc}{I}$

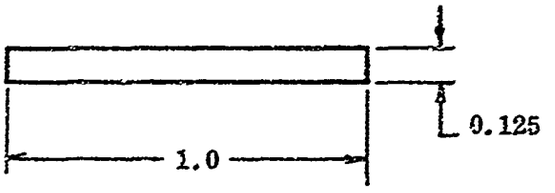

$I = \frac{1}{12} bh^3 = \frac{1}{12}(1)(0.125)^3 = 0.000162 \text{ in.}^4$

$c = 0.0625$ in.

$F_b = \frac{Mc}{I} = \frac{(0.133)(0.0625)}{0.000162} = 51.3$ ksi tension and compression

$F_{tu} = 88$ ksi M.S. $= \frac{88}{51.3} - 1 = 0.71$

$F_{cy} = 71.8$ ksi M.S. $= \frac{71.8}{51.3} - 1 = 0.40$

Check for Bending Along the Vane

Use full depth of vane = 7.50 in.

Assume t entire load acting down on the vanes is reacted by 0.25 x 2 in. strip at bottom of vanes.

Total force acting down = 18 (1.5)(3)(7.5) = 607 lb (ult)

Assume this load acting uniformly along strip.

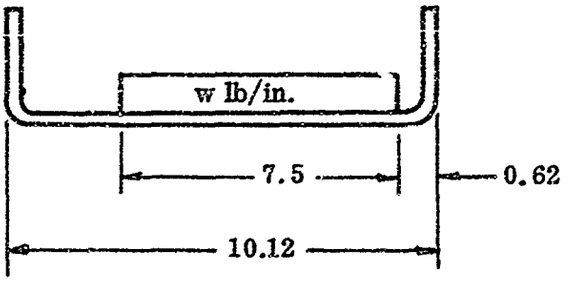

$w = \frac{P}{L} = \frac{607}{7.5} = 81$ lb/in.

Assume ends simply supported

$R_L = \frac{(7.5)(81)(4.37)}{10.12} = 262$ lb

$R_R = 607 - 262 = 345$ lb

Max. moment occurs at zero shear

$\sum V = 0 = 345 - x\,81$

$x = \frac{345}{81} = 4.27$ in.

Max. moment occurs $4.27 + 0.62 = 4.89$ in. from right end

$M = (4.89)(345) - 4.27(81)(4.27/2)$

$M = 1705 - 735 = 970$ in. lb $= 0.97$ in. kips.

$F_b = \frac{Mc}{I}$ $\qquad t = 0.25$

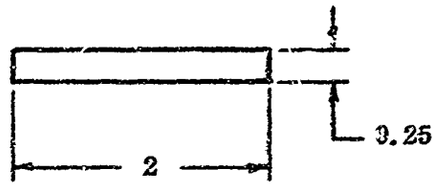

$I = \frac{1}{12} bh^3 = \frac{1}{12}(2)(0.25)^3 = 0.0026$ in.^{2}

$c = 0.125$ in.

$F_b = \frac{Mc}{I} \frac{(0.97)(0.125)}{0.0026} = 45$ ksi tension and compression

$F_{tu} = 88$ ksi $\qquad$ M.S. $= \frac{88}{45} - 1 = 0.95$ tension

$F_{cy} = 71.4$ ksi $\qquad$ M.S. $= \frac{71.4}{45} - 1 = 0.60$ compression

Check of Support

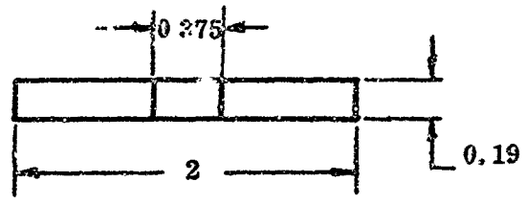

$A = 0.38 - 0.375\,(0.19) = 0.31$ in.^{2}

$P_{all} = A\,F_{tu} = 0.31\,(88) = 27.3$ kips $\qquad$ M.S. = ample

10. Analysis of Floor Sheet at 1200°F, Using A-286 Steel - 20,000-lb Aircraft (Reference Figure 9)

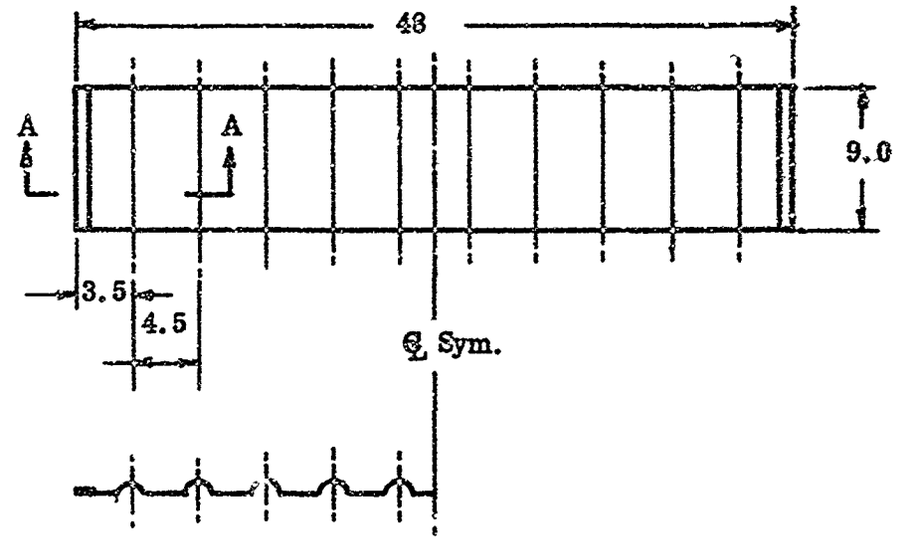

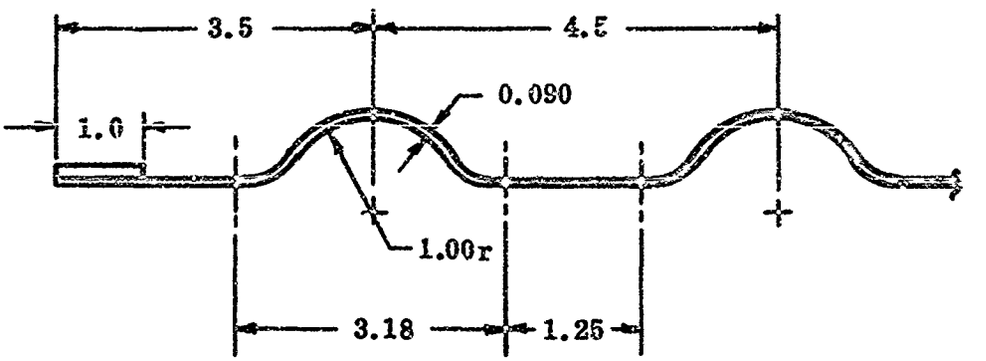

Section A-A

Use pressure = 18 psi over entire sheet (limit value).

p = 18 (1.5) = 27.0 psi (ult.)

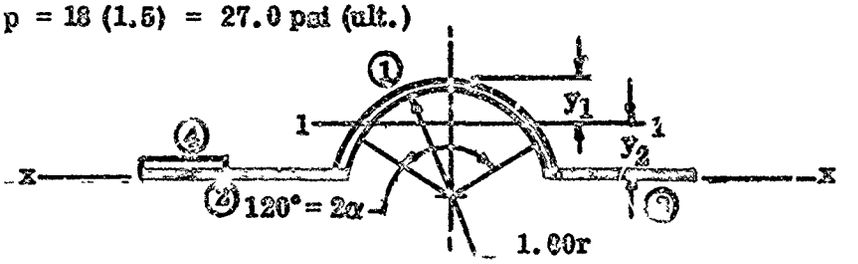

α = 30° = 1.05 radians

For Section ① only (thin circular shell)

$A = 2\alpha\, rt = (2)(1.05)(1.0)(0.09) = 0.189 \text{ in.}^2$

$y_1 = r\left(1 - \frac{\sin\alpha}{\alpha}\right) = 1\,(1 - 0.825) = 0.175 \text{ in.}$

$I_1 = r^3 t\left(\alpha + \sin\alpha\cos\alpha - \frac{2\sin^2\alpha}{\alpha}\right) = (1)^3\,(0.09)\,(1.05 + 0.433 - 1.43)$

$I_1 = 0.00477 \text{ in.}^4$

For entire section

Section	b	h	A	y	Ay	Ay^2	I
1	-	-	0.1890	0.505	0.0954	0.0482	0.00477
2	2.5	0.09	0.2250	0.045	0.0102	0.0046	0.00015
3	1.25	0.09	0.1125	0.045	0.0051	0.0023	0.00008
4	1.0	0.125	0.1250	0.153	0.0194	0.0030	0.00016
$\sum$			0.6515		0.1301	0.0581	0.00516

$\bar{y} = \frac{\sum Ay}{\sum A} = \frac{0.1301}{0.6515} = 0.200 \text{ in.}$

$I = \sum I + \sum Ay^2 - \bar{y}^2 \sum A = 0.00516 + 0.0581 - 0.0261$

$= 0.0372 \text{ in.}^4$

Beam span = 9.0 in.

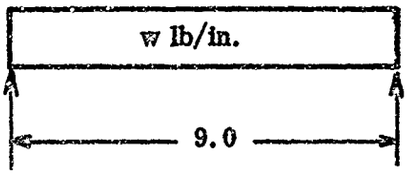

$w = (27 \text{ lb/in.}^2)\,(5.75 \text{ in.}) = 155.3 \text{ lb/in.}$

Maximum bending moment (M) at center

$M = \frac{wL^2}{8} = \frac{(155.3)(9)^2}{8} = 1570 \text{ in. lb.} = 1.57 \text{ in kips}$

$$F_b = \frac{Mc}{I} = \frac{(1.57)(0.48)}{0.0372} = 20.3 \text{ ksi compression}$$

$F_{cy} = 71.4$ ksi M.S. = ample

$$F_b = \frac{My}{I} = \frac{(1.57)(0.2)}{0.0372} = 8.45 \text{ ksi tension}$$

$F_{tu} = 88$ ksi M.S. = ample

Maximum reaction = $R = \frac{wL}{2} = 700$ lb $= 0.7$ kips

Max. shear stress $= \frac{P}{A} = \frac{0.7}{0.6515} = 1.07$ ksi

$F_{su} = 68$ ksi M.S. = ample

Maximum Deflection (at limit load)

Δ_{max} at center

$$\Delta_{max} = \frac{5wL^4}{384EI} = \frac{5(103.5)(9)^4}{384(29.0 \times 10^6)(0.0372)}$$

$= 0.017$ in.

11. Weight Calculation of Module

Weight of Outside Trusses

Top angles = area x length x 0.287
= (1.1408)(48)(0.287) = 15.7 lb/truss

Tubing = area x total length x 0.287
= (0.443)(125)(0.287) = 15.9 lb/truss

Bottom angles and plates = area x length x 0.287
= (1.719)(48)(0.287) = 23.8 lb/truss

Total weight of outside trusses = 110.8 lb

Weight of Inside Truss

Top angles = area x length x 0.287
= (0.9688)(48)(0.287) = 13.4 lb

Tubing = area x total length x 0.287
= (0.443)(125)(0.287) = 15.9 lb

Bottom angles and plates = area x length x
= (1.719)(48)(0.287) = 23.8 lb

Total weight of inside truss = 53.1 lbs

Weight of Tension Bars and Fittings = 40 lb

Weight of Deflecting Vanes (8 vanes) = 13.5 lb

Weight of Floor Sheet = 18.7 lb

Hardware = 10 lb

Total Weight Without Grid = 246.1 lb

Weight of Grid = 150.7 lb

Total Weight of Module and Grid = 396.8 lb

TABLE 3. CRITICAL STRESS LEVELS AT 1000°F

Wt. A/C in lb	20000	30000	40000	50000	F_{all}
Top Outside Angles					
1) Max. Ten.	63.3	68.6	71	60	103.5
2) Max. Comp.	54.5	57.8	58	50	72
3) Max. Bearing	123	155	189	145	198
4) Max. Shear	19.0	25.2	31.6	26.9	68
Top Inside Angles					
1) Max. Ten.	73.5	79.6	78.5	653	103.5
2) Max. Comp.	36.5	43	45	38.6	36.5
3) Max. Bearing	123	155	189	145	123
4) Max. Shear	23.1	31	36.9	31.4	23.1
Upper Pins					
1) Max. Ten.	124	122	136	137	175
2) Max. Comp.	124	122	136	137	175
3) Max. Shear	31.3	32.6	37.1	40	68
Tubing					
1) Max. Comp.	43.3	65	78.5	62.2	80
2) Max. Bearing	175	204*	205*	177	198
Lower Pins					
1) Max. Shear	64	58	43.5	54.5	68
Lower Angles					
1) Max. Ten.	36.7	54.3	72.8	62.8	103.5
2) Max. Comp.	10	15.1	20.2	21.8	72
3) Max. Bearing	176	202*	200*	168.5	198
4) Max. Shear	11.7	19.6	24.5	25.5	68
Tension Bars					
1) Max. Tens.	15	22.5	30	37.5	103.5
2) Max. Comp.	15	22.5	30	37.5	50

* Acceptable negative margin

All stresses in ksi.

TABLE 4. STRUCTURAL ANALYSIS SUMMARY

Aircraft Weight (lb)			20,000	30,000	40,000	50,000	50,000
Temperature °F							
	Under load		1000	1000	1000	1000	70
	Maximum		1200	1200	1200	1200	70
Material (except grid)			A-286 steel	A-286 steel	A-286 steel	A-286 steel	4130 steel HT 180-220
Grid (Ref. Figure 10)	Bearing bars		3" x .25"	3.5" x .25"	4" x .25"	4.5" x .25"	3.5" x .25"
	Cross bars		1.75" x .25"	1.75" x .25"	1.75" x .25"	1.75" x .25"	1.75" x .25"
	Banding bars		1.75" x .25"	1.75" x .25"	1.75" x .25"	1.75" x .25"	1.75" x .25"
	Material		316 steel	316 steel	316 steel	316 steel	4130 steel HT 180-220
Top angles on outside trusses (Ref. Figure 11)	Fig. a	t(in.)	0.125	0.125	0.125	0.188	0.125
		a(in.)	2.50	3.00	3.50	3.50	3.50
		b(in.)	0.50	0.50	0.50	0.50	0.50
		c(in.)	1.50	1.50	1.50	1.50	1.50
		d(in.)	1.00	1.00	1.00	1.00	1.00
Top angles on inside trusses (Ref. Figure 11)	Fig. b	t(in.)	0.125	0.125	0.125	0.188	0.125
		a(in.)	2.50	3.00	3.50	3.50	3.50
		b(in.)	0.50	0.50	0.50	0.50	0.50
		c(in.)	3.50	3.50	3.50	3.50	3.50
Pins attaching truss tubes to top angles (Ref. Figure 11)	Dia. (in.)		0.625	0.750	0.812	0.875	0.750

TABLE 4. STRUCTURAL ANALYSIS SUMMARY (Cont'd)

Aircraft Weight (lb)		20,000	30,000	40,000	50,000	50,000
Truss Tubes (Ref. Fig. 11)	O.D. (in.)	1.25	1.25	1.375	1.50	1.25
	Wall (in.)	0.125	0.125	0.125	0.188	0.125
Pins attaching truss tubes to bottom angles (Ref. Figure 11)	Dia. (in.)	0.437	0.562	0.750	0.750	0.750
Bottom Angles (Ref. Figure 11)	t(in.)	0.125	0.125	0.125	0.188	0.125
	a(in.)	2.25	2.25	2.25	2.25	2.25
Fig. c	b(in.)	0.50	0.50	0.50	0.50	0.50
	c(in.)	0.25	0.25	0.25	0.25	0.25
	d(in.)	3.50	3.50	3.50	3.50	3.50
Tension bars (Ref. Figure 12)		Same for all modules				
Air deflecting vanes (Ref. Figure 12)		Same for all modules				
Floor sheet (Ref. Figure 12)		Same for all modules				

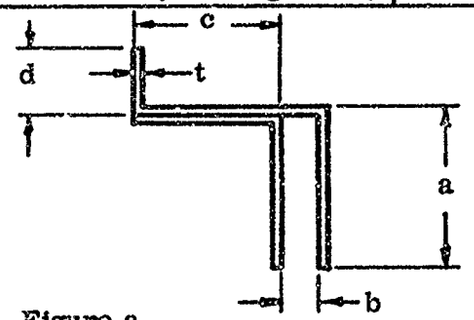

Figure a

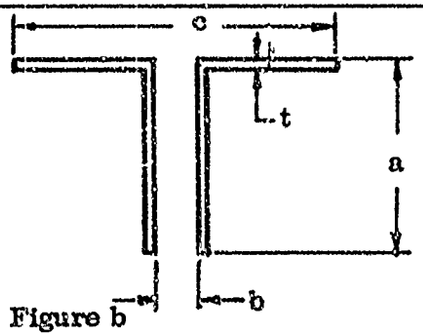

Figure b

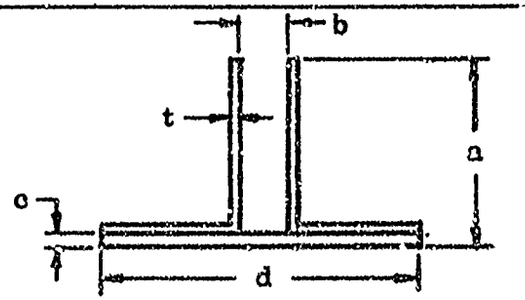

Figure c

TABLE 5. MODULE WEIGHTS (Lb)

Aircraft Weight (lb)		20,000	30,000	40,000	50,000	50,000
Temperature °F		1000	1000	1000	1000	70
Grid		150.7	169.2	187.2	205.2	169.2
Top angles on	outside truss	15.7	17.4	19.2	28.6	18.1
	inside truss	13.4	15.1	16.8	25.2	16.8
Truss tubes		15.9	15.9	17.6	27.7	15.9
Bottom angles		23.8	23.8	23.8	29.4	23.8
Tension bars		40.0	40.0	40.0	40.0	40.0
Air deflecting vanes		13.5	13.5	13.5	13.5	13.5
Floor sheet		18.7	18.7	18.7	18.7	18.7
Hardware		10.0	10.0	10.0	10.0	10.0
Total Weight	without grid	246.1	261.2	261.6	335.9	245.7
	with grid	396.8	420.4	448.8	541.1	414.9

REFERENCES

1. Republic Aviation Structures Manual (see Appendix A)

2. "A.I.S.C. Manual of Steel Construction," A.I.S.C. Institute of Steel Construction, Inc., 1965

3. MIL-HDBK-5A dated February 8, 1966

4. "Formulas for Stress and Strain," by Raymond J. Roark, McGraw-Hill Book Co., 1965

SECTION VIII

CONCLUSIONS AND RECOMMENDATIONS

A. SUMMARY

A research study was conducted to determine the design and manufacturing requirements for a portable VTOL blast controlling platform. In this study, thermodynamic considerations, design criteria, a materials survey, and structural analyses were combined with a review of manufacturing requirements to produce a design concept for such a platform.

The formulation of this design concept was also based on ease of handling and erection of the platform in the field. The minimization of special tooling, the use of the simplest manufacturing procedures, and cost savings in all areas were also considered as factors affecting design.

B. CONCLUSIONS

A portable modular VTOL blast controlling platform is entirely feasible for use with aircraft of various weights and engine exhaust characteristics. Manufacturing methods required to produce such a platform are in no way specialized. The design concept conceived meets the established requirements for field use.

C. RECOMMENDATIONS

Before detail design of production modules and platforms can be accomplished, intermediate programs must be conducted. The first of these is the design and construction of an experimental platform with a configuration which allows for angular adjustment and replacement of the deflecting vanes and variation of the exhaust area. This platform should be tested with engines and simulated aircraft structure (only engine exhaust loading and temperatures to be applied) to investigate such factors as optimum platform configuration, effects of temperature on platform and aircraft, heat dissipation, and effect of the platform on noise level and thrust.

In the second program, the results of this investigation should be applied to the design concept and a prototype platform designed. Prototype modules must be subjected to static testing. Subsequent to this a prototype platform large enough for the takeoff and landing of VTOL aircraft should be manufactured and tested not only for validity of platform characteristics, but also for effect of the platform on the aircraft.

The results of this second (prototype) construction and test program will then be combined with all previous data in order to optimize design condiguration of production platforms.

APPENDIX A

REPUBLIC AVIATION

STRUCTURES MANUAL

SECTION 1.6200: ANALYSIS OF LUGS

1.6210: REFERENCES

(a): ANC-5 (Including Amendment 1)—"Strength of Aircraft Elements"—June 1951

(b): RAC Structures Handbook—Vol. II—"Structural Methods"

1.6210: NOTATION

The notation used herein is in accordance with the standard notation described in Section 0.1000 and listed as follows:—

A = Area (*usually minimum appropriate area*), Square inches
B = Load distribution factor for outside lugs, non dimensional
D = Diameter of hole in lug, inches
e = Edge distance from center of hole, inches
F = Material allowable stress, ksi
f = Calculated stress, ksi
g = Gap between mating lugs (*if any*), inches
K = Efficiency factor
M = Applied bending moment, inch-kips
n = Total number of lugs, (*both fittings*)
P = Applied load, kips (*without subscript, refers to total load; with subscript, refers to appropriate condition, lug, or bushing*)
P = allowable load, kips
r = Geometric factor, non-dimensional = $\frac{e - D/2}{t}$
t = Lug thickness, inches
W = Lug width (see figure 1.62001-1), inches
θ = Angle between loading direction and lug center line, degrees
{$\theta = 0°$, refers to axial load} {$\theta = 90°$, refers to transverse load}
γ = Pin bending moment reduction factor for peaking of loading.

Subscripts

$_1$ = inside lugs of female fitting (see figure 1.6200-2)
$_{B1}$ = outside lugs of female fitting (see figure 1.6200-2)
$_2$ = lugs of male fitting
$_a$ = axial load
$_b$ = bending, (F_b, bending modulus of rupture)
$_{br}$ = bearing, (P_{br}, refers to a combined shear—bearing failure)
$_{bu}$ = bushing
$_g$ = grain direction
$_c$ = compression
$_L$ = longitudinal grain direction

$_T$ = transverse grain direction
$_N$ = short transverse grain direction
$_{min.}$ = minimum, $[(P_u)_{min}$ is the smaller of P_{br}, and $P_{tu}]$
$_p$ = pin
$_s$ = shear
$_t$ = tension
$_{tr}$ = transverse
$_u$ = ultimate
$_y$ = yield

1.6220: SUMMARY

A method for the structural design analysis of lugs and shear pins is presented herein. Design curves for the various correction factors necessary for the design analysis are shown in Figures 1.6200-7 to 1.6200-12.

The necessity for this new method was emphasized when experimental investigations of lug-pin combinations, with lugs of various materials and geometries, disclosed that the existing conventional methods of analysis were conservative in some respects and unconservative in others. The two predominating factors which adversely affected the use of the conventional methods are:

(a) *effect of ductility of the materials (which varies with grain direction)*
(b) *incomplete evaluation of the effect of stress concentrations. Correction factors have been determined to take into account all possible effects and are shown in Figures 1.6200-7 to 1.6200-12.*

1.6230: LIMITATIONS OF METHOD OF ANALYSIS

(a) The method of analysis presented herein is applicable to aluminum and steel alloy lugs of *uniform thickness* and *under loading conditions shown in figure 1.6200-1.*

(b) The method of analysis is applicable *only when the lug thickness is less than the hole diameter.* $\left(\frac{D}{t} > 1.0\right)$

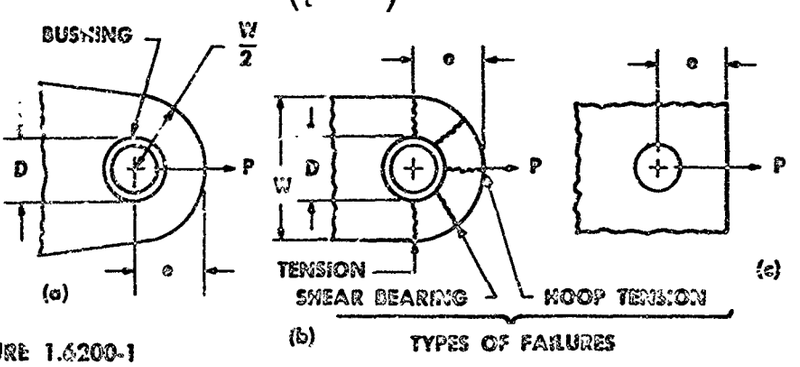

FIGURE 1.6200-1

1.6240: LOAD DISTRIBUTION TO LUGS

A satisfactory design analysis of an individual lug can only be made if the correct distribution of the total load to each of the lugs is determined. Consider first the three-lug connection as shown in figure 1.6200-2(a). The load distribution to the lugs is

$$P_1 = P_{B_1} = \frac{P}{2}$$

$$P_2 = P$$

This load distribution is shown in the form of a factor in the B column of table 1.6200-1.

For multiple-lug connections, figure 1.6200-2(b), the load distribution is more complicated. The load distribution factor B is obtained from Table 1.6200-1 for the proper total number of lugs (n). Therefore the load distributions to each of the lugs is obtained as follows, assuming that the thickness t_{B_1} of the outer female fitting is $\geq$ nt_1:

$$P_1 = \frac{2P}{4B + n - 3}$$

$$P_{B1} = BP_1 = \frac{2BP}{4B + n - 3}$$

$$P_2 = \frac{2P}{n - 1}$$

As an example, for the lug-pin connection shown in figure 1.6200-2(b).

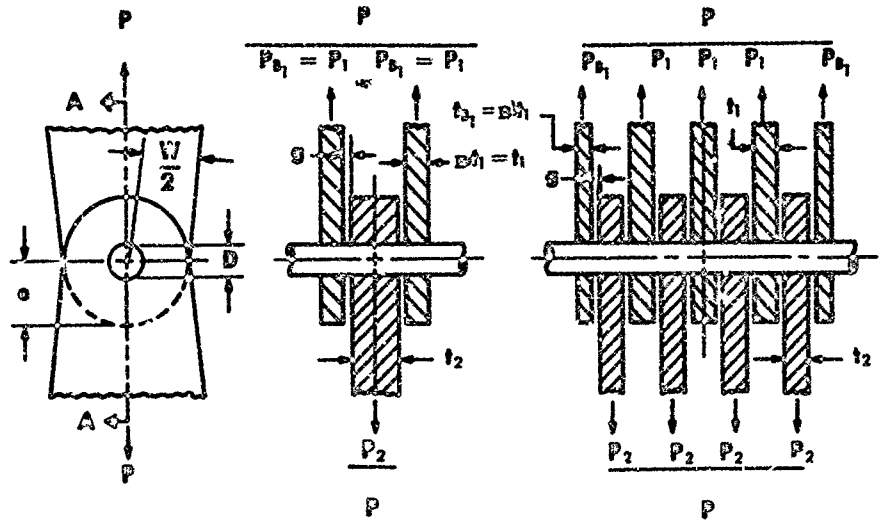

(a) GENERAL (b) SEC. A-A 3 LUGS (c) SEC. A-A 9 LUGS

FIGURE 1.6200-2

$$n = 9$$

Therefore

$$P_1 = \frac{2P}{4(.43) + 9 - 3} = .259P$$

$$P_{B1} = .43\,(.259P) = .1114P$$

$$P_2 = \frac{2P}{(9 - 1)} = .250P$$

TABLE 1.6200-I: LOAD-COEFFICIENTS

Item		Coefficients	
Total Number of Lugs (Both Sides) n	s	(a) K_s	(b) K_b
3	$st_1 = t_1 = .50t_2$	1.00	$.250(2t_1 + 4g + \gamma t_2)$
5	.35	.50	$.070(t_1 + 4g + \gamma t_2)$
7	.40	.53	$.083(t_1 + 4g + \gamma t_2)$
9	.43	.54	$.093(t_1 + 4g + \gamma t_2)$
11	.44	.54	$.098(t_1 + 4g + \gamma t_2)$
∞	.50	.50	$.125(t_1 + 4g + \gamma t_2)$

(a) K_s = Shear Factor, Non-Dimensional
(b) K_b = Bending Factor, Non-Dimensional

1.6250: METHOD OF ANALYSIS

In the analysis of lug-pin combinations under axial tension load the following modes of failure should be checked for by the methods presented:

(a) Tension across the net section. Because of the inherent stress concentration, the load carrying capacity is reduced.

(b) Shear tear-out or bearing. These two are closely related and are covered by a single computation based on empirical curves.

(c) Hoop tension at the tip of the lug. No separate calculation is required since the shear-bearing allowables preclude hoop tension failure.

(d) Yielding of the lug. This is considered excessive beyond a permanent set of (.02 x pin diameter).

(e) Excessive yielding of the bushing (if a bushing is used).

(d) Shearing of the pin.

(e) Bending of the pin. The pin ultimate strength is based on modulus of rupture.

1.6260: FACTORS AND DESIGN NOTES

(a) Pertinent fitting, casting, or bearing factors shall always be used in the analysis. For "joints having motion" the provisions of paragraph 2.61122, reference (a), are applicable to bearing stresses only. If in any application, more than one of these factors are applicable, they shall not be multiplied, but only the largest shall be used.

(b) It is desirable for the analysis of important lug-pin assemblies to show a minimum margin of safety of 0.20, for both lug and pin. This shall be considered in both yield and ultimate strengths.

(c) If no bushing is included in the original design, strength should be provided to maintain the desired margins of safety should the hole diameter be increased to include a bushing, i.e., equivalent to the next size bolt or pin. Margins of safety, however, shall be expressed on the basis of the actual pin size and lug hole diameter shown on the engineering drawing.

(d) For three-lug connections, one lug on each side must be analyzed unless it is obvious which lug is critical. For multiply-lug connections one outer female lug $_{B1}$, one inner female lug $_{(1)}$, and one male lug $_{(2)}$ must be checked to determine the minimum margin of safety.

1.6270: ANALYSIS PROCEDURE—AXIAL LOAD

(a) Determine the yield and ultimate loads for each lug by the load distribution procedure (Table 1.6200-1).

(b) Determine the pertinent fitting, casting and/or bearing factors.

(c) Given the pin and lug materials and the dimensions e, D, t, and W (see figure 1.6200-1).

(d) Obtain applicable material properties from reference (a) and for aluminum alloys, include the cross grain data listed in Table II.

TABLE 1.6200-II

SHORT — TRANSVERSE GRAIN TENSION PROPERTIES ALUMINUM ALLOY

Material	$(F_{tu})_N$	$(F_{ty})_N$
14ST and 75ST hand forged billet	$0.90(F_{tu})_T$	$0.96(F_{ty})_T$
14ST and 75ST die forgings*	$0.85(F_{tu})_T$	$0.90(F_{ty})_T$
75ST plate (these values may also be used to approximate values for other aluminum alloy plate)	$0.85(F_{tu})_T$	$0.85(F_{ty})_T$
75S-T6 extrusion	$0.98(F_{tu})_T$	$0.98(F_{ty})_T$
14S-T6 extrusion	$0.97(F_{tu})_T$	$0.98(F_{ty})_T$

*—Die forgings ordinarily do not have a definite and predictable grain direction; the 'N' values given are properties across the parting plane and ordinarily need not be used elsewhere.

NOTE:—Subscript T = long — transverse grain direction
Subscript N = short — transverse grain direction

(e) COMPUTATIONS

Determine

$$\frac{e_2}{D} \quad \frac{W_2}{D} \quad \frac{t_2}{D} \qquad A_{br} \doteq Dt, \quad A_t = (W - D)t$$

(f) *i) Lug*

(use appropriate subscript; $_1$, $_{B1}$, or $_2$ for each lug; $_2$ used as example)

Allowable *shear-bearing ultimate* load:

$$(P_{bru})_2 = [K_{br}(F_{tu})_g A_{br}]_2$$

K_{br} from figure 1.6200-8

$$(M.S._{bru})_2 = \left(\frac{P_{bru}}{P_u}\right)_2 - 1$$

Allowable *tensile ultimate load:*

$$(P_{tu})_2 = [K_t(F_{tu})_g A_t]_2$$

K_t from figure 1.6200-7

$$(M.S._{tu})_2 = \left(\frac{P_{tu}}{P_u}\right)_2 - 1$$

Allowable *yield* load:

$$(P_y)_1 = [K_{bry} (F_{ty})_g A_{br}]_2$$

K_{bry} from figure 1.6200-9

$$(M.S._y)_2 = \left(\frac{P_y}{P_y}\right)_2 - 1$$

(Note: Yield test for lug should always be checked as it is frequently reached at a lower load than would be anticipated from the ratio of F_{ty} to F_{tu} for the material)

ii) Bushing

(use proper subscript; $_1$, $_{B1}$ or $_2$ for each bushing $_2$ used as example)

Allowable *yield bearing* load:

$$(P_{bry})_2 = [1.85\ F_{cy} A_{br}]_2 \qquad (M.S._{bry})_2 = \left(\frac{P_{bry}}{P_y}\right)_2 - 1$$

iii) Pin

Compute

$$r = \left[\left(\frac{e}{D} - \frac{1}{2}\right)\frac{D}{t}\right]_2$$

Take the smaller of $(P_{bru})_2$ and $(P_{tu})_2$, found in preceding paragraph, and designate it as $(P_u)_1$

As

Compute $\left[\frac{(P_u)_2}{(F_{tu})_g A_{br}}\right]_2$

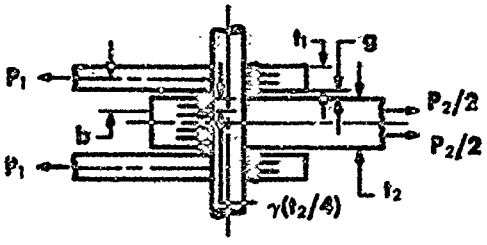

FIGURE 1.6200-3

Determine γ from Figure 1.6200-10 and K_b from Table 1.6200-I. The factor γ corrects for the fact that the load on the pin is not uniformly distributed.

Calculate the maximum bending moment

$$M_p = K_b (P)_1 \quad \text{(in-kips)} \quad [K_b \text{ from Table 1.6200-I}]$$

Corresponding bending stress

$$f_b = \frac{Mc}{I} \quad \text{(ksi)}$$

$$M.S._{bu} = \frac{F_b}{f_b} - 1$$

Maximum calculated shear stress

$$f_s = \frac{1.33\, K_s (P)_1}{A_p} \quad \text{(ksi)}$$

K_s from Table 1.6200-I

$$M.S._{tu} = \frac{F_s}{f_s} - 1$$

1.6280: OBLIQUE AND TRANSVERSE LOADING ANALYSIS

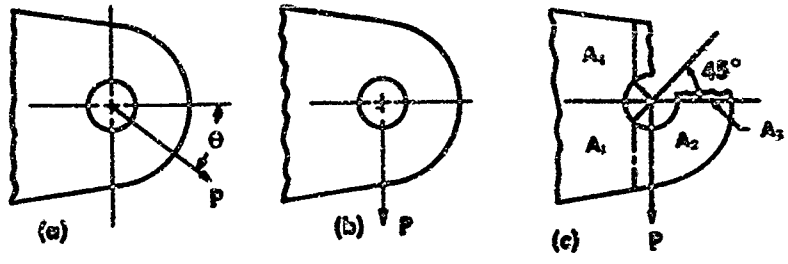

FIGURE 1.6200-4

Lugs may be loaded either obliquely or transverse to the axial direction as shown in figure 1.6200-4. An empirical correction factor was determined experimentally from tests to take this type of loading into account. The empirical curve is shown in figure 1.6200-11. Multiplication of the axial allowable load of the lug by this correction factor gives the allowable load when the load is applied at an angle to the axis of symmetry.

It should be noted that the allowable transverse load should never be taken as less than that which could be carried by cantilever beam action on the area A_1 as shown in figure 1.6200-4(c).

This load is very approximately indicated by the curve shown in Figure 1.6200-12. If K_{tru} is below the curve, make a separate cantilever beam action for section A_1.

The minimum transverse allowable load may be calculated as follows:

Allowable *ultimate* load

$$(P_{tru})_2 = [K_{tru}\,(F_{tu})_g\,A_{tu}]_2$$

Allowable *yield* load

$$(P_{try})_2 = [K_{try}\,(F_{ty})_g\,A_{tu}]_2$$

1.6290: SPECIAL NOTES AND APPLICATION

(A) ALLOWABLE BEARING STRESS OF MATERIALS

Reference (a) lists for the pertinent materials the applicable values of allowable bearing stress for $\frac{e}{D}$ values of 1.5 and 2.0, but they are only valid for $\frac{D}{t}$ less than or equal to 5.50.

For geometrical conditions outside of the above ranges, the allowable bearing stress may be determined in the following manner:

(i) Ultimate allowable bearing stress;

For particular $\frac{D}{t}$ and $\frac{e}{D}$ obtain K_{br} from figure 1.6200-8. Then

$$F_{bru} = K_{br}\,(F_{tu})_g$$

(ii) Yield allowable bearing stress; use the K_{br} of (i) as the abscissa for Figure 1.6200-9 and obtain K_{bry}. Then

$$F_{bry} = K_y\,K_{bry}\,(F_{ty})_g$$

(B) IRREGULAR LUG SECTION — BEARING LOAD DISTRIBUTE OVER ENTIRE THICKNESS.

For lugs of irregular section having bearing stress distributed over the entire thickness, an analysis should be made based on an equivalent lug with rectangular sections having areas equal to the original sections.

Example:

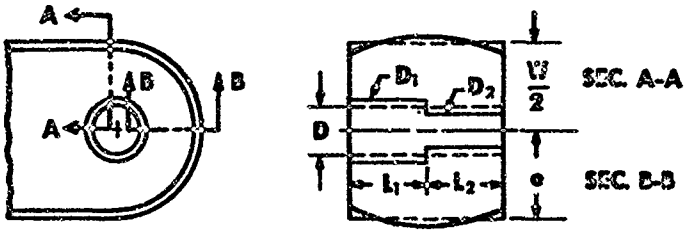

FIGURE 1.6200-5

Solid lines show actual lug. Dotted lines show equivalent lug for calculation.

(C) ECCENTRIC HOLE

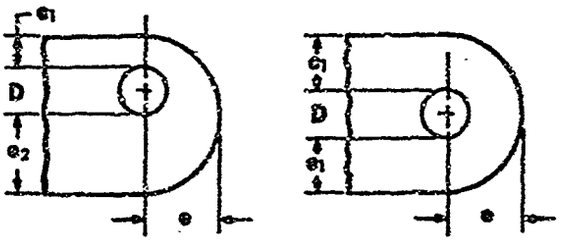

FIGURE 1.6200-6

If the hole is laterally eccentric as shown in Figure 1.6200.6(a), (e_1 less than e_2); Assume $e_2 = e_1$ and make edge distance 'e' of equivalent lug equal to edge distance 'e' of actual lug. The lug allowables shall be determined by obtaining P_{bru}, P_{tu}, and P_y for the equivalent lug shown in Figue 1.6200-6(b) and multiplying them by—

$$\frac{e_1 + e_2 + 2D}{2e_2 + 2D}$$

Example — Axial Load

Consider the three lug-pin combination shown, (comparable to Figure 1.6200-2(a)).

Determine the minimum M.S. for an applied axial load of

P_u (ultimate) = 150 kips
P_y (yield) = 100 kips

The lug is made of 7075S-T6, the bushing is 4130 steel (hardened) and the pin is 4340 steel (180-195 ksi).

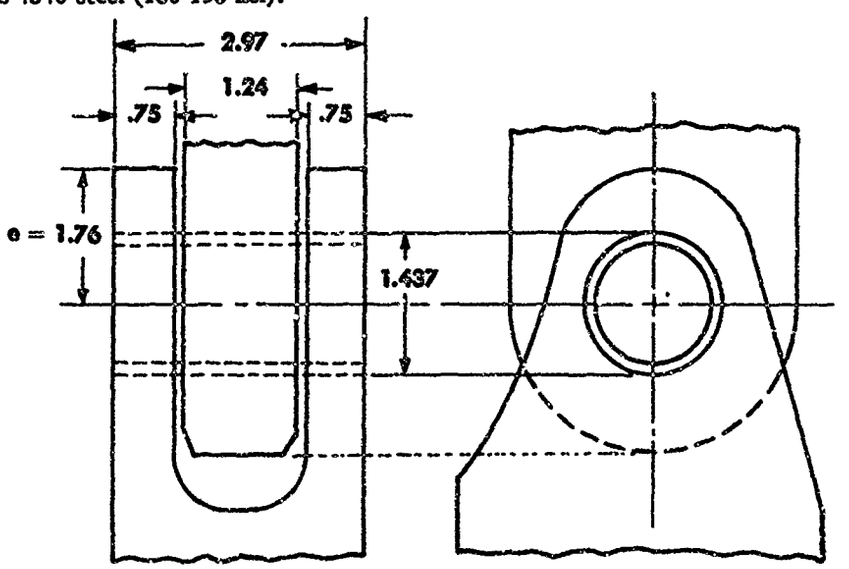

Load Distribution: (refer to Table 1.6200-1)

$$(P_u)_{g_1} = \frac{P_u}{2} = 75 \text{ kips}$$

$$(P_u)_2 = P_u = 150 \text{ kips}$$
$$(P_y)_2 = P_y = 100 \text{ kips}$$

1. Check lug (1):

(a) $\left(\frac{e}{D}\right)_1 = 1.31$ $\left(\frac{W}{D}\right)_1 = 2.07$ $\left(\frac{D}{t}\right)_2 = 1.915$

$$(A_e)_1 = 1.150 \text{ in}^2$$
$$(A_{br})_1 = 1.077 \text{ in}^2$$

(b) $(P_{bru})_1 = [K_{br} (F_{tu})_g \ A_{br}]_1$

$(K_{br})_1 = 1.21$ (Figure 1.6200-7)

$(F_{tu})_g = 68$ ksi (Reference (a))

$(P_{bru})_1 = 1.21 (68) (1.077) = 88.7$ kips

$$(M.S.)_{bru} = \frac{88.7}{75} - 1 = .18$$

(c) $(P_{tu})_1 = [K_t (F_{tu})_g \ A_t]_1$

$(K_t)_1 = .963$ (Figure 1.6200-8)

$(P_{tu})_1 = .963 (68) (1.150) = 75.3$ kips

$$(M.S.)_{tu} = \frac{75.3}{75} - 1 = .002$$

(d) $(P_y)_1 = [K_{bry} (F_{ty})_g \ A_{br}]_1$

$(K_{bry})_1 = 1.06$ (Figure 1.6200-9)

$(F_{ty})_g = 58$ ksi (Reference (a))

$(P_y)_1 = 1.06 (58) (1.077) = 66.3$ kips

$$(M.S.)_{bry} = \frac{66.3}{50} - 1 = .32$$

2. Check Bushing:

$(P_{bry})_1 = [1.85 F_{cy} A_{br}]_1$

$F_{cy} = 62$ ksi (Reference (a))

$(P_{bry})_1 = 1.85 (62) (1.077) = 123.6$ kips

M.S. = Exc.

3. Check Pin:

(a) $r = \left[\left(\frac{e}{D} - \frac{1}{2}\right)\frac{D}{t}\right]_1 = (1.31 - .50) 1.915 = 1.552$

(b) $(P_u)_{min} = 75.3$ kips

$$\frac{(P_u)_{min}}{[A_{br}\,(F_{tu})_{gli}} = 1.028$$

$\gamma = .508$ (Figure 1.6200-10)

$K_b = .250\,(2t_1 + 4g + \gamma\, t_2)$ (Table 1.6200-1)

$K_b = .250\,[2(.75) + 4(.23) + .508(.75)] = .700$ in.

(c) $M = K_b(P_u)_1 = .700(75) = 52.5$ in-kips

(d)

$$f_b = \frac{Mc}{I} \text{ for pin} \qquad \frac{I}{c} = .291 \text{ in}^3$$

$f_b = 52.5/.291 = 180.2$ ksi

$F_b = 285$ ksi (Reference (a))

M.S. = Exc.

(e) $f_s = 1.33\,K_s(P_u)_1/A_p$ $K_s = 1.0$ (Table 1.6200-1)

$A_p = 1.622$ in^2

$f_s = 1.33(1.0)\,(75)/1.622 = 61.5$ ksi

$F_s = 105$ ksi (Reference (a))

$$\text{M.S.} = \frac{105}{61.5} - 1 = .736$$

The minimum M.S. is .002 and the lug is critical in net tension.

FIGURE 1.6200-7: TENSION EFFICIENCY FACTORS FOR LUGS

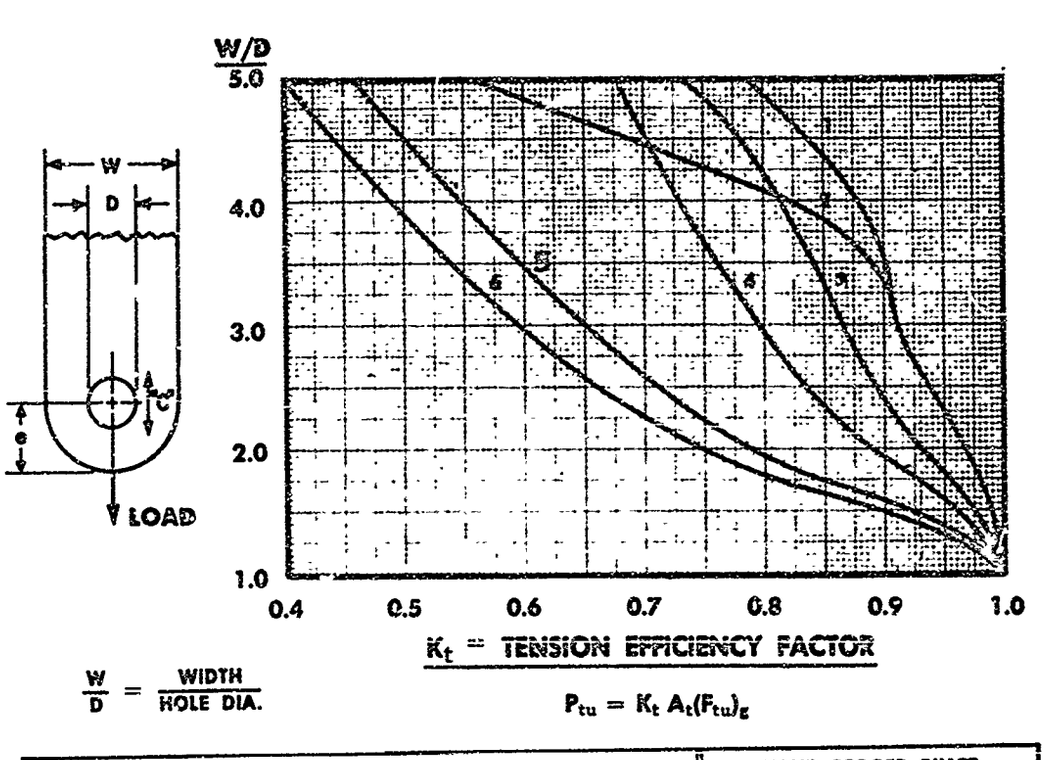

K_t = TENSION EFFICIENCY FACTOR

$\frac{W}{D} = \frac{\text{WIDTH}}{\text{HOLE DIA.}}$

$P_{tu} = K_t A_t (F_{tu})_g$

	STEEL ALLOYS (ANC-5a) TABLE 2.111b: USE CURVE 1													HAND FORGED BILLET				
	ALUM. CASTINGS 195-T6, 220-T4 & 356-T6: USE CURVE 5													14S-T6				*
		BAR			DIE FORG.			EXT.			PLATE				≤144(L)	>144(L)	≤36(T)	>36(T)	
	‡	L	T	N	L	T	N	L	T	N	(L, T)	(L, T)	(L, T)	N	75S-T6				
	*										≤0.5	0.5≤1	>1.0		≤36(L)	>36(L)	≤16(T)	>16(T)	*
	14S-T6			6	1	2	6				1	2	4	6	1	2	2	5	6
†	24S-T6,42	4	4	6				3	3	3	4	4	4	6					
	75S-T6	1	6	6	1	2	6	1	2	2	1	2	4	6	2	4	4	5	6

NOTES:

† NUMBERED CURVES APPLY TO THE MATERIALS NOTED IN TABLE

‡ LEGEND: L, T AND N, INDICATE GRAIN IN DIRECTION "C" IN SKETCH
L = LONGITUDINAL (WITH)
T = TRANSVERSE (CROSS)
N = SHORT TRANSVERSE (NORMAL)
FOR DIE FORGINGS 'N' DIRECTION EXISTS ONLY AT THE PARTING PLANE

* NUMERALS INDICATE THICKNESS OF PLATE AND/OR AREA OF BILLET

FIGURE 1.6200-8: SHEAR BEARING EFFICIENCY FACTOR FOR LUGS

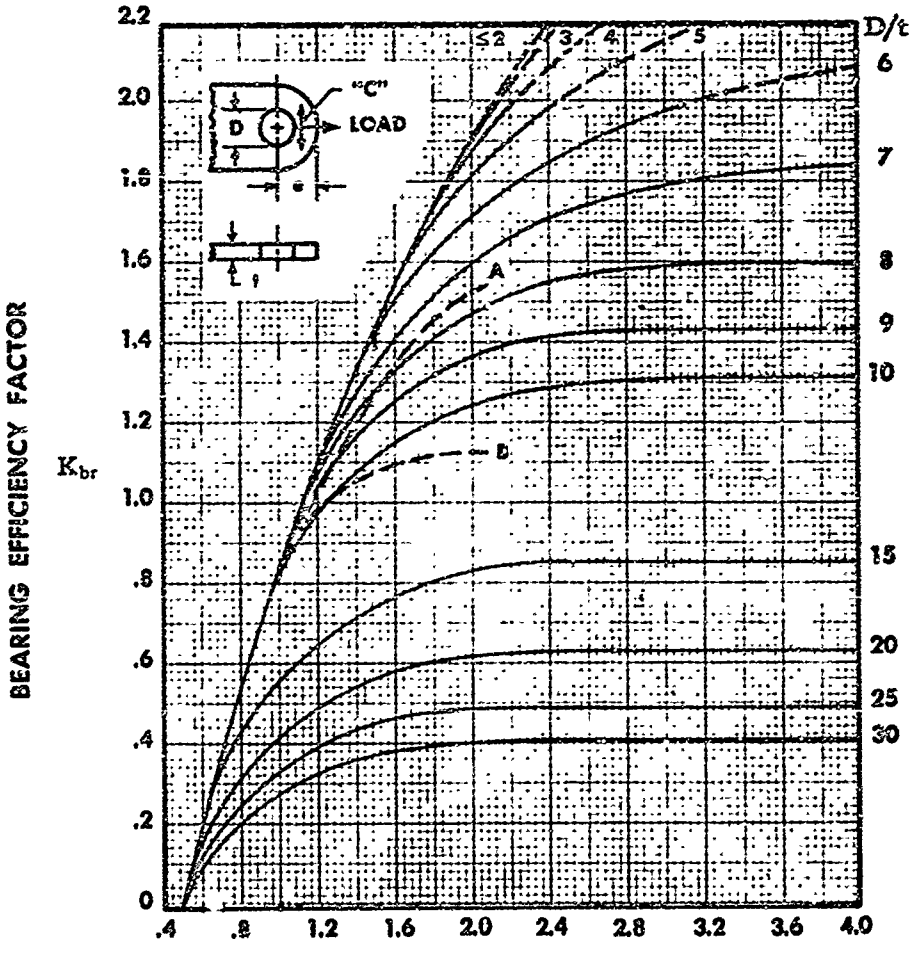

$$\frac{e}{D} = \frac{\text{EDGE DISTANCE}}{\text{HOLE DIAMETER}}$$

$$P_{bru} = K_{br}\, A_{br}\, (F_{tu})_g$$

NOTES:

1. CURVE "A" IS A CUTOFF TO BE USED FOR ALL ALUMINUM ALLOY HAND FORGED BILLET WHEN THE LONG TRANSVERSE GRAIN DIRECTION HAS THE GENERAL DIRECTION "C" IN THE SKETCH.
2. CURVE "B" IS A CUTOFF TO BE USED FOR ALL ALUMINUM ALLOY PLATE, BAR, AND HAND FORGED BILLET WHEN THE SHORT TRANSVERSE GRAIN DIRECTION HAS THE GENERAL DIRECTION "C" IN THE SKETCH, AND FOR DIE FORGINGS WHEN THE LUG CONTAINS THE PARTING PLANE IN A DIRECTION APPROXIMATELY NORMAL TO THE DIRECTION "C".
3. IN ADDITION TO THE LIMITATIONS PROVIDED BY CURVES "A" AND "B", IN NO EVENT SHALL A K_{br} GREATER THAN 2.00 BE USED FOR LUGS MADE FROM 5" THICK OR THICKER ALUMINUM ALLOY, PLATE, BAR, OR HAND FORGED BILLET.

FIGURE 1.6200-9: YIELD FACTOR FOR LUGS

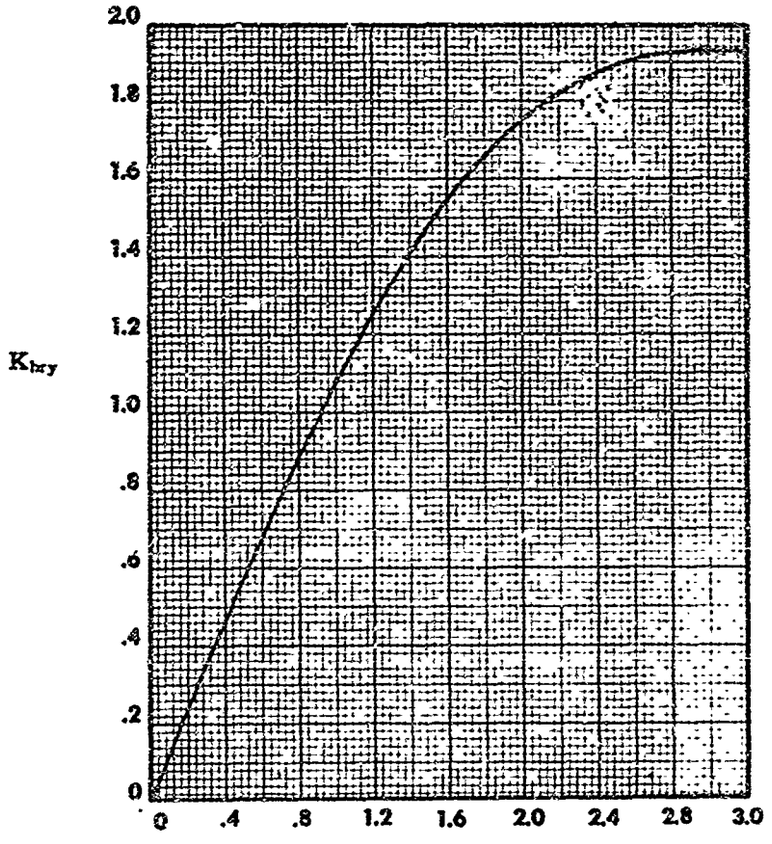

(WHICHEVER IS LOWER)

$$P_y = K_{bry} (F_{tu})_g A_b$$

FIGURE 1.6200-10: PIN BEARING MOMENT REDUCTION FACTORS

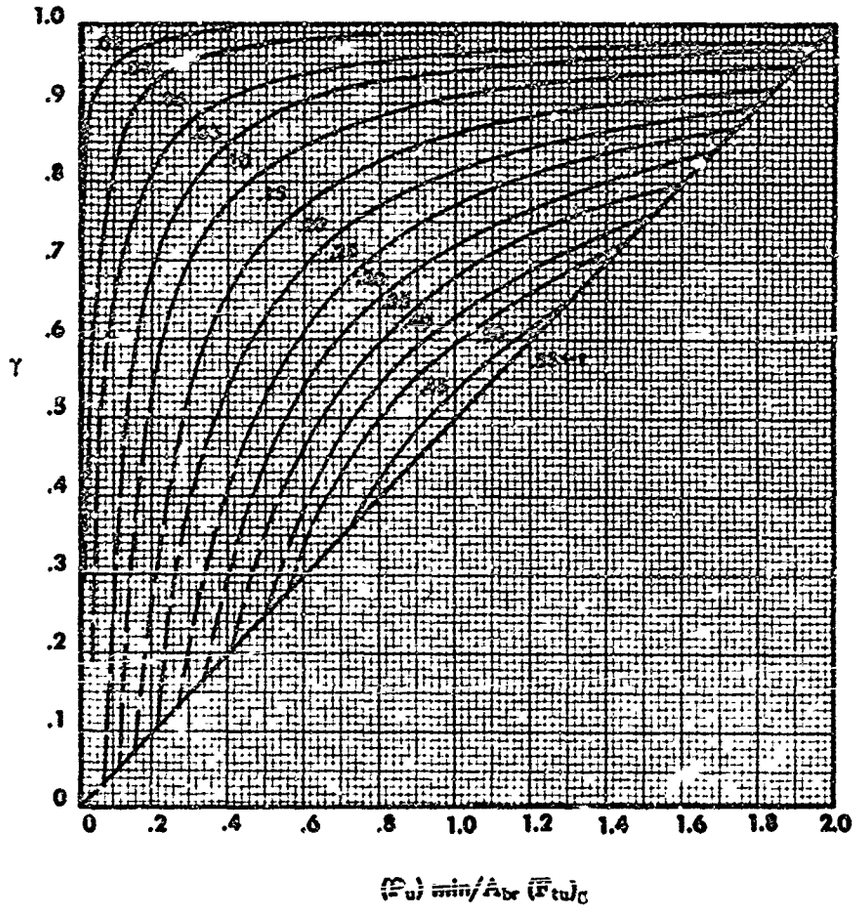

$(P_u)_{min} / A_{br} (F_{tu})_c$

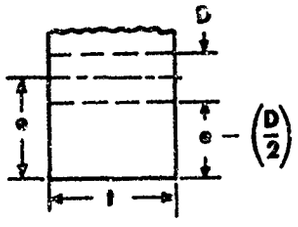

$$r = \frac{e - \frac{D}{2}}{t} = \left(\frac{e}{D} - \frac{1}{2}\right)\frac{D}{t}$$

NOTE:
DASH LINES INDICATE REGION WHERE THEORETICAL CURVES HAVE NOT BEEN SUBSTANTIATED BY TEST DATA

FIGURE 1.6200-11: ALLOWABLE LATERAL BEARING PRESSURE LOADINGS FOR LUGS

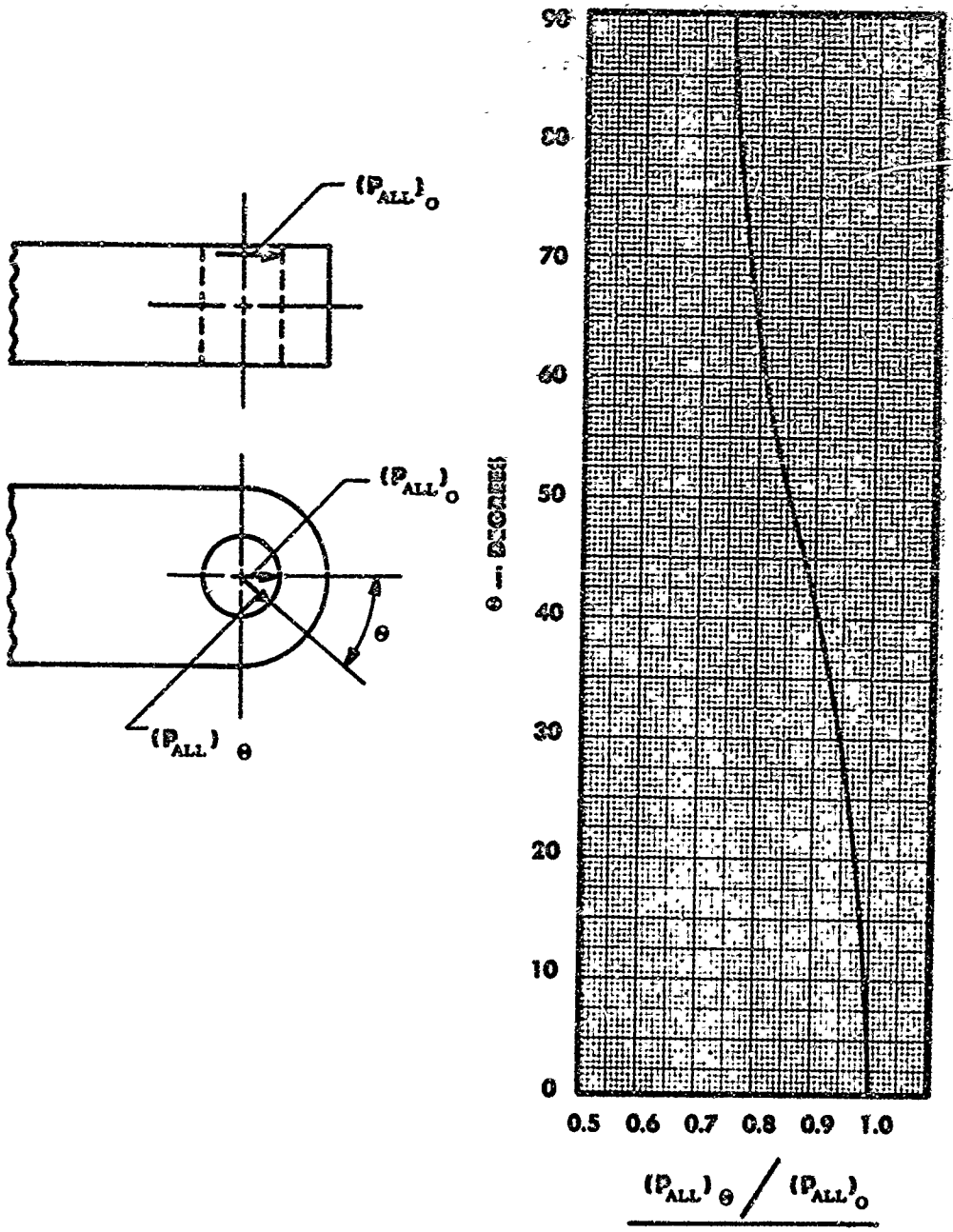

FIGURE 1.6200-12: LUG EFFICIENCY FACTOR FOR TRANSVERSE LOAD

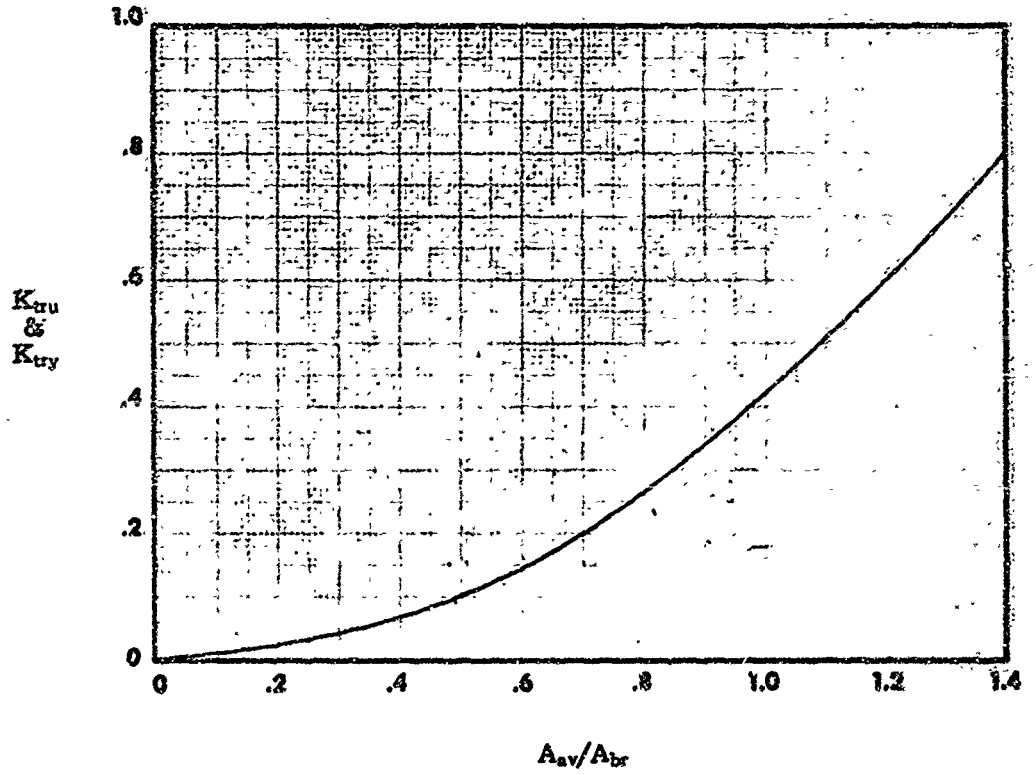

NOTE:
CURVE — APPROXIMATE CANTILEVER STRENGTH

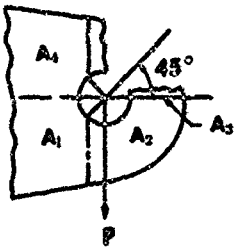

$$A_{av} = \frac{6}{(3/A_1) + (1/A_2) + (1/A_3) + (1/A_4)}$$

FIGURE 1.1630-1: COLUMN CURVES—LONGITUDINAL—STAINLESS STEEL (18-8)

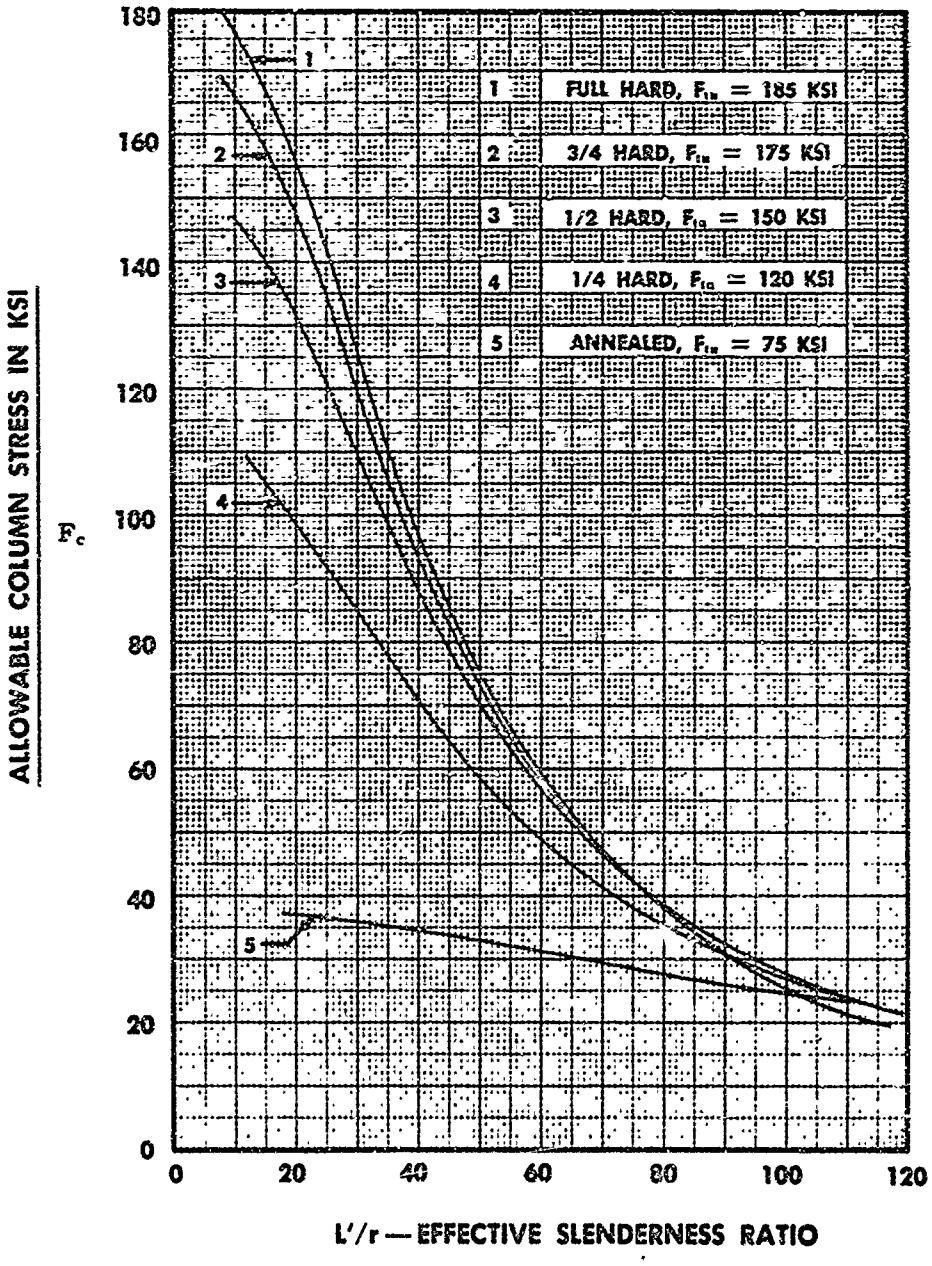

FIGURE 1.1630-3: COLUMN CURVES—ALLOY STEEL